A MITOCHONDRIAL UPR NEGATIVE FEEDBACK LOOP LIMITS LONGEVITY AND IS EXPLOITED DURING INFECTION

A Dissertation

Presented to the Faculty of the Weill Cornell Graduate School

of Medical Sciences

in Partial Fulfillment of the Requirements for the Degree of

Doctor of Philosophy

by

Pan Deng

December 2018

A MITOCHONDRIAL UPR NEGATIVE FEEDBACK LOOP LIMITS LONGEVITY AND IS EXPLOITED DURING INFECTION

Pan Deng, Ph.D.

Cornell University 2018

Mitochondria degenerate during aging and are perturbed by multiple pathogens during infection. In response, metazoans activate an unfolded protein response (UPR^{mt}) regulated by the transcription factor ATFS-1 that promotes mitochondrial recovery and innate immunity. UPR^{mt} activation promotes longevity caused by modest mitochondrial perturbations and also limits infection of pathogens that perturb mitochondrial function such as *Pseudomonas aeruginosa*. However, prolonged UPR^{mt} activation is detrimental. Here, we identify a UPR^{mt} negative feedback loop mediated by accumulation of the bZIP protein ZIP-3 which is induced by ATFS-1 and degraded by proteasomes. Interestingly, *zip-3*-deletion increases longevity in long-lived animals by enhancing UPR^{mt} activation, although development is severely impaired upon exposure to mitochondrial toxins demonstrating the UPR^{mt} must be appropriately regulated. During infection, the *P. aeruginosa* virulence response impairs UPR^{mt} activation. And, worms lacking *zip-3* were impervious to *P. aeruginosa*-mediated UPR^{mt} repression, and resistant to infection. Thus, we identified an intrinsic UPR^{mt} negative feedback loop that regulates the UPR^{mt}, and a pathogen that has evolved means to engage a UPR^{mt} negative regulator to promote infection.

BIOGRAPHICAL SKETCH

Pan Deng was born in Shijiazhuang, a city in Northern China, in 1990. She attended Tsinghua University in Beijing from 2008 to 2012, where she attained a B.S. in Biological Sciences. During the second year of undergraduate, Pan studied at Laboratory of Diabetes mellitus type 2, under the supervision of Dr. Zhen Li, and was then selected as a member of “Spark” Innovative Talent Cultivation Program in Tsinghua University because of her work on the formation and secretion of adiponectin polymers. Then, Pan joined the newly established Laboratory of Stem Cell and Germ Cell Development of Dr. Kehkooi Kee, where Pan carried out the project of reprogramming human fibroblast cells to iPS cells with *in vitro* transcribed mRNA. After graduation with honor, Pan moved to New York City and enrolled in the graduate program at Weill Cornell Graduate School of Medical Sciences in 2012. She joined the lab of Dr. Cole Haynes for her doctoral study in the following year. For her thesis research at Memorial Sloan Kettering Cancer Center and the University of Massachusetts Medical School, she focused on the regulation of mitochondrial unfolded protein response (UPR^{mt}) and the interaction between pathogen infection and mitochondrial UPR with using the animal model *Caenorhabditis elegans.*

ACKNOWLEDGEMENTS

First, I would like to express my deepest gratitude to Dr. Cole Haynes, for being the greatest mentor. With his guidance, I was able to learn to conduct scientific research independently with critical thinking, while having support all the time. He inspired me with his dedication for science and enthusiasm for research during my thesis research, and will keep inspiring me in my future career.

I would also like to thank my thesis committee members, Dr. Andy Koff and Dr. Mary Baylies, who offered numerous suggestions on my thesis project, with their valuable insights over the years.

I thank Drs. Amrita Nargund, Mark Pellegrino, Yi-Fan Lin, and Christopher Fiorese, for their tremendous help and since I joined Haynes' lab. They are great scientists with passion and patience. I'd also like to give my grateful thanks to Josh Lavelle, Dr. Qiyuan Yang, and Dr. Andy Melber, for their considerate company and kind support in and out of labs, from research to life, in Worcester. I am also grateful to have the opportunities working with other members of Haynes lab: Dr. Anna Schulz, Dr. Lilian Lamech, Dr. Tomer Shpilka, Yunguang Du, Nandhitha UmaNaresh and Bradford Trembley, all of whom are helpful and welcoming, making the sometimes-not-so-cheerful days of research less painful.

I'd also like to thank my friends in graduate school: Dr. Kan Lin, a wonderful listener who can always come up with wise advice, who guided me through the anxiety and confusion of PhD study; Linlin Cao and Yan Zhang, my former roommates and best friends, with whom I had the best moments during graduate school, which I would value for my entire life; Xiaojing Mu, the girl I admire and learn from, taught me how to embrace life.

I am also grateful to Yunxiao Zhang, who accompanied me the most time of graduate school. Yunxiao is the most intelligent person I have met, and I couldn't express my appreciation for all I learned from him over the years. We had a wonderful time together, and I wish him all the best with life and research in the future.

Lastly, I am most grateful to my parents, Hui Deng and Xuehong Wang. My parents were both engineers, then professors in a college in Shijiazhuang, China. They encouraged me to keep pursuing higher goals all the time. Also, they took care of my life since I was a kid, and are still backing me up when I am thousands of miles away from home. Without their support, I would not be able to achieve what I have today.

TABLE OF CONTENTS

LIST OF FIGURES

LIST OF TABLES

Chapter 1 Introduction

1.1 A brief introduction to mitochondria

1.1.1 Multifaceted mitochondria

Mitochondria are cellular compartments that form a dynamic network located throughout the cytosol and play pivotal roles in cells and organisms that rely on aerobic metabolism. Mitochondria harbor the tricarboxylic acid (TCA) cycle and oxidative phosphorylation (OXPHOS) machinery. These two processes convert acetyl-CoA generated from carbohydrate, protein and fat catabolism into ATP via the electron transport chain (respiratory chain) complexes and the ATP synthase (Jay 1987, Brown 1992, Alberts, Johnson et al. 2002). Meanwhile, mitochondria are also required for many other essential cellular activities, including the metabolism of amino acids, lipids, and nucleotides, iron-sulfur cluster synthesis, as well as calcium homeostasis (Figure 1.1)(Lill and Muhlenhoff 2008, Osman, Voelker et al. 2011).

Beyond metabolism, mitochondria significantly contribute to multiple signal transduction events including the regulation of programmed cell death via apoptosis, cell differentiation and growth (Liu, Kim et al. 1996, Sciacovelli, Guzzo et al. 2013, Ito and Suda 2014, Kasahara and Scorrano 2014, Weinberg, Sena et al. 2015). Crucial roles of mitochondria in the immune response are also revealed in recent years. ATP and metabolites produced from the TCA

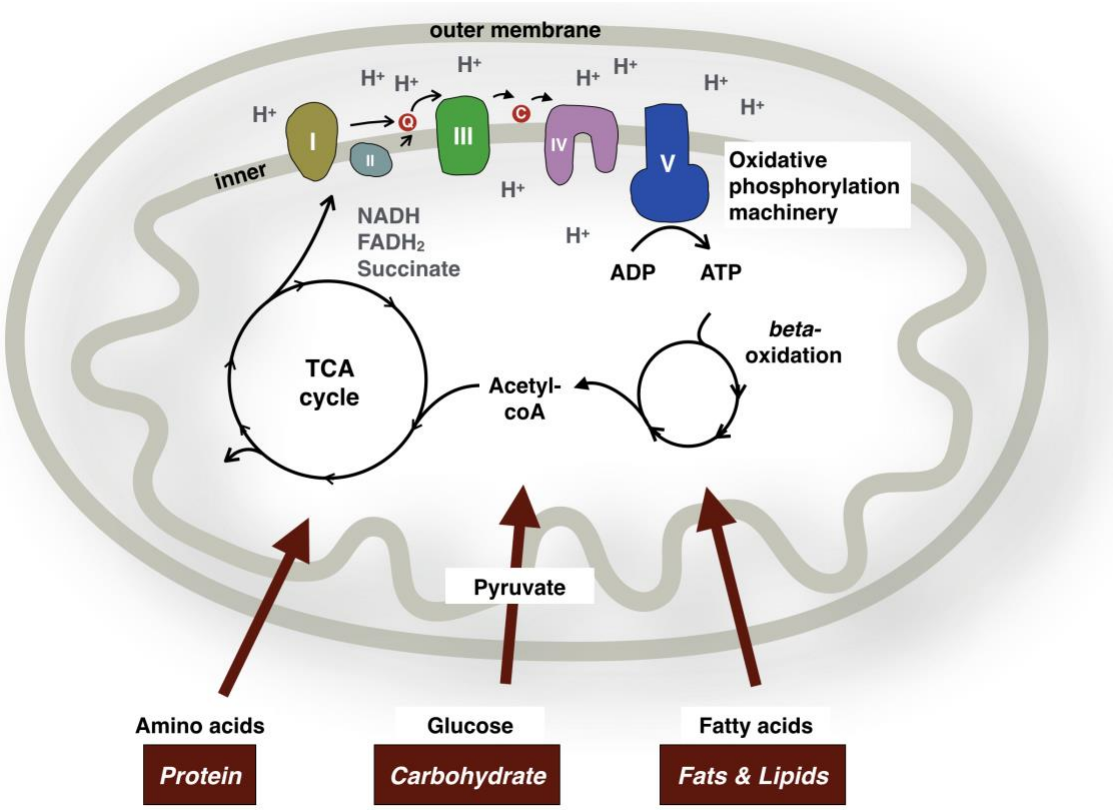

Figure 1.1 Mitochondria produce ATP from protein, carbohydrates and fat via the TCA cycle and oxidative phosphorylation

Amino acids, pyruvate and fatty acids derived from catabolized protein, carbohydrates, fats and lipids are transported into mitochondria, where they are incorporated in the TCA cycle. The TCA cycle, coupled with the electron transport chain complexes and the H^+-driven ATP synthase located on the inner membrane of mitochondria, promotes ATP production.

cycle or electron transport chain regulate the formation, differentiation and activation of T cells during adaptive immunity (Weinberg, Sena et al. 2015), while a great number of mitochondrial molecules and metabolites are essential signals for innate immunity activation in nematodes and mammals (West, Shadel et al. 2011, Liu, Samuel et al. 2014, Pellegrino, Nargund et al. 2014).

In mammals, Pattern-Recognition Receptors (PPRs) detect pathogen-associated and damage-associate molecular patterns, which initiate the innate immune response in hosts during pathogen infection or trauma injury (Kumar, Kawai et al. 2011, Mahla, Reddy et al. 2013). Defensive pathways activated by several types of PPRs are dependent on mitochondria signals. For example, mitochondrial DNA released from mitochondria can activate membrane-bound Toll-like receptors (TLR), the receptors recognizing conserved molecules derived from microbes, while elevated reactive oxygen species and the TCA cycle intermediate succinate produced by malfunctioned mitochondria promote the inflammatory cytokine signaling downstream of the TLR signaling pathway (Zhang, Raoof et al. 2010, Bulua, Simon et al. 2011, Infantino, Convertini et al. 2011). In addition, mitochondrial membrane potential, mitochondrial DNA and MAVS, a type of mitochondrial adaptor protein located on the mitochondrial outer membrane, can invoke the anti-viral singling pathway via RIG-I-like receptors (Seth, Sun et al. 2005, Koshiba, Yasukawa et al. 2011, White, McArthur et al. 2014). While the innate immune system in nematodes is much simpler, studies have shown that a mitochondrial retrograde signaling protective

pathway is essential for activating the defense response in hosts during pathogen infection, such as the infection of *P. aeruginosa* (Pellegrino, Nargund et al. 2014).

1.1.2 Mitochondrial assembly and mitochondrial quality control

Mitochondria are double membrane bound organelles consisting of about 1200 proteins. Nearly 99% of mitochondrial proteins are encoded by nuclear genes and synthesized on cytosolic ribosomes (Hartl, Pfanner et al. 1989). These proteins harbor mitochondrial targeting sequences (MTS) that direct them to the mitochondrial outer membrane where they engage the mitochondrial protein import machinery. First, they interact with the TOM complex (translocase of the outer membrane) and then TIM complex (translocase of the inner membrane) to traverse both mitochondrial membranes and enter the mitochondrial matrix (Figure 1.2)(Hoogenraad, Ward et al. 2002, Truscott, Wiedemann et al. 2002). In addition to the channels, transportation across the inner membrane requires a proton gradient generated by the respiratory chain as well as molecular chaperones located in the mitochondrial matrix (Simon, Peskin et al. 1992, Schatz and Dobberstein 1996). Once in the matrix, the MTS is typically cleaved and the protein folds and/or assembles, a process facilitated by molecular chaperones and complex assembly factors (Ostermann, Horwich et al. 1989, Hartl 1996, Martin 1997).

The remaining components of the mitochondrial proteome are encoded by the

mitochondrial genome (mtDNA). Typically, human cells harbor hundreds, or even thousands of mtDNA copies, which require extensive cellular machinery to maintain (Miller, Rosenfeldt et al. 2003, Wachsmuth, Hubner et al. 2016). Human mtDNA encodes 13 essential components of the OXPHOS complexes as well as 2 rRNAs and 22 tRNAs, which are required for the synthesis of mtDNA-encoded proteins within the mitochondrial matrix (Taanman 1999).

As the OXPHOS system is composed of large multi-subunits complexes encoded by separate genomes, transcription, protein expression and complex assembly must be tightly coordinated to prevent the accumulation of toxic protein folding or assembly intermediates in the mitochondria. Multiple mitochondria quality control pathways have evolved to maintain the normal functionality of mitochondria (Baker and Haynes 2011). For example, nuclear-encoded mitochondrial chaperone proteins, including mtHsp70, Hsp60 and Hsp78, function beyond folding nascent peptides: they promote the unfolding and refolding of misfolded or aggregated proteins (Baker, Tatsuta et al. 2011, Schreiner, Westerburg et al. 2012). In addition, mitochondrial proteases help to maintain mitochondrial proteostasis. Lon and ClpXP, two mitochondrial matrix-localized ATP-dependent proteases degrade damaged or misfolded proteins, while ATP-dependent AAA proteases located on the mitochondrial inner membrane selectively target damaged proteins in intermembrane space or on mitochondria inner membrane (Figure 1.2)(Tatsuta and Langer 2008).

When damaged proteins overload mitochondrial chaperones and proteases, mitochondria transmit stress signals to the nucleus via several retrograde responses. Retrograde response is a communication pathway from non-nucleus compartment to nucleus, which allows rapid transcription adaptation in nucleus according to the functional state of sub-cellular compartments (Liu and Butow 2006). During one such response, overloaded mitochondrial proteases can trigger a retrograde response called the mitochondrial unfolded protein response (UPR^{mt}), during which the compromised mitochondrial import efficiency leads to the relocation of a transcription factor from the cytosol into nucleus, and thus alters the transcription profile to adapt metabolism, alleviate mitochondrial stress and promote mitochondrial recovery (Haynes, Yang et al. 2010, Nargund, Pellegrino et al. 2012). The UPR^{mt} is further discussed in Chapter 1.3 and beyond.

The damages to mitochondria can be irreversible. Severely stressed mitochondria undergo fission, during which the damaged compartments are fragmented and sequestered (Youle and van der Bliek 2012), and degraded via mitophagy, or mitochondrial specific-autophagy (Lemasters 2005, Youle and Narendra 2011). These mechanisms will not be discussed in detail since they

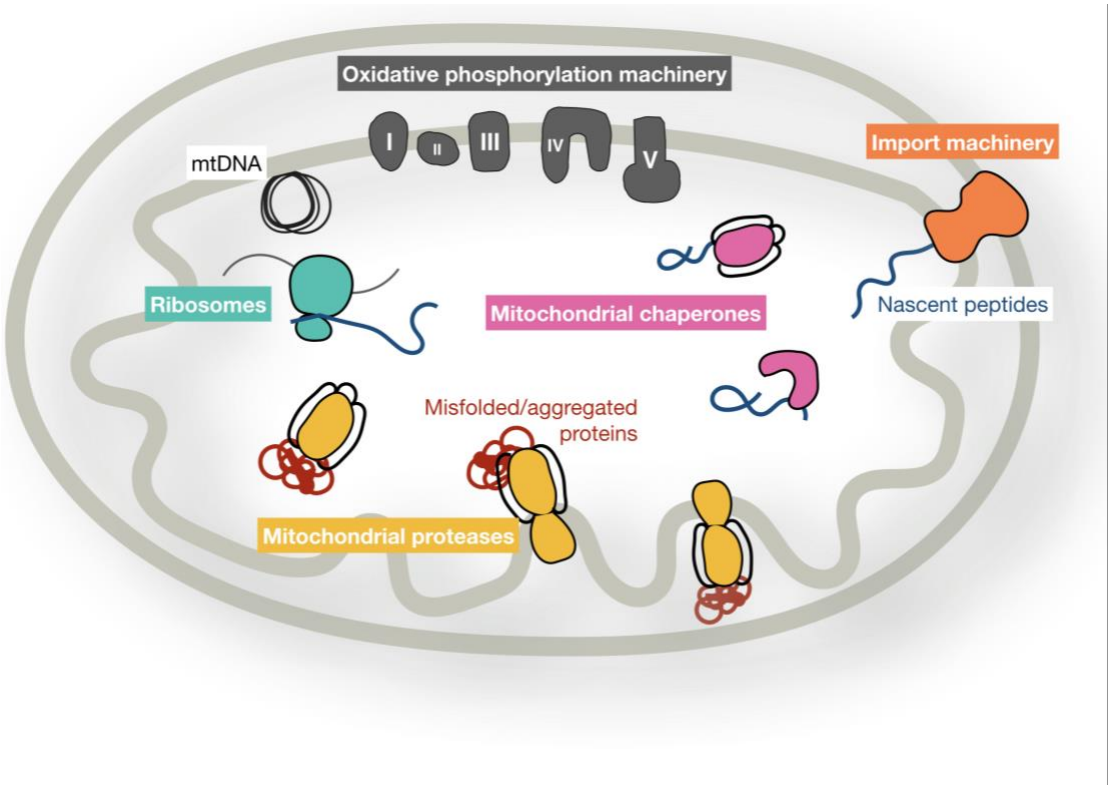

Figure 1.2 Mitochondrial machinery assembly and mitochondrial quality control.

99% of mitochondrial proteins are imported from cytosol as mRNAs or nascent proteins. Imported nascent peptides and peptides translated by mitochondrial ribosomes are folded and assembled by chaperones located in mitochondrial matrix. Mitochondrial proteases spanning matrix and inner membrane are required for quality control of mitochondrial proteins, via turning over misfolded or aggregated proteins, and activating retrograde signaling (Haynes, Yang et al. 2010).

are beyond the scope of this thesis. In summary, due to the importance of mitochondria in cellular activities and complexity of coordinating mitochondrial machinery, mitochondria are surveilled and regulated by multiple pathways related to different mitochondrial stress levels.

1.2 Mitochondrial dysfunction, and why it matters

1.2.1 Mitochondrial dysfunction

Though cells utilize many strategies to surveil and defend mitochondria, mitochondrial dysfunction arises from mitochondrial toxins, mtDNA mutations, and accumulative oxidative damage, which also orchestrate with each other and lead to inevitable mitochondrial function decline during aging and pathogenesis processes.

Apart from metabolic changes and ATP production decrease, stressed mitochondria further aggravate the damage to cells and organisms and lead to a variety of diseases. For example, Alzheimer's disease is a chronic neurodegenerative disease associated with β-amyloid protein (Aβ) deposition and progressive memory loss, while the pathogenesis of the disease remains mostly unknown (Obregon, Hou et al. 2012). Recent studies have found that the oxidative damage produced from aerobic metabolism of mitochondria promotes the production and aggregation of Aβ protein, and thus triggers some types of Alzheimer's disease (Swerdlow and Khan 2004). Consistent with the findings,

mitochondria-specific anti-oxidants that limit the mitochondrial oxidative stress level might be a potential therapy for Alzheimer's Disease (Moreira, Carvalho et al. 2010, Wang, Wang et al. 2014).

Mitochondrial dysfunction also contribute to other diseases mostly present as neuro-muscular disorders, such as Parkinson's Disease, Huntington's Disease, amyotrophic lateral sclerosis, as well as cardiac and skeletal muscle disorders (Lin and Beal 2006, Subramaniam and Chesselet 2013, Russell, Foletta et al. 2014, Schwarz, Siddiqi et al. 2014), and metabolic diseases, such as type II diabetes and Alper's syndrome (Naviaux, Nyhan et al. 1999, Lowell and Shulman 2005), likely due to the importance of mitochondria in metabolism and for neural and muscular activities.

1.2.2 Mitochondria and cancer

Mutations or lesions in mtDNA have been found in a variety of cancers, suggesting a relationship between mitochondrial dysregulation and cancer cell biology (Larman, DePalma et al. 2012, Gaude and Frezza 2014). Many of these mutations reduce oxidative phosphorylation efficiency in mitochondria (Petros, Baumann et al. 2005, Bonora, Porcelli et al. 2006, Singh, Ayyasamy et al. 2009) and force cells to rely more heavily on anaerobic glycolysis for ATP production. These observations potentially provides an underlying mechanism for what Warburg observed in cancer cells nearly 100 years ago; that cancer cells rely heavily on glycolysis even in the presence of oxygen (Warburg, Wind et al.

1927).

However, a bevy of recent studies have found that cancer cells rely more heavily on mitochondrial functions than previously thought, as mitochondrial dysfunction can impair the tumorigenicity of specific cancers cells. For example, depletion of mtDNA in glioblastoma and breast carcinoma cells significantly impairs proliferation (Dickinson, Yeung et al. 2013, Tan, Baty et al. 2015). Additionally, inhibition of mtDNA replication or mitochondrial biogenesis by suppressing PGC-1α or TFAM also reduced the invasion and metastasis of mammary epithelial cancer cells and lung cancer cells respectively (Weinberg, Hamanaka et al. 2010, LeBleu, O'Connell et al. 2014). These studies suggest that cancer cells rely on mitochondrial activities as well cellular pathways that evolved to maintain and recover mitochondrial function.

Interestingly, considerable evidence suggests that signals emanating from stressed or dysfunctional mitochondria promote cancer cell growth and survival. For example, mutations in the TCA cycle enzyme, such as isocitrate dehydrogenase (IDH), leads to an over-production of the onco-metabolite 2HG, which contributes to glioma formation and leukemogensis (Dang, White et al. 2010, Losman, Looper et al. 2013). And, succinate dehydrogenase (SDH) or fumarate hydratase (FH) mutations also cause accumulation of the TCA cycle metabolic intermediates, succinate and fumarate, that activate hypoxia-inducible factor 1 alpha (HIF-1α), which promotes cancer cell growth and

survival (Isaacs, Jung et al. 2005, Selak, Armour et al. 2005, Semenza 2010, Laukka, Mariani et al. 2016). Moreover, mutations in genes encoding complex III, components of the electron transport chain, impair apoptosis, thus contributing to tumor progression (Dasgupta, Hoque et al. 2009).

Further suggestive of a contribution of dysfunctional mitochondria to tumor progression, several mtDNA mutations, such as mutations in cytochrome c oxidase subunit 1 (MTCO1) and NADH dehydrogenase (ND5), are found in tumors of patients with diverse mtDNA backgrounds (Petros, Baumann et al. 2005, Gasparre, Hervouet et al. 2008). Although the impact on cancer biology remains controversial, several studies have suggested that mtDNA mutations perturb the respiratory chain can cause increased reactive oxygen species (ROS) which engage components of pro-growth or pro-survival pathways such as K-Ras, Akt and TLR4 (Ishikawa, Takenaga et al. 2008, Weinberg, Hamanaka et al. 2010, Sharma, Fang et al. 2011, Sabharwal and Schumacker 2014, Boroughs and DeBerardinis 2015, Liu, Pei et al. 2015). While it is well-documented that mtDNA lesions are relatively common in cancer cells, it should be noted that some studies have found no effect of mtDNA mutations on cancer cell biology (Deichmann, Kahle et al. 2004). Hopefully, future studies will be able to determine if mtDNA mutations are correlative or causative in tumorigenesis.

1.2.3 Mitochondria and longevity

Mitochondrial function has tremendous impact on lifespan. The free radical theory of aging has been dominant in the past tens of years, which suggested

that aging and related degenerative diseases are attributed to deleterious effects of reactive oxygen species (ROS), or free radicals, the by-products of aerobic metabolism (Harman 1956). The oxidative stress caused by excessive ROS accumulates mtDNA mutations, disturbs the normal function of mitochondrial proteins and damages lipid formation as well as plasma membrane fluidity (Shigenaga, Hagen et al. 1994). Consistent with the theory, high metabolic rates usually negatively correlate with lifespans.

However, the traditional theory of aging has been questioned recently. A bevy of studies showed that ROS are signaling molecules critical in a broad variety of cellular processes (Thannickal and Fanburg 2000, Apel and Hirt 2004, Janssen-Heininger, Mossman et al. 2008, Ray, Huang et al. 2012, Sena, Li et al. 2013). Moreover, evidence suggest that modest level of ROS increases lifespan (Balaban, Nemoto et al. 2005, Munkacsy and Rea 2014).

The conserved protein CLK-1 is an enzyme required for the synthesis of coenzyme Q, a critical component of complex III of the electron transport chain (Ewbank, Barnes et al. 1997). More than 20 years ago, research in *C. elegans* identified that several mutations in c*lk-1* gene significantly extended the lifespan of worms (Wong, Boutis et al. 1995, Ewbank, Barnes et al. 1997). In addition, worms with mutation in *isp-1*, iron-sulfur protein of the mitochondrial complex III, also showed similar lifespan extension compared to wildtype worms (Feng, Bussiere et al. 2001). Research found that, despite the potential oxidative stress

and damage on cellular components, the key triggering signaling molecule to the longevity in *clk-1* and *isp-1* mutants is the modest elevation of ROS (Lee, Hwang et al. 2010).

In addition, mutations in the mitochondrial tRNA synthetase *lrs-2*, cytochrome *c* heme lyase *cchl-1*, as well as knock-down of several essential components of electron transport chain have also been reported extending the lifespan of *C. elegans*, *D. melanogaster* and *M. musculus* (Dillin, Hsu et al. 2002, Lee, Lee et al. 2003, Liu, Jiang et al. 2005, Houtkooper, Mouchiroud et al. 2013, Owusu-Ansah, Song et al. 2013), supporting the hypothesis that modest mitochondrial dysfunction could lead to longevity. While several mitochondrial mutants shortened the lifespan of worms in an inconclusive way (Munkacsy and Rea 2014), an dsRNA titration experiment showed that the effect of mitochondrial dysfunction of lifespan is not monotonic (Rea, Ventura et al. 2007). Beyond a certain threshold, RNAis that target individual electron transport chain components start to shorten the lifespan with the increase of concentration, indicating the dual role of ROS and mitochondrial dysfunction on cellular activities lifespan.

Beyond the free radical theory, many other hypotheses have been raised to explain the effect of mitochondria on aging. These hypotheses involve nutrient-sensing pathways or cellular damage response pathways (Kirkwood 2005, Vijg and Campisi 2008, Gems and Partridge 2013, Lopez-Otin, Blasco et al. 2013).

For example, it has been reported that the proofreading-deficient mitochondrial DNA polymerase γ POLG-derived mtDNA mutation accumulation in mice contributes to aging via activating the cytochrome *c*-mediated apoptosis pathway (Kujoth, Hiona et al. 2005). Thus, mitochondria have a complicated role in regulating lifespan, and the mechanisms remain to be elucidated.

1.3 Mitochondrial UPR

Considerable evidence has suggested the existence of adaptive transcriptional responses to mitochondrial dysfunction. Transcription profiling studies comparing affected tissues in patients with mitochondrial diseases demonstrated a variety of potentially adaptive transcriptional alterations (Cizkova, Stranecky et al. 2008). Consistent with the patient studies, mitochondrial dysfunction in cultured cells caused by depletion of mtDNA or the overexpression of a terminally misfolded mitochondrial protein (ΔOTC) caused transcriptional induction of a number of mitochondrial-specific molecular chaperones and proteases (Martinus, Garth et al. 1996, Zhao, Wang et al. 2002). As these findings were conceptually similar to a well-studied response that mediates endoplasmic reticulum protein homeostasis known as the unfolded protein response (UPR), it was dubbed a mitochondrial stress response, and later a UPR^{mt} (Yoneda, Benedetti et al. 2004). While conceptually similar, regulation of the UPR^{mt} is different and completely independent from the UPR^{ER} likely deriving from differences in the two protein folding compartments. And,

the scope of the response is reflective of diverse cellular activities affected by mitochondrial functions.

In line with an organelle-specific response, the UPR^{mt} is specifically activated by mitochondrial perturbations (Yoneda, Benedetti et al. 2004). In addition to mtDNA depletion and mitochondrial unfolded protein accumulation, OXPHOS defects, inhibition of mitochondrial protein synthesis, mtDNA mutants, reactive oxygen species, hypoxia, as well as pathogenic bacteria that target mitochondria as part of a virulence response can trigger the UPR^{mt} (Liu, Wise et al. 2008, Nargund, Pellegrino et al. 2012, Houtkooper, Mouchiroud et al. 2013, Cano, Wang et al. 2014, Pellegrino, Nargund et al. 2014, Jovaisaite and Auwerx 2015, Rauthan, Ranji et al. 2015, Shao, Niu et al. 2016). As indicated in the previous section, many of the listed mitochondrial defects can be observed in cancer cells suggesting activation of the UPR^{mt}.

1.3.1 UPR^{mt} in worms

Genetic and biochemical studies in *C. elegans* have indicated that cells evaluate or monitor mitochondrial protein import efficiency to regulate the UPR^{mt}. Mitochondrial import likely serves as a useful surrogate for mitochondrial function, as multiple activities including OXPHOS and mitochondrial protein homeostasis, are required for efficient mitochondrial import (Wright, Terada et al. 2001). Several components that regulate UPR^{mt} activation have been discovered via genetic screens. The bZIP transcription factor, ATFS-1, directly

regulates UPR^{mt} gene promoters during mitochondrial dysfunction and is regulated by organellar compartmentalization. ATFS-1 harbors both a mitochondrial targeting sequence as well as a nuclear localization sequence allowing it to respond to mitochondrial import efficiency (Nargund, Pellegrino et al. 2012). In cells with a healthy mitochondrial network, ATFS-1 is synthesized and rapidly imported into mitochondria where it is degraded. However, during mitochondrial stress or dysfunction, reduced mitochondrial protein import efficiency causes a percentage of mitochondrial-targeted proteins to accumulate in the cytosol. As ATFS-1 harbors a nuclear localization sequence, it traffics to the nucleus to regulate a broad transcriptional response (Figure 1.3)(Haynes, Yang et al. 2010, Nargund, Pellegrino et al. 2012). In addition to transcriptional adaptations, UPR^{mt} activation also results in chromatin rearrangements required for a sustained response (Cole, Wang et al. 2015). Interestingly, UPR^{mt} activation can also be communicated between cells or different tissues presumably to allow for metabolic coordination or to prepare tissues for future conditions that may impact mitochondrial functions, although the signaling mechanism remains to be further defined (Berendzen, Durieux et al. 2016, Shao, Niu et al. 2016).

Once in the nucleus, ATFS-1 regulates transcription of over 500 genes that orchestrate a coherent mitochondrial stress response, including genes that promote mitochondrial protein homeostasis (chaperones, proteases and antioxidant genes). ATFS-1 also regulates diverse metabolic adaptations

including an increase of all glycolysis genes while simultaneously limiting transcription of TCA cycle and OXPHOS genes, presumably to reduce mitochondrial metabolic loads and maintain cellular ATP levels via glycolysis occurring in the cytosol. And lastly, the UPR^{mt} coordinates a mitochondrial repair and recovery program that includes a mitochondrial biogenesis pathway (Nargund, Fiorese et al. 2015). Concomitantly, ATFS-1 regulates expression of xenobiotic detoxifying genes and an innate immune response likely to reduce the effects of toxic metabolic intermediates or environmental toxins, and detect those pathogens that perturb mitochondrial function as part of their virulence response. For example, the pathogen *Pseudomonas aeruginosa*, which produces the OXPHOS inhibitor cyanide as a virulence factor, activates the UPR^{mt}, which is required to clear the infection (Pellegrino, Nargund et al. 2014, Nargund, Fiorese et al. 2015).

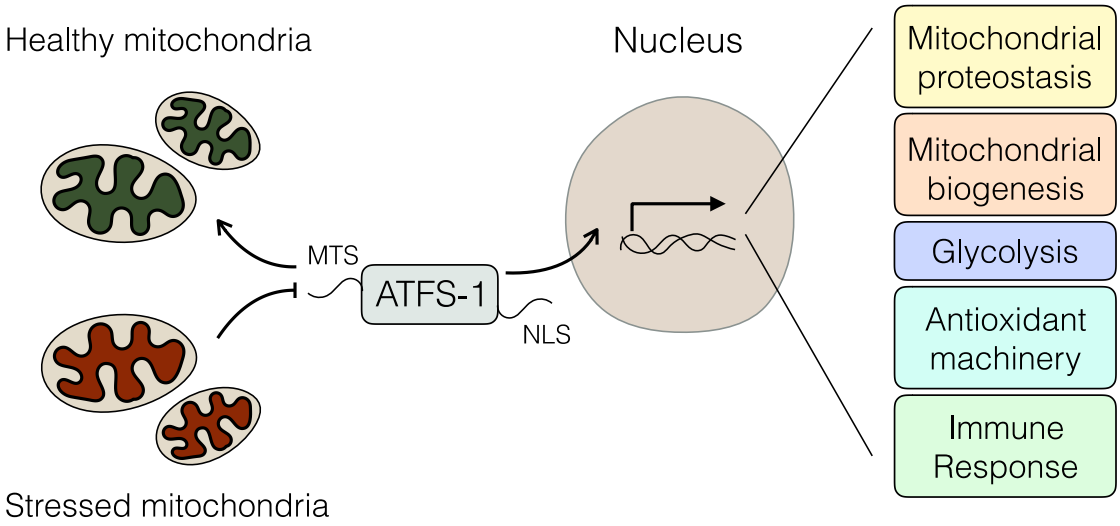

Figure 1.3 UPR^{mt} signaling in *C. elegans*

In the absence of mitochondrial stress, ATFS-1 is targeted to mitochondria via an amino-terminal mitochondrial targeting sequence (MTS) and is subsequently degraded in mitochondrial matrix. During mitochondrial stress or dysfunction, mitochondrial protein import is impaired, causing ATFS-1 to accumulate in the cytosol. Subsequently, ATFS-1 traffics to nucleus via its nuclear localization signal (NLS) and regulates the transcription of ~500 genes that promote mitochondrial protein homeostasis (proteostasis), mitochondrial recovery or biogenesis, metabolic adaptations such as glycolysis, antioxidants, and genes involved in xenobiotic detoxification to promote survival and resolution of mitochondrial stress.

1.3.2 UPR^{mt} in mammals

Mitochondrial stress response signaling in mammals also relies on similar mechanisms and bZIP transcription factors such as CHOP, ATF4 and ATF5, yet signaling in mammals may be more intricate (Figure 1.4). The interaction or coordination of these three transcription factors is rapidly emerging. However, it is clear that CHOP is induced during mitochondrial stress and was recently shown to be required for UPR^{mt} induction (Zhao, Wang et al. 2002, Munch and Harper 2016). However, CHOP is also induced during many forms of cellular stress, so how it contributes specifically during mitochondrial dysfunction remains unclear. ATF4 has also been shown to respond to mitochondrial dysfunction and induce mitochondrial proteases as well as the hormone FGF21 that coordinates metabolism between cells and tissues (Kim, Jeong et al. 2013, Kim and Lee 2014, Munch and Harper 2016). And most recently, ATF5 was found to regulate a UPR^{mt}, by mediating a transcription response that includes mitochondrial chaperones and proteases similar to ATFS-1 in *C. elegans* (Fiorese, Schulz et al. 2016). Interestingly, ATF5 is transcriptionally induced in several mitochondrial disorders (Endo, Sano et al. 2009, Tyynismaa, Carroll et al. 2010, Torres-Peraza, Engel et al. 2013, Yap, Llanos et al. 2016), and cells with impaired ATF5 are susceptible to mitochondrial stress (Fiorese, Schulz et al. 2016).

Accumulating evidence indicates that, like in *C. elegans*, the UPR^{mt} in mammals is regulated at least in part by mitochondrial import efficiency. For example,

during mitochondrial dysfunction, a subunit of the TIM23 mitochondrial protein import complex is rapidly degraded, resulting in reduced import efficiency and induction of a UPR^{mt} (Rainbolt, Atanassova et al. 2013). Importantly, ATF5 is regulated by mitochondrial protein import efficiency similar to ATFS-1 (Fiorese, Schulz et al. 2016), and potentially responds to degradation of Tim17a or other forms of mitochondrial stress that perturb protein import. Similar to ATFS-1, the steady-state localization of ATF5 is within mitochondria when expressed in healthy cells. However, during mitochondrial stress it accumulates in nuclei and induces the expression of mitochondrial-protective genes. Importantly, ATF5 is required for survival and recovery from mitochondrial dysfunction (Fiorese, Schulz et al. 2016).

1.3.3 UPR^{mt} and diseases

Numerous studies showed that ATF5 and the mitochondrial UPR pathway are important for maintaining mitochondrial functions and cellular activities. ATF5 promotes the proliferation of neural progenitor cells, and regulates the differentiation of mature neurons or glial cells (Hansen, Mitchelmore et al. 2002, Angelastro, Ignatova et al. 2003, Angelastro, Mason et al. 2005), which is consistent with the knowledge that neural system relies heavily on mitochondria

Figure 1.4 UPR^{mt} signaling in mammals

UPR^{mt} signaling in mammalian cells. The mammalian UPR^{mt} is regulated by multiple bZIP transcription factors such as ATF5, which is regulated by at least two mechanisms. Expression of ATF5 is regulated by the phosphorylation of the translation initiation factor eIF2α, which is regulated by the kinases GCN2, PERK or PKR. Because the ATF5-encoding mRNA harbors upstream open reading frames (uORFs) in the 5' untranslated region, its synthesis requires phosphorylated eIF2α which can be stimulated during nutrient deprivation, mitochondria or endoplasmic reticulum dysfunction or the accumulation of double-stranded RNA in the cytosol by the above-mentioned kinases. Once it is expressed, ATF5 is regulated by mitochondrial protein import efficiency. In the absence of mitochondrial stress, ATF5 is targeted to mitochondria via its amino-terminal mitochondrial targeting sequence (MTS). However, during mitochondrial dysfunction, ATF5 fails to be imported into mitochondria and traffics to the nucleus via its nuclear localization signal (NLS) to induce transcription of genes that influence mitochondrial proteostasis, anti-apoptotic machinery, cell growth and migration.

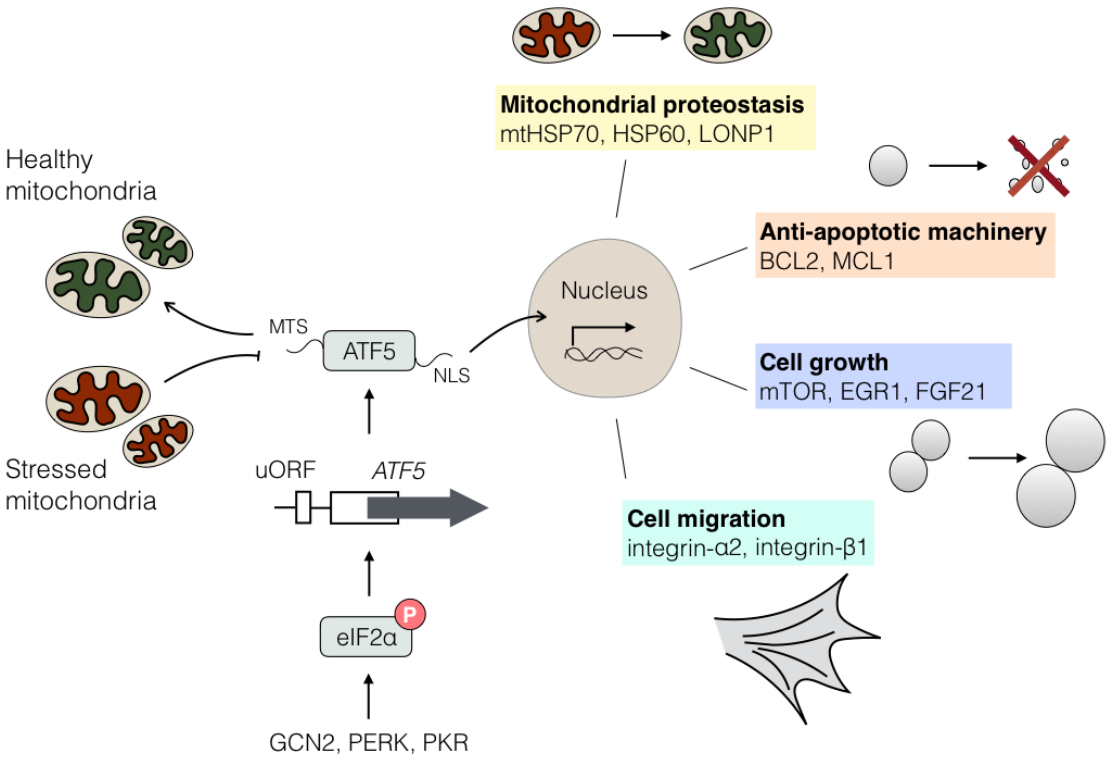
Mitochondrial proteostasis
mtHSP70, HSP60, LONP1
Healthy
mitochondria
Anti-apoptotic machinery
BCL2, MCL1
Nucleus
MTS
ATF5
NLS
Cell growth
mTOR, EGR1, FGF21
Stressed
mitochondria
uORF
ATF5
Cell migration
integrin-α2, integrin-β1
P
eIF2α
GCN2, PERK, PKR

for their normal activities. UPR^{mt} also prevents aging. Studies in mice showed that the UPR^{mt} rejuvenates muscle stem cells and hematopoietic stem cells (Mohrin, Shin et al. 2015, Zhang, Ryu et al. 2016). Moreover, ATF5 is activated during metabolic changes that leads to mitochondrial stress, such as fasting or amino acid limitation (Watatani, Kimura et al. 2007, Shimizu, Morita et al. 2009).

Further, the UPR^{mt} protects mitochondria and cells from mitochondrial toxins, such as paraquat, ethidium bromide, statins, cadmium and arsenite in worms and mammalian cell lines (Uekusa, Namimatsu et al. 2009, Nargund, Pellegrino et al. 2012, Rauthan, Ranji et al. 2013). Pre-activation of the UPR^{mt} extended the survival of worms on *P. aeruginosa*, a type of pathogen secreting a group of mitochondrial toxins (Chapter 3.1), via inducing innate immune response in worms (Pellegrino, Nargund et al. 2014).

Meanwhile, UPR^{mt} is important for mitochondrial repair and metabolic adaptations during diseases with mitochondrial dysfunction. Muscle disorders caused by respiratory chain deficiencies, such as cardiomyopathy, require ATF5-mediated mitochondrial stress responsive pathway to promote mitochondrial biogenesis and maintain mitochondrial homeostasis (Tyynismaa, Carroll et al. 2010, Dogan, Pujol et al. 2014). Huntington's Disease is a fatal genetic neurodegenerative disease, the genetic mutations during which cause aggregation of polyglutamine chain proteins in human brains, and thus lead to cellular damages and death of cells. UPR^{mt} activation also displayed positive

impact on preventing polyglutamine aggregation in human patients' tissue, mice and nematodes (Berendzen, Durieux et al. 2016, Tian, Garcia et al. 2016, Hernandez, Torres-Peraza et al. 2017). In addition, eliciting the UPR^{mt} via supplementing diet with nicotinamide riboside, a precursor of NAD(+) biosynthesis, successfully reversed the nonalcoholic fatty liver disease caused by high-fat high-sucrose diet in mice (Gariani, Menzies et al. 2016).

However, the UPR^{mt} also promotes cell growth and survival by ensuring mitochondrial function in the presence of mitochondrial stress related to cell physiology or mutation accumulation in tumors. The UPR^{mt}-induced genes such as mitochondrial chaperones and proteases are highly induced in many cancers (Czarnecka, Campanella et al. 2006, Cerami, Gao et al. 2012, Gao, Aksoy et al. 2013, Goard and Schimmer 2014), some of which have been shown to be ATF5-dependent. On the contrary, inhibition of the UPR^{mt} can selectively repress the growth and progression of tumor cells. A dominant-negative form of ATF5, CP-d/n-ATF5-S1, has been developed as an ATF5-specific inhibitor, which impairs the growth of prostate cancer, glioblastoma, melanoma and triple receptor-negative breast cancer cells in cell culture and xenograft models by inducing apoptosis (Karpel-Massler, Horst et al. 2016).

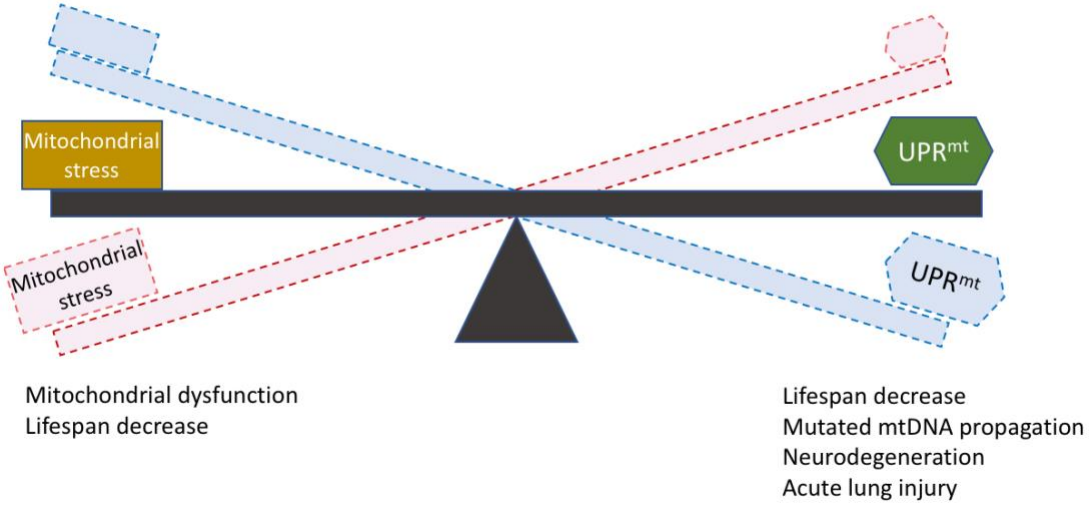

Figure 1.5 Matching mitochondrial UPR activity and mitochondrial stress level is important for the normal function of cells and organisms

While accumulating mitochondrial stress can lead to mitochondrial dysfunction and decrease in lifespan, prolonged UPR^{mt} activity with no mitochondrial stress also result in lifespan decrease, as well as neurodegeneration and acute lung injury.

1.3.4 Toxicity of the UPR^{mt}

While mild level of UPR^{mt} is positive associated with longevity (Owusu-Ansah, Song et al. 2013, Munkacsy and Rea 2014), prolonged UPR^{mt} activation can be toxic to normal cells. Due to the inefficient import to mitochondria caused by a point mutation in the MTS of the protein, in ATFS-1 gain-of-function mutant, ATFS-1 constitutively traffics to nucleus, and induces UPR^{mt} activity (Rauthan, Ranji et al. 2013). Though resistant to mitochondrial toxins such as statins and gliotoxin, ATFS-1 gain-of-function worm strain has shorter lifespan compared to wildtype worms. Then, it was found that ATFS-1 gain-of-function leads to the propagation of mutated mitochondrial DNA, which compromises the efficiency of respiratory chain (Lin, Schulz et al. 2016). Prolonged UPR^{mt} activity is also reported leading to loss of dopamine neurons, development impairment and acute lung injury (Rauthan, Ranji et al. 2013, Martinez, Petersen et al. 2017, Zhang, Zhuang et al. 2018).

Thus, balanced mitochondrial UPR activity is essential for mitochondrial function and cellular activities (Figure 1.5). While the previous studies demonstrated that mitochondrial stress and mitochondrial import efficiency induce the UPR^{mt}, it is important to for us learn how UPR^{mt} is regulated to match the cellular mitochondrial stress. MET-2-mediated H3K9 methylation and the consequential nuclear translocation of LIN-65 leads to chromatin reorganization, which promotes ATFS-1 binding to UPR^{mt} genes and initiating the UPR^{mt} transcription program (Tian, Garcia et al. 2016). As both MET-2 and LIN-65 are

activated by mitochondrial stress in an ATFS-1 independent way, chromatin remodeling serves as an approach to modulate UPR^{mt} activity. However, regulations involving changes of methylation patterns are usually enduring, which means it cannot provide prompt feedback on UPR^{mt} activity. This thesis described an intrinsic UPR^{mt} repressor, ZIP-3, which is transcriptionally induced by ATFS-1, and thus composes a negative feedback loop regulating UPR^{mt} during various mitochondrial stress. Also, we showed that pathogen *P. aeruginosa* evolved to exploit ZIP-3, to repress the UPR^{mt} and promote infection.

Chapter 2 ZIP-3: A repressor of the UPR^{mt}

2.1 ZIP-3: A bZIP transcription factor regulated by ATFS-1

bZIP proteins form homo- or hetero- dimers in the nucleus to regulate gene expressions. Firstly, we asked if other bZIP proteins hetero-dimerize with ATFS-1 to activate the UPR^{mt}.

An *in vitro* experiment identified 3 transcription factors whose bZIP domains dimerize with the bZIP domain of ATFS-1: C48E7.11, *ces-2* and *zip-3* (Reinke, Baek et al. 2013). Among them, the transcription *zip-3* was robustly induced in an ATFS-1 dependent manner during mitochondrial stress caused by knock-down of mitochondrial protease SPG-7 (Nargund, Pellegrino et al. 2012)(Figure 2.1a). *zip-3* was also transcriptionally induced in a strain expressing constitutively active ATFS-1, *et15*, which harbors a mutation that impairs the MTS and promotes its nuclear accumulation (Rauthan, Ranji et al. 2013, Lin, Schulz et al. 2016) (Figure 2.1b). Combined, these results indicate that the nuclear ATFS-1 induces the transcription of *zip-3* gene.

ZIP-3 protein contains a Basic Leucine Zipper domain (bZIP domain) on its C-terminus and is composed of 307 amino acids (Figure 2.1c). A previous ChIP-sequencing experiment identified the UPR^{mt}E consensus sequence, the sequence to which ATFS-1 binds during *spg-7*(RNAi) induced mitochondrial stress (Nargund, Fiorese et al. 2015). And, the consensus sequence is also

present in the promoter region of *zip-3*, consistent with the ChIP-seq experiment that ATFS-1 protein is enriched at the promoter and genomic coding region of *zip-3* during *spg*-7(RNAi) treatment (Figure 2.1d). As the expression of *zip-3* mRNA is also induced by ATFS-1 during mitochondrial stress, the combined results suggest that ATFS-1 directly regulates the transcription of the *zip-3* gene during mitochondrial stress.

Though *spg-7*(RNAi) experiment indicates that ZIP-3 is not required for UPR^{mt} activation, the close connection between ZIP-3 and ATFS-1 drew our attention. Since *spg-7*(RNAi) is a strong UPR^{mt} inducer that leads to transient UPR^{mt} burst, we then switched to models other than *spg-7* knock-down, to test the hypothesis that ZIP-3 regulates the UPR^{mt}, probably via regulating ATFS-1 activity in a feedback approach.

2.2 ZIP-3 and the mitochondrial UPR

2.2.1 Loss of ZIP-3 enhanced UPR^{mt} activity

zip-3(gk3164) is a *zip-3* deletion strain with exon2 and the flanking introns removed in the *zip-3* gene (Figure 2.2a). HSP-6 and HSP-60 are mitochondrial chaperones that promote folding and refolding of nascent peptides or misfolded proteins in mitochondrial matrix. *hsp-6 and hsp-60* genes are induced during

Figure 2.1 ATFS-1 regulates the transcription of bZIP protein ZIP-3 via directly binding to ZIP-3 promoter during mitochondrial stress

a, *zip-3* mRNA as determined by qRT-PCR in wildtype and *atfs-1(tm4525)* worms on control versus *spg-7*(RNAi) (n=3, ±s.d.). **P*<0.05 (Student's *t*-test). **b,** *zip-3* mRNA as determined by qRT-PCR in wildtype and *atfs-1(et15)* worms (n=3, ±s.d.). **P*<0.05 (Student's *t*-test). **c,** ZIP-3 protein. bZIP domain: The Basic Leucine Zipper Domain which mediates sequence specific DNA binding properties. NLS: nuclear localization signal. PY motif: a conserved motif targeted by E3 ubiquitin ligase WWP-1 and is essential for ZIP-3 degradation. PY motif is further described in Chapter 2.3. **d,** ChIP-seq profile of the *zip-3* promoter and genomic coding region in wildtype worms raised on *spg-7*(RNAi) using ATFS-1 antibody or no antibody. ATFS-1 binding motif, or the UPR^{mt}E consensus sequence, is identified previously (Nargund, Fiorese et al. 2015).

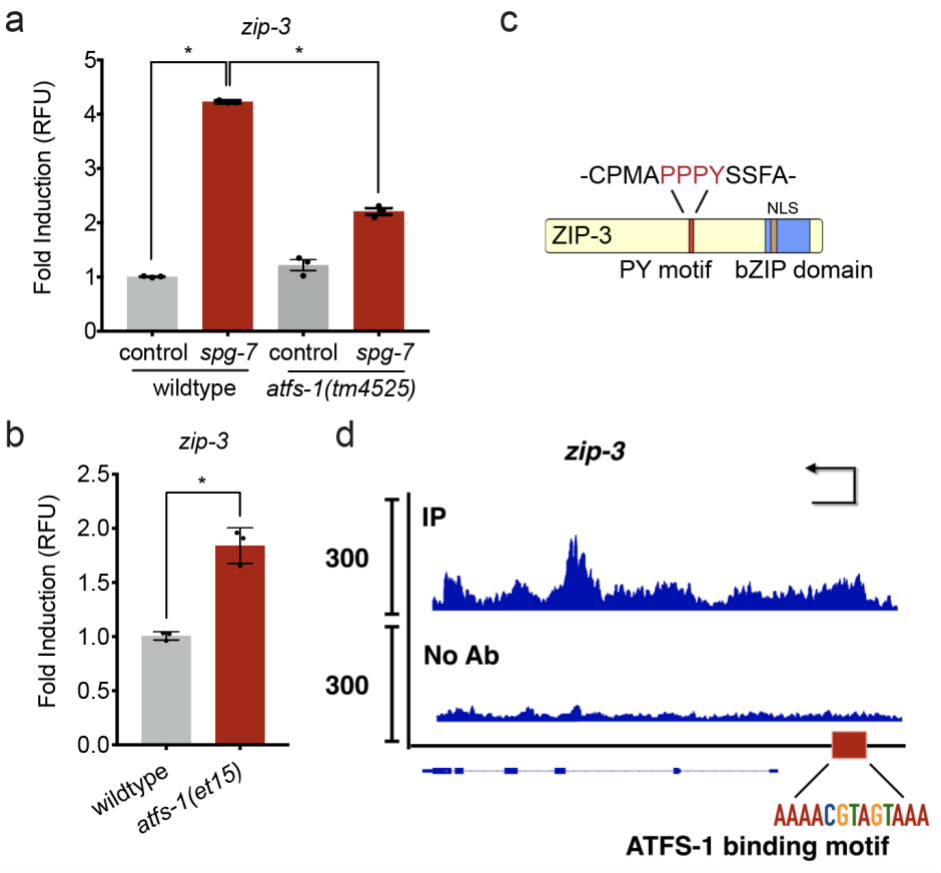
a
zip-3
Fold Induction (RFU)
control
spg-7
control
spg-7
wildtype
atfs-1(tm4525)
b
zip-3
Fold Induction (RFU)
wildtype
atfs-1(et15)
c
-CPMAPPPYSSFA-
NLS
ZIP-3
PY motif
bZIP domain
d
zip-3
IP
No Ab
300
300
AAAACGTAGTAAA
ATFS-1 binding motif

various mitochondrial stress, including *spg-7*(RNAi) exposure, to promote the recovery of mitochondrial proteostasis. GFP driven by the promoters of the two chaperone genes, *hsp-6$_{pr}$::gfp* and *hsp-60$_{pr}$::gfp*, are constructed as reporters to evaluate UPR^{mt} activity (Yoneda, Benedetti et al. 2004, Haynes, Yang et al. 2010, Nargund, Pellegrino et al. 2012). To evaluate the effect of *zip-3* on the UPR^{mt}, we crossed *zip-3* deletion strain with the mitochondrial UPR reporter strain *hsp-6$_{pr}$::gfp.* While the deletion of *zip-3* gene, consistent with knock-down of *zip-3* mRNA, has no effect on the lifespan of worms fed *E. coli* in the absence of additional mitochondrial stress (Figure 2.2b), *zip-3* deletion strain showed mild UPR^{mt} induction (Figure 2.2c).

We then examined how *zip-3* affects the UPR^{mt} during mitochondrial stress. Transient loss of mitochondrial protease SPG-7 leads to ATFS-1-dependent activation of the UPR^{mt} (Nargund, Pellegrino et al. 2012). With higher UPR^{mt} activity to start with, we didn't observe stronger UPR^{mt} activation in *zip-3* deletion strain compared to wildtype strain during the *spg-7* knock-down (Figure 2.3a).

Considering that *spg-7* knock-down leads to strong mitochondrial dysfunction and activation of *hsp-6$_{pr}$::gfp* reporter, we asked if the mitochondrial stress induced by *spg-7* knock-down overshadows the effect of ZIP-3 on UPR^{mt}.

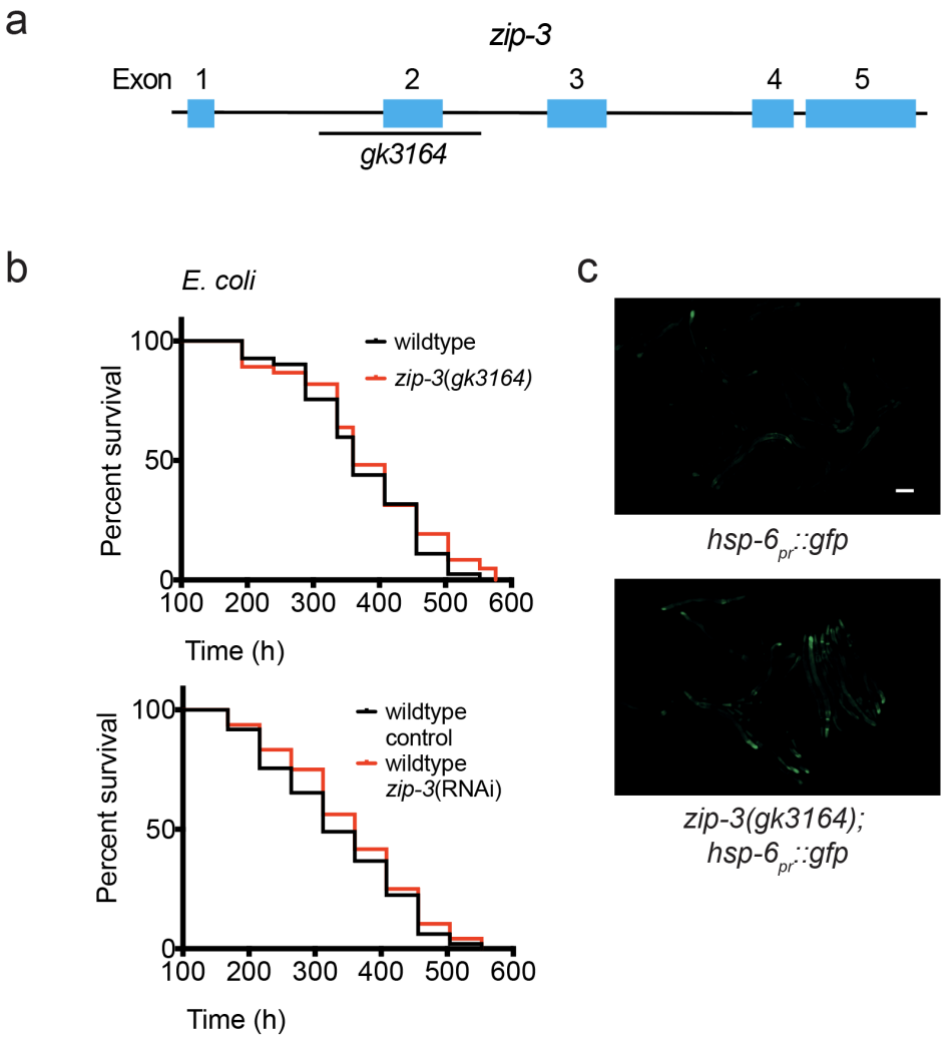

Figure 2.2 *zip-3* deletion induces mild UPR^{mt} activation, but does not affect worm lifespan

a, Schematic of the *zip-3(gk3164)* deletion that removes 1275 base pairs and all of exon 2 from *zip-3*. **b,** Lifespan of wildtype or *zip-3(gk3164)* worms exposed to *E. coli*, and wildtype worms on control or *zip-3*(RNAi). Statistics are in Table A.4. **c,** Representative images of *hsp-6$_{pr}$::gfp* and *zip-3(gk3164);hsp-6$_{pr}$::gfp* worms on *E. coli.* Scale bar, 0.1mm.

Figure 2.3 *zip-3* deletion delays the development and extends the lifespan of long-lived mutants via further activating the UPR^{mt}

a, UPR^{mt} activity of *hsp-6$_{pr}$::gfp* and *zip-3(gk3164);hsp-6$_{pr}$::gfp* worms on *spg-7*(RNAi). **b,** Representative images of UPR^{mt} activation in *clk-1(qm30)* and *clk-1(qm30); zip-3(gk3164)* worms raised on *E. coli.* Scale bar, 0.1mm. **c,** Representative images of *clk-1(qm30)* or *clk-1(qm30); zip-3(gk3164)* worms raised on *E. coli.* **d,** Representative images of *isp-1(qm150)* or *isp-1(qm150); zip-3(gk3164)* worms raised on *E. coli.* **e,** Lifespan of *clk-1(qm30)* or *clk-1(qm30); zip-3(gk3164)* worms raised on *E. coli*. Statistics are in Table A.4. **f,** Lifespan of *isp-1(qm150)* or *isp-1(qm150); zip-3(gk3164)* worms raised on *E. coli*. Statistics are in Table A.4.

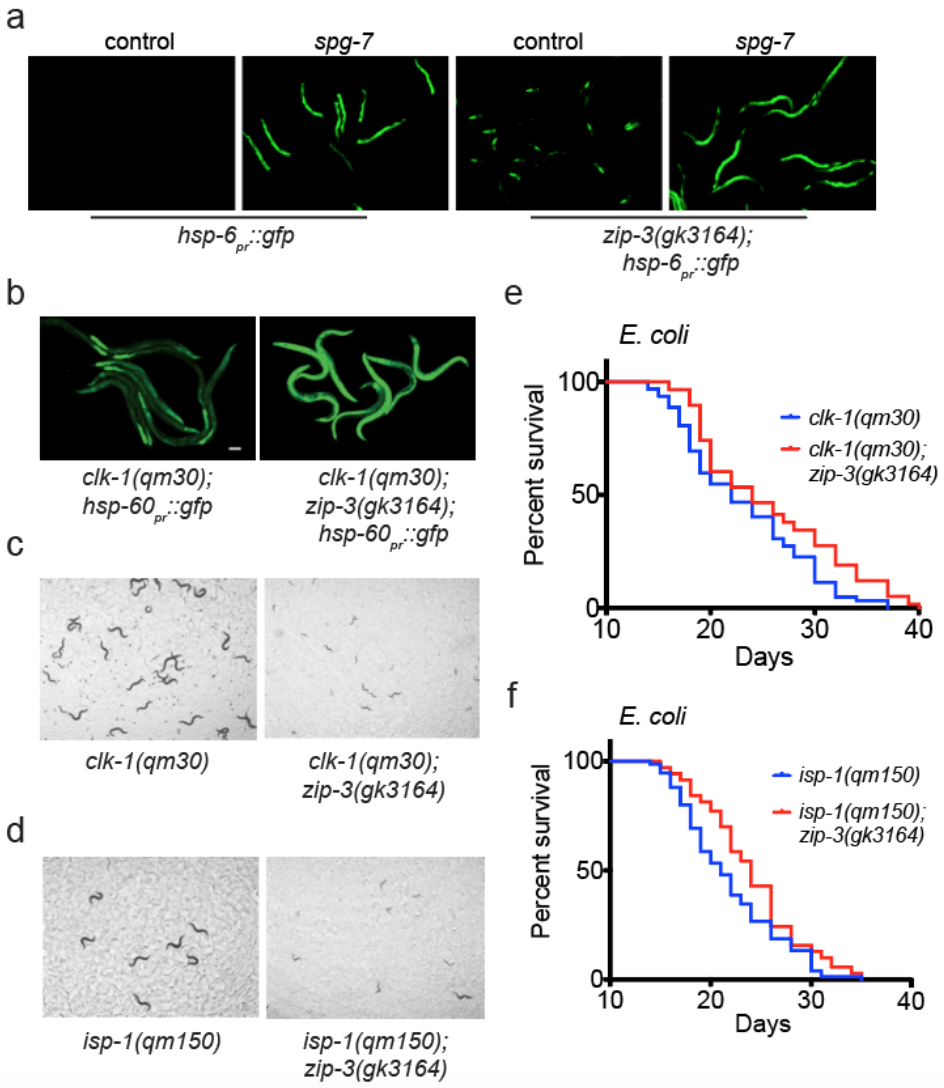
a
control
spg-7
control
spg-7
hsp-6pr::gfp
zip-3(gk3164);
hsp-6pr::gfp
b
clk-1(qm30);
hsp-60pr::gfp
clk-1(qm30);
zip-3(gk3164);
hsp-60pr::gfp
c
clk-1(qm30)
clk-1(qm30);
zip-3(gk3164)
d
isp-1(qm150)
isp-1(qm150);
zip-3(gk3164)
e
E. coli
Percent survival
100
50
0
10
20
30
40
Days
clk-1(qm30)
clk-1(qm30);
zip-3(gk3164)
f
E. coli
Percent survival
100
50
0
10
20
30
40
Days
isp-1(qm150)
isp-1(qm150);
zip-3(gk3164)

Thus, we examined the worm strains with modest mitochondrial stress. As stated previously, modest mitochondrial dysfunction caused by loss of function in mutations in genes encoding oxidative phosphorylation components, such as *clk-1* and *isp-1*, activates the UPR^{mt} and extends worm lifespan. Next, we asked whether ZIP-3 affects the UPR^{mt} activation in worm strains with *clk-1* or *isp-1* mutations.

Strikingly, unlike *spg-7*(RNAi), we observed a tremendously increased expression of *hsp-60$_{pr}$::gfp* reporter upon deleting *zip-3* in *clk-1(qm30)* worms (Figure 2.3b), suggesting that *zip-3* deletion further activates the UPR^{mt} during modest mitochondrial stress induced by *clk-1* mutation.

To understand why the loss of *zip-3* leads to activation of the UPR^{mt}, we investigated the physiological impact of *zip-3* on *clk-1* and *isp-1* mutants. Loss of *zip-3* in *clk-1* or *isp-1* mutants result in further development impairment in the worms (Figure 2.3c, d), suggesting that ZIP-3 is probably required for maintaining mitochondrial function similar to mitochondrial protease SPG-7 (Nargund, Pellegrino et al. 2012, Shao, Niu et al. 2016). However, both *clk-1(qm30);zip-3(gk3164)* and *isp-1(qm150);zip-3(gk3164)* double mutant strains showed extended lifespan compared to *clk-1(qm30)* mutant strain (Figure 2.3e, f). Since several reports have demonstrated that UPR^{mt}-regulatory components including ATFS-1 are required for the extended lifespan of both *clk-1(qm30)* and *isp-1(qm150)* strains (Durieux, Wolff et al. 2011, Bennett, Kwon et al. 2017), the

extended lifespan in *zip-3* loss-of-function background is likely induced by enhanced UPR^{mt} activity. This supports the hypothesis that ZIP-3 functions as a negative regulator of ATFS-1 and together, ATFS-1 and ZIP-3 form a negative feedback loop regulating UPR^{mt} activity.

2.2.2 UPR^{mt} genes are further induced in the absence of ZIP-3 during mitochondrial stress

We have shown paradoxical impact of *zip-3* during mitochondrial stress induced by *spg-7*(RNAi) and *clk-1* or *isp-1* mutations. To assess if the impact of ZIP-3 on the UPR^{mt} is specific to certain types of mitochondrial stress, and to determine the role of ZIP-3 during mitochondrial stress, we exposed both wildtype and *zip-3* deletion strains to *spg*-7(RNAi), then checked the genomic-wide RNA expression level in wildtype and *zip-3* deletion strains with RNA-seq experiment.

To be more specific, we raised wildtype, *zip-3* deletion and an *atfs-1* loss-of-function strain *atfs-1(tm4919)* on control RNAi and *spg-7* (RNAi) for the same duration of time. We defined the UPR^{mt} genes as those genes that are induced by *spg-7*(RNAi) in wildtype worms and are however, less induced in *atfs-1(tm4919)* during stress compared to wildtype worms. First, we identified 560

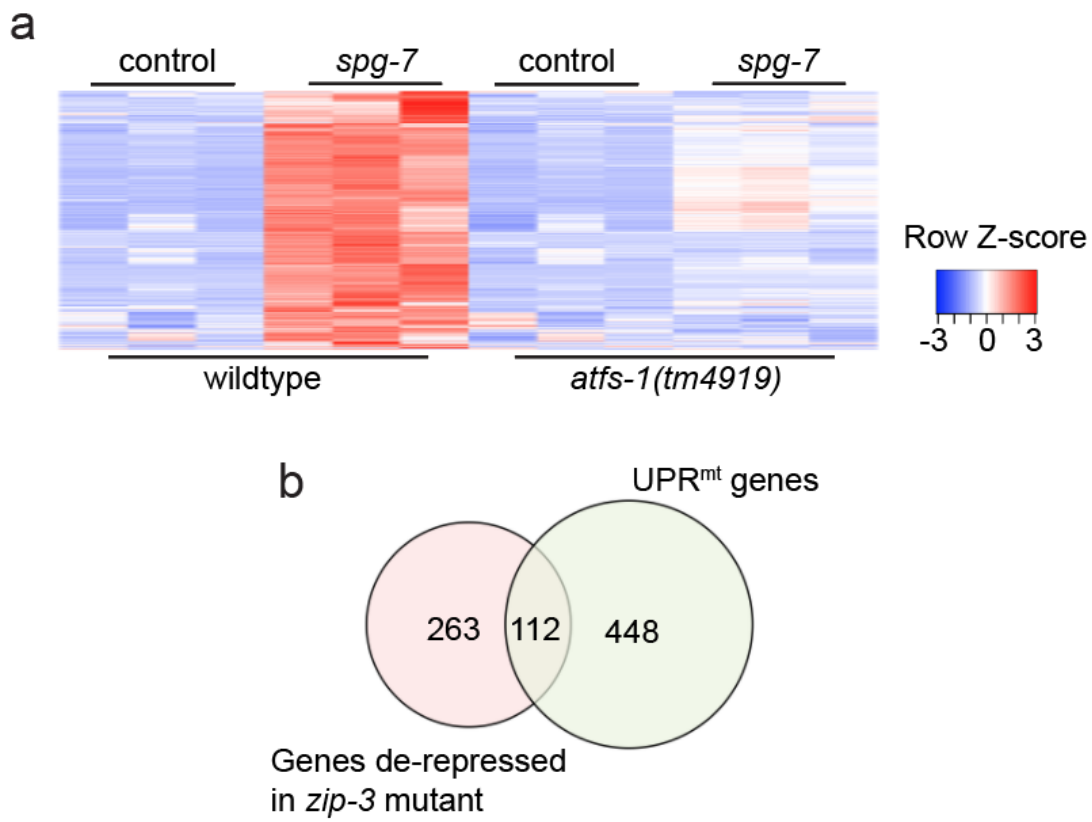

Figure 2.4 Genes regulated by ATFS-1 or ZIP-3 during mitochondrial stress

a, Heat map comparing gene expression patterns of wildtype or *atfs-1(tm4919)* (Pellegrino, Nargund et al. 2014) worms raised on control (RNAi) or *spg-7*(RNAi). **b,** Venn diagram showing ATFS-1-dependent UPR^{mt} genes that are further induced in *zip-3(gk3164)* mutant compared to wildtype worms.

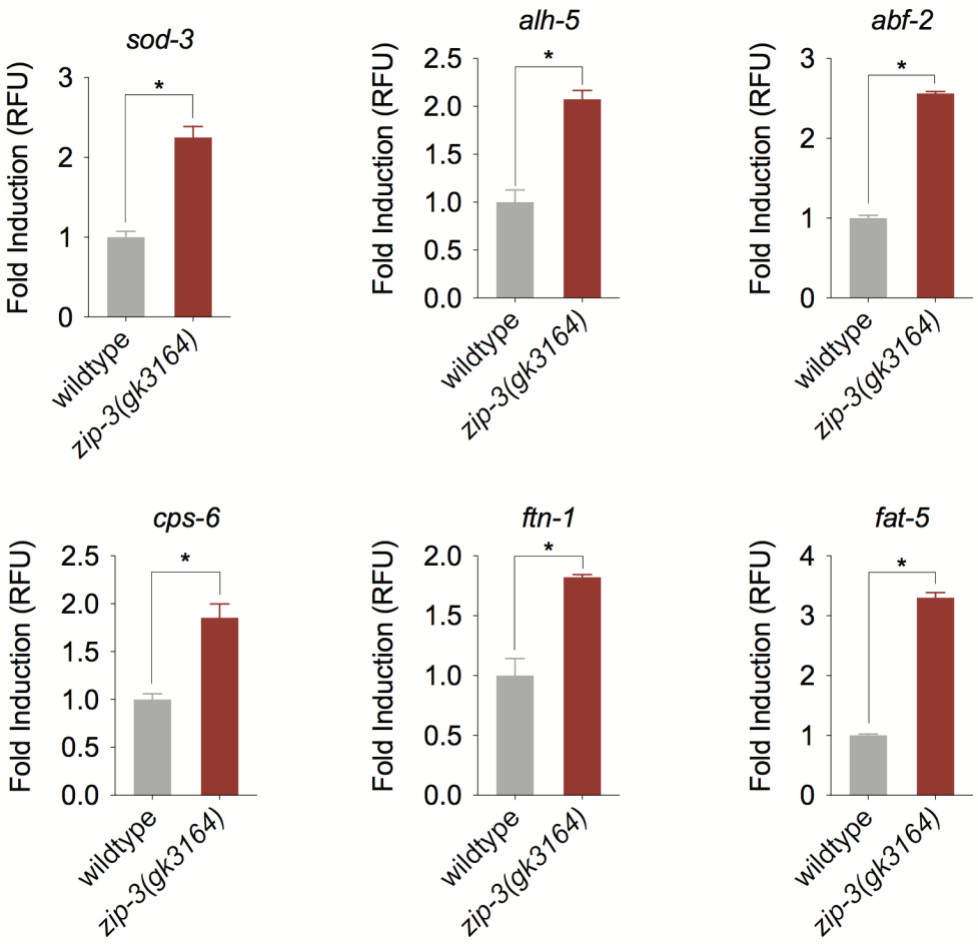

Figure 2.5 Representative ATFS-1-dependent UPR^{mt} genes further induced in *zip-3(gk3164)* worms during *spg-7*(RNAi)

sod-3, alh-5, abf-2, cps-6, ftn-1 and *fat-5* transcripts as determined by qRT-PCR in wildtype or *zip-3(gk3164)* worms on *spg-7*(RNAi) (n = 3, ±s.d.); **P* < 0.05 (Student's *t*-test).

Table 1. UPR^{mt} genes induced in *zip-3* deletion strains exposed to *spg-7*(RNAi)

Gene name	Description
AMPK pathway	
aakg-4	AMPK gamma subunit
Glycolysis and glucose metabolism	
T26H5.8	galactoside 2-alpha-L-fucosyltransferase
Oxidative phosphorylation	
nnt-1	nicotinamide nucleotide transhydrogenase
Innate Immunity	
abf-2	antimicrobial peptide
spp-2	antimicrobial peptide
dod-22	Involved in innate immune response
Xenobiotic detoxification	
cyp-13A2	cytochrome P450
cyp-13A3	cytochrome P450
cyp-33C1	cytochrome P450
cyp-33C2	cytochrome P450
cyp-34A5	cytochrome P450
cyp-34A7	cytochrome P450
cyp-34A9	cytochrome P450
gst-12	glutathione S-transferase
gst-33	glutathione S-transferase
alh-5	aldehyde dehydrogenase
dlhd-1	dienelactone hydrolase
C52A10.2	carboxylic ester hydrolase
Antioxidant	
sod-3	superoxide dismutase, mitochondrial
Cell structure	
chil-18	chitinase-like
cutl-10	cuticlin-like

(Table 1 Continued)

Lipid and cholesterol metabolism	
faah-5	fatty acid amide hydrolase
fat-5	delta(9)-fatty-acid desaturase
oac-14	o-acyltransferase
C06E4.3	hydroxysteroid dehydrogenase
C06E4.6	hydroxysteroid dehydrogenase
F12E12.12	hydroxysteroid dehydrogenase
stdh-2	putative steroid dehydrogenase
lips-10	lipase related
Transporters	
ifta-1	intraflagellar transport associated
ZC196.2	VAPA and VAPB ortholog
B0281.6	potassium channel tetramerization domain
Iron metabolism	
ftn-1	ferritin; intracellular iron storage
Proteolysis	
fbxa-117	F-box protein
fbxa-118	F-box protein
fbxa-165	F-box protein
Transcription factors	
nhr-30	nuclear hormone receptor
nhr-142	nuclear hormone receptor
nhr-265	nuclear hormone receptor
mdl-1	bHLH transcription factor
Signaling	
cal-6	calmodulin related genes
ins-35	insulin-related peptides
dct-3	DAF-16/FOXO controlled

UPR^{mt} genes from the RNA-seq, spanning from mitochondrial chaperones to immune response genes, which is consistent with previous studies (Figure 2.4a, b) (Nargund, Pellegrino et al. 2012, Pellegrino, Nargund et al. 2014, Nargund, Fiorese et al. 2015). With *clk-1* and *isp-1* mutants, we learned that the loss of ZIP-3 further induces the UPR^{mt} activity. Thus, we checked the genes that are further induced in zip-3 deletion worms during *spg-7*(RNAi) treatment compared to wildtype strain. We identified 375 genes that are further induced in *zip-3* deletion worms, and 112 of them are UPR^{mt} genes (Figure 2.4b, Table 1, Table A.1). For example, ZIP-3 represses UPR^{mt}-induced antioxidant, xenobiotic and innate immune genes, including the superoxide dismutase *sod-3*, aldehyde dehydrogenase *alh-5*, and the antimicrobial peptide *abf-2* (Figure 2.5a, b, c) (Scandalios 1993, Kato, Aizawa et al. 2002, Rodriguez-Torres and Allan 2016). ZIP-3 also represses metabolism genes including ferritin *ftn-1*, fatty-acid desaturase fat-5, and apoptosis gene endonuclease G *cps-6* (Figure 2.5d, e, f) (Watts and Browse 2000, Parrish, Li et al. 2001, Arosio, Ingrassia et al. 2009). The RNA-seq analysis results showed that the presence of ZIP-3 impairs the UPR^{mt} activity during *spg-7*(RNAi) treatment, and the regulation of ZIP-3 on UPR^{mt} goes beyond *clk-1* and *isp-1*-induced mitochondrial stress.

2.2.3 *zip-3* deletion strain phenocopies *atfs-1* gain-of-function strain during mitochondrial stress

Next, we examined the phenotype of *zip-3* deletion worms exposed to other mitochondrial stress inducers. Antimycin A is a secondary metabolite produced

by bacteria *Streptomyces* (Neft and Farley 1972), which disrupts oxidative phosphorylation by inhibiting the Q-cycle of cytochrome *c* reductase in complex III (Alexandre and Lehninger 1984, Xia, Yu et al. 1997). Treatment with antimycin A activates the UPR^{mt} level in worms (Liu, Samuel et al. 2014), and not surprisingly, *atfs-1* deletion strain developed slower when exposed to a modest level of antimycin A. However, interestingly, *zip-3* deletion worms arrest at earlier developmental stage with a lower concentration of antimycin A (Figure 2.6).

RNA-seq experiment suggests that ZIP-3 have functions independent of UPR^{mt} regulation (Figure. 2.4b), which is further discussed in Chapter 4.3, and could possibly account for the sensitivity of *zip-3* deletion strains to the drug. However, it is possible that the over activation of ATFS-1 in the *zip-3* deletion strain caused the abnormal behavior of worms on antimycin A, consistent with the hypothesis that ZIP-3 negatively regulates the UPR^{mt}. ATFS-1^{et15} harbors an impaired MTS, which causes nuclear accumulation of ATFS-1 and constitutive activation of the UPR^{mt} independent of mitochondrial stress (Rauthan, Ranji et al. 2013)(Figure. 2.7a). We examined the development of *atfs-1(et15)* on antimycin A. Interestingly, *atfs-1(et15)* worms are also sensitive to antimycin A and showed similar sensitivity to drug treatment with *zip-3* deletion strain (Figure. 2.7b), supporting the hypothesis that ZIP-3 negatively regulates the UPR^{mt}.

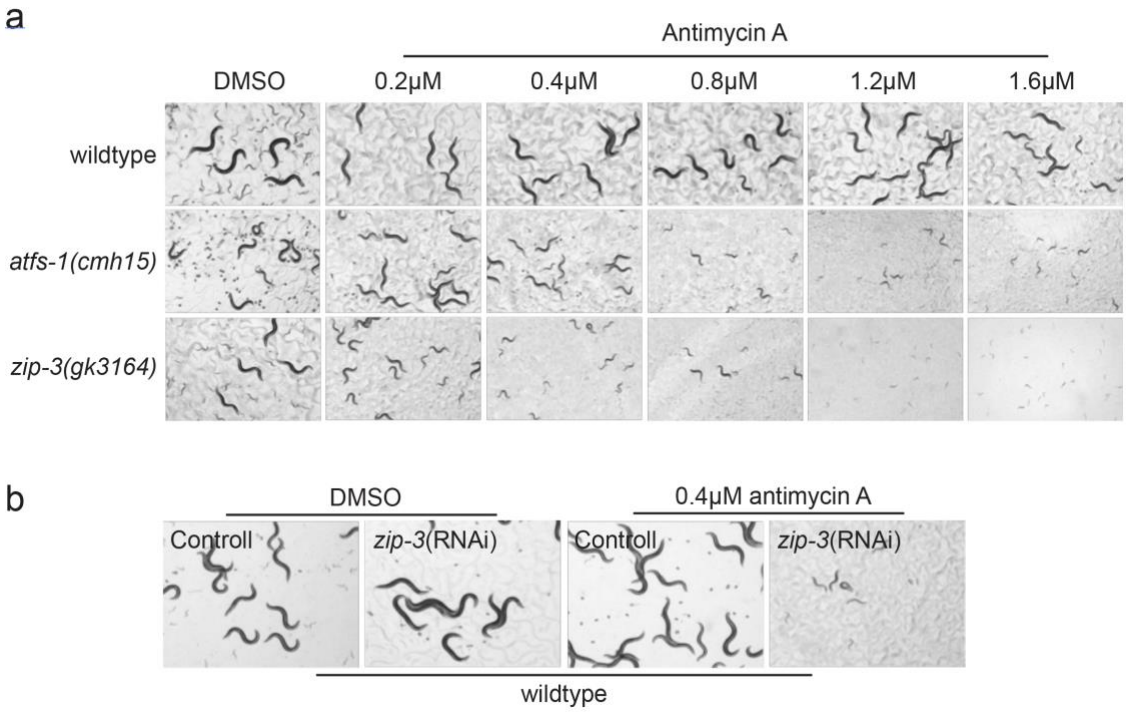

Figure 2.6 *zip-3* deletion strain is sensitive to mitochondrial toxin antimycin A

a, Development of wildtype, *atfs-1(cmh15)* and *zip-3(gk3164)* worms on DMSO or titration of antimycin A. **b,** Development of wildtype worms raised on control or *zip-3* (RNAi) exposed to DMSO or antimycin A.

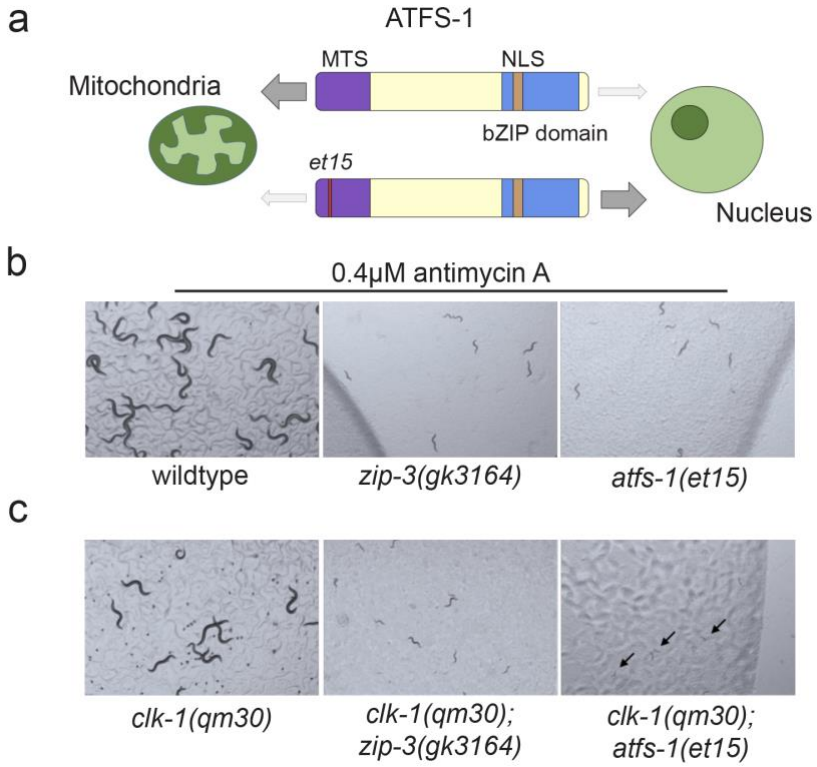

Figure 2.7 Impaired growth of *atfs-1* gain-of-function and *zip-3* deletion worms during mitochondrial stresses

a, Schematic of wildtype ATFS-1 and ATFS-1^{et15}. **b,** Growth of wildtype, *zip-3(gk3164)* and *atfs-1(et15)* worms raised on *E. coli* exposed to DMSO or titrated antimycin A. **c,** Growth of *clk-1(qm30)*, *clk-1(qm30);zip-3(gk3164)* and *clk-1(qm30);atfs-1(et15)* worms raised on *E. coli.*

It was long suggested that ATFS-1 and the UPR^{mt} are protective during chronic mitochondrial stress such as *clk-1* mutation. However, after introducing ATFS-1^{et15} into *clk-1(qm30)* background, we observed that *clk-1(qm30);atfs-1(et15)* barely develops on *E. coli*, which is similar to *clk-1(qm30);zip-3(gk3164)* mutant (Figure. 2.7c). With previous results showing that ZIP-3 is regulated by ATFS-1, we inferred that the UPR^{mt} involves ZIP-3 as an intrinsic repressor to dynamically regulate its own activity. In addition, these data further support a protective role for the UPR^{mt} during mitochondrial dysfunction both in development and longevity. However, if UPR^{mt} activation is not regulated or limited by *zip-3*, excessive UPR^{mt} activation enhances longevity at the expense of development.

2.3 ZIP-3 is degraded by the ubiquitin-proteasome system

To better understand the mechanism by which ZIP-3 is regulated and impacts ATFS-1 function, we tried to quantify ZIP-3 protein expression via immunoblot. However, though the ZIP-3 specific antibody binds to recombinant ZIP-3 protein expressed in *E. coli* strain BL21, we couldn't recover native ZIP-3 protein in worms (data not shown). To investigate if this is due to the rapid turnover of ZIP-3 protein, we generated transgenic strains in which GFP or a ZIP-3::GFP fusion protein were expressed via the *zip-3* promoter. In the *zip-3$_{pr}$::gfp* strain, GFP was expressed at high levels, indicating that the *zip-3* promoter was active (Figure. 2.8a). However, the ZIP-3::GFP fusion protein under the same promoter was difficult to detect (Figure. 2.8a), suggesting the ZIP-3 protein is

degraded rapidly.

Consistent with previous findings that the transcription of *zip-3* is induced during mitochondrial stress, *spg-7*(RNAi), *clk-1* mutation, antimycin A treatment and mitochondrial OXPHOS machinery toxin paraquat induce the expression of *zip-3* and accumulate ZIP-3 protein in nucleus (Figure. 2.8b). In addition, ATFS-1 is required for nuclear ZIP-3 accumulation during mitochondrial dysfunction (Figure. 2.8b), supporting that ATFS-1 induces *zip-3* transcription.

Impressively, inhibition of a core proteasomal subunit via *pbs-1*(RNAi) caused ZIP-3::GFP accumulation within intestinal nuclei (Figure. 2.9a), indicating that ZIP-3 is regulated by protein stability.

Proteins are typically targeted for proteasomal degradation by the ubiquitin system. E3 ubiquitin ligases specifically ubiquitinate substrate proteins by recognizing domains on substrates. Later, the ubiquitinated proteins are recruited and degraded by proteasome (Pickart 2001). Thus, we hypothesized that ZIP-3 is a target of a ubiquitin ligase. Within ZIP-3 we identified a -PPxY- motif (Figure. 2.1c), a conserved motif that is recognized by the WW-domain E3 ubiquitin ligases (Harvey and Kumar 1999, Bruce, Kanelis et al. 2008, Rotin and Kumar 2009).

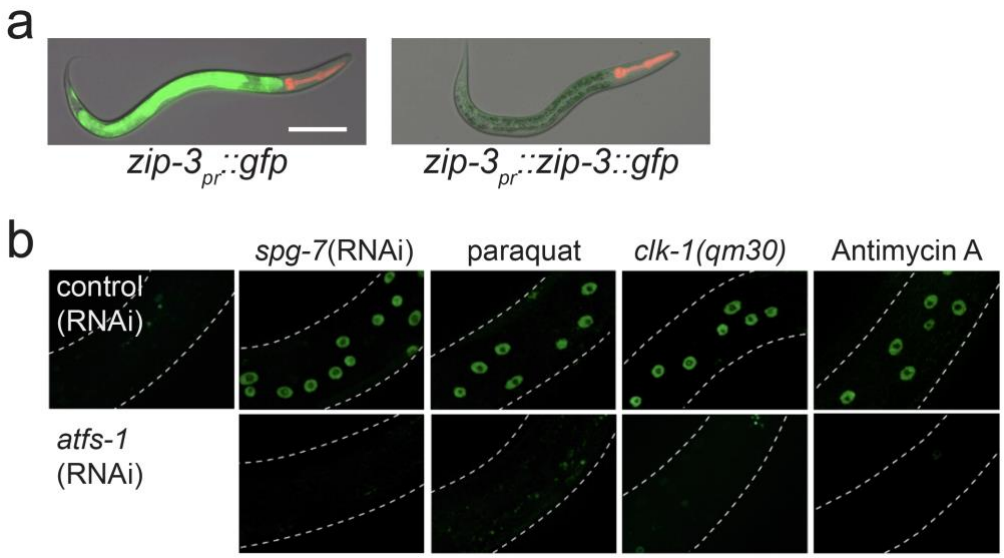

Figure 2.8 *zip-3$_{pr}$::gfp* has higher GFP expression level compared to *zip-3$_{pr}$::zip-3::gfp* worm

a, Representative photomicrographs of *zip-3$_{pr}$::gfp* and *zip-3$_{pr}$:zip-3::gfp* worms raised on *E. coli*. Images are overlays of DIC and GFP. Scale bar, 0.1 mm. **b,** Representative photomicrographs of *zip-3$_{pr}$:zip-3::gfp* exposed to *spg-7*(RNAi), 0.3mM paraquat or 1.2μM antimycin A, or in the *clk-1(qm30)* background, raised on control or *atfs-1*(RNAi). Dashed lines outline the worm body.

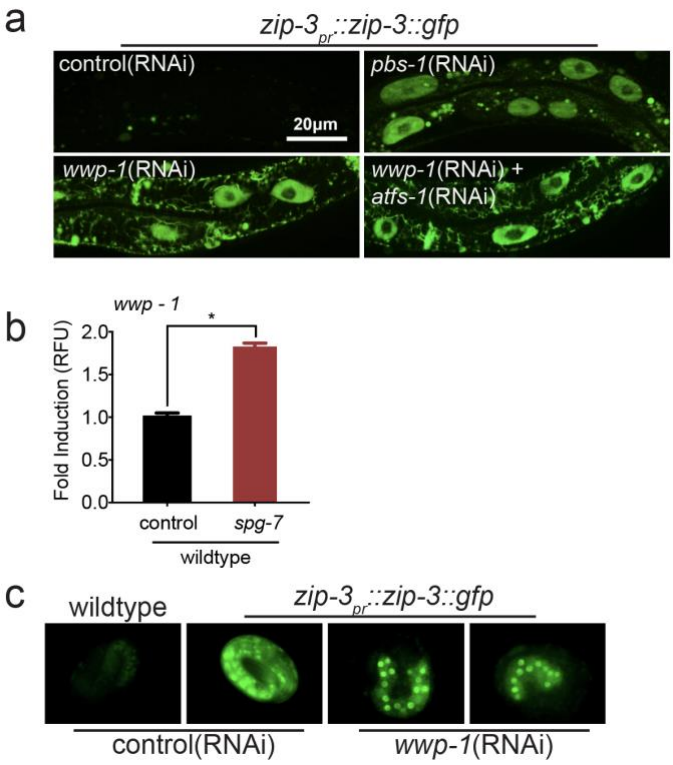

Figure 2.9 ZIP-3 is degraded in a manner dependent on the ubiquitin ligase WWP-1 and proteasome

a, Representative photomicrographs of *zip-3*$_{pr}$*:zip-3::gfp* worms raised on control, *pbs-1*(RNAi), *wwp-1*(RNAi), or *wwp-1+atfs-1* double RNAi. Scale bar, 0.02 mm. **b,** qRT-PCR showing the transcription induction of the *wwp-1* mRNA during *spg-7*(RNAi). **c,** Representative photomicrographs of wildtype and *zip-3*$_{pr}$*:zip-3::gfp* worms raised on control or *wwp-1*(RNAi).

A single WW-domain ubiquitin ligase, WWP-1, was transcriptionally induced during mitochondrial stress (Carrano, Dillin et al. 2014)(Figure 2.9b). Strikingly, *wwp-1*(RNAi) increased nuclear-localized ZIP-3::GFP in both adult worms and embryos (Figure. 2.9a, c), suggesting that ZIP-3 is ubiquitinated by WWP-1. Of note, ZIP-3::GFP accumulation caused by *wwp-1*(RNAi) is not entirely *atfs-1*-dependent (Figure. 2.9a), consistent with the previous result that the basal transcription of ZIP-3 is ATFS-1 independent (Figure. 2.1a), indicating that additional mechanisms also regulate expression of ZIP-3.

Next, to support the above findings, we created a strain expressing GFP::ZIP-3 from the native locus utilizing CRISPR-Cas9 tool. In the CRISPR-Cas9 engineered *gfp::zip-3* strain, knock-down of the ubiquitin ligase WWP-1 and proteasome component PBS-1 increased nuclear accumulation of GFP::ZIP-3 (Figure. 2.10a), which is consistent with the previous data.

To assess if the PY motif is essential for WWP-1-mediated ZIP-3 degradation, we generated two mutants that to potentially impair the putative WWP-1 binding site within ZIP-3, The tyrosine residue (Y) in the -PPxY- motif was altered to either alanine (A) or phenylalanine (F) (Figure. 2.10b). And, similar to *wwp*-1(RNAi), both mutants accumulated in intestinal nuclei (Figure. 2.10a), indicating that the -PPxY- motif promotes proteasomal degradation of ZIP-3::GFP. Taken together, these data indicate that *zip-3* can be transcriptionally induced by ATFS-1 and that ZIP-3 is recognized and ubiquitinated by WWP-1,

and degraded by proteasomes.

2.4 ZIP-3 represses the UPR^{mt}

To test if ZIP-3 is the repressor of the UPR^{mt}, we examined the UPR^{mt} activity in worms with stabilized ZIP-3 protein. We generated transgenic strains in which stabilized ZIP-3 mutant protein, ZIP-3^{PPxA} protein, was expressed via the *zip-3* promoter. In contrast with CRISPR-Cas9 engineered strain, multi-copies of *zip-3$_{pr}$::zip-3^{PPxA}* are randomly integrated into a single locus of worm genome and are stably inherited. The transgenic *zip-3$_{pr}$::zip-3^{PPxA}* rescued the growth defect of *zip-3* deletion worms on antimycin A, suggesting that the ZIP-3^{PPxA} protein is expressed from the exogenous locus and the mutated protein is functional (Figure. 2.11a).

With the multi-copy integration, we expected higher expression level of stabilized ZIP-3 mutant protein compared to CRISPR-Cas9 engineered ZIP-3^{PPxA} from native locus. We utilized the transgenic expression ZIP-3^{PPxA} to assess if the stabilized ZIP-3 decreases the UPR^{mt} activity via repressing the UPR^{mt}.

First, we examined the impact of ZIP-3 on UPR^{mt} activation in ATFS-1^{et15} mutant. In *atfs-1(et15)* mutant, due to the point mutation in the mitochondrial targeting

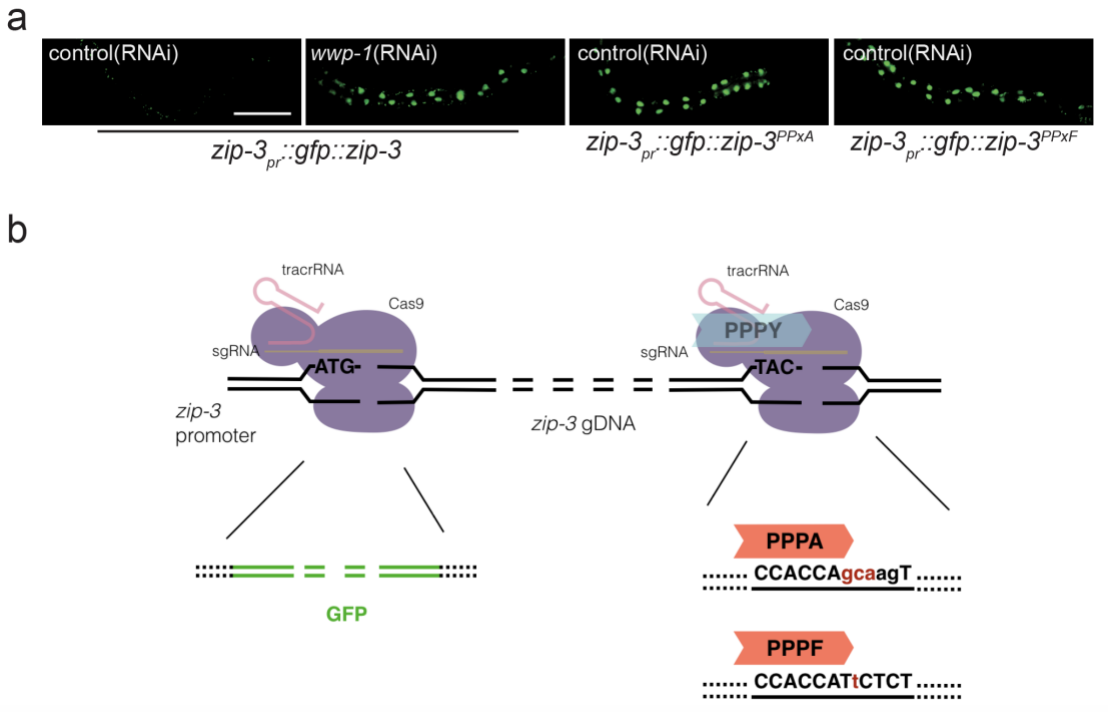

Figure 2.10 GFP::ZIP-3 is degraded in a manner dependent on the ubiquitin ligase WWP-1 and the -PPxY- motif within ZIP-3

a, *zip-3*$_{pr}$*::gfp::zip-3*, *zip-3*$_{pr}$*::gfp::zip-3*^{PPxA} and *zip-3*$_{pr}$*::gfp::zip-3*^{PPxF} worms raised on control or *wwp-1*(RNAi). Scale bar, 0.1mm. **b,** Schematics of CRISPR-Cas9 engineered GFP::ZIP-3 and GFP::ZIP-3 mutants.

sequence of ATFS-1^{et15} protein, the UPR^{mt} is constitutively active independent of mitochondrial stress in *atfs-1(et15)* strain. Thus, we can decouple the mitochondrial stress and UPR^{mt} activity in *atfs-1(et15)* worms. Impressively, ZIP-3^{PPxA} reduced UPR^{mt} activity in *atfs-1(et15)* worms (Figure. 2.11b). The reduction is blocked by *zip-3*(RNAi), indicating that the repression is ZIP-3 dependent. Also, the results indicated that ZIP-3 inhibits the activated form of ATFS-1, rather than perturbing mitochondrial function, consistent with ZIP-3 being localized in the nucleus.

In contrast with *zip-3* loss-of-function strain, ZIP-3 stabilization caused by either *wwp-1*(RNAi) or ZIP-3^{PPxA} was sufficient to repress *clk-1(qm30)*-induced UPR^{mt} activation (Figure. 2.11c), suggesting that ZIP-3 stabilization impairs the UPR^{mt} in worms with mitochondrial stress.

Due to the lack of the UPR^{mt}, *atfs-1* deletion worms are sensitive to many mitochondrial toxins. Paraquat is a redox-active organic compound that inhibits the mitochondrial OXPHOS machinery and leads to oxidative stress (Cocheme and Murphy 2008). *atfs-1* deletion worms exposed to paraquat showed severe growth delay, while the *zip-3* deletion strain is not sensitive to paraquat. The phenotype suggested that, in contrast to antimycin A, worms treated with paraquat may be more sensitive to insufficient UPR^{mt} activity. Not surprisingly, *zip-3*$_{pr}$::*zip-3*^{PPxA} strain showed similar growth delay as *atfs-1* deletion worm

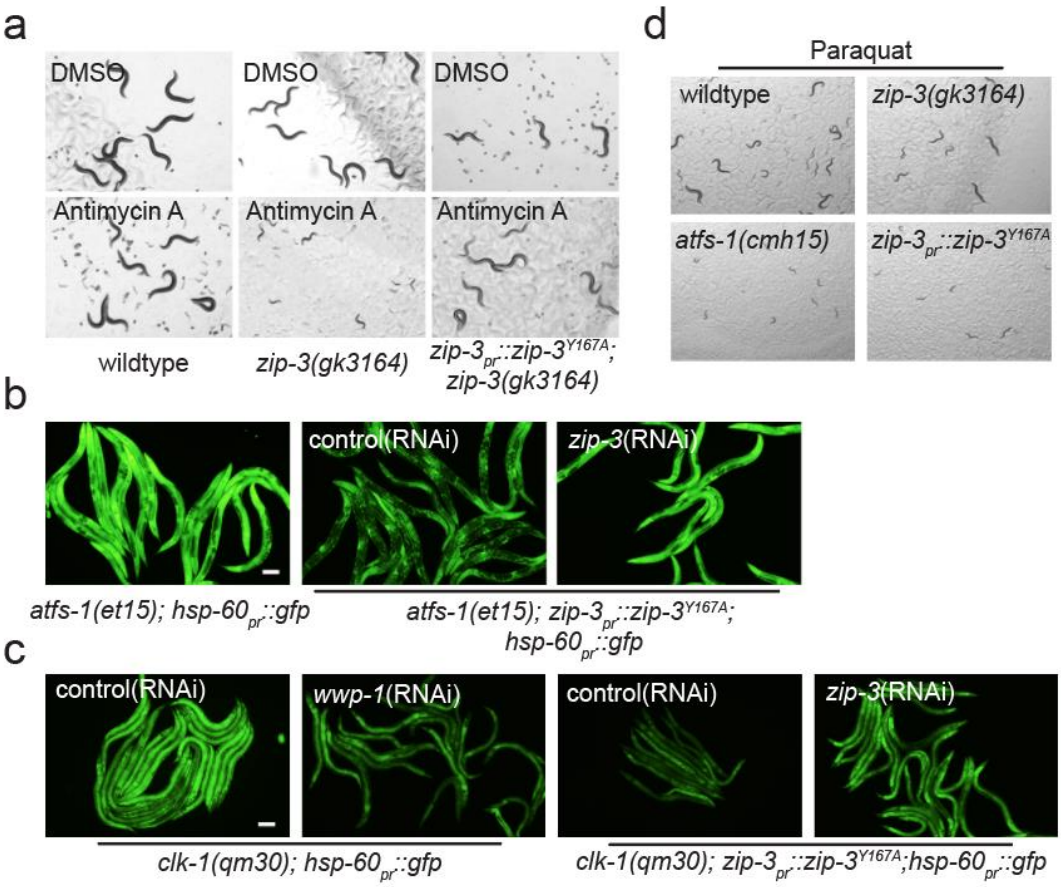

Figure 2.11 Functionally stabilized ZIP-3 represses the UPR^{mt}

a, Growth of wildtype, *zip-3(gk3164)* and *zip-3^{PPxA};zip-3(gk3164)* exposed to DMSO or antimycin A. **b,** *atfs-1(et15);hsp-60$_{pr}$::gfp* or *atfs-1(et15);zip-3^{PPxA};hsp-60$_{pr}$::gfp* on control or *zip-3*(RNAi). Scale bar, 0.1 mm. **c,** *clk-1(qm30);hsp-60$_{pr}$::gfp* worms on control or *wwp-1*(RNAi) and *clk-1(qm30);zip-3^{PPxA};hsp-60$_{pr}$::gfp* on control or *zip-3*(RNAi). Scale bar, 0.1 mm. **d,** Growth of wildtype, *zip-3(gk3164)*, *atfs-1(cmh15)* and *zip-3^{PPxA}* exposed to paraquat.

(Figure 2.11d), which is consistent with the hypothesis that ZIP-3 represses the UPR^{mt} activity.

With the results from experiments with *zip-3* deletion worms and *zip-3* stabilized worms, we conclude that the ZIP-3 protein functions as a negative regulator of ATFS-1 and the UPR^{mt}. As the ZIP-3 protein is partially regulated by ATFS-1, we believe that ATFS-1 and ZIP-3 form a negative feedback loop which allows dynamic regulation and rapid adaptation of UPR^{mt} activity, in response to mitochondrial stress while limiting the detrimental effect of UPR^{mt} over activation.

Chapter 3 *P. aeruginosa* exploits ZIP-3 to repress the UPR^{mt} during infection

3.1 *Pseudomonas aeruginosa:* A pathogen that targets mitochondrial functions

Pathogen infection is a common cause of mitochondrial dysfunction (Jendrossek, Grassme et al. 2001, Willhite and Blanke 2004, Ma, Wickham et al. 2006, Shin, Shin et al. 2008, Stavru, Bouillaud et al. 2011). *Pseudomonas aeruginosa* is a human opportunistic pathogen that infects immunocompromised and cystic fibrosis patients (Wood 1976, Evans, Turner et al. 1996, Emerson, Rosenfeld et al. 2002), and occasionally colonizes in healthy people (Morrison and Wenzel 1984). *P. aeruginosa* produces virulence factors that target mitochondrial and cellular activities, which then result in cell death and cytochrome *c*-mediated apoptosis, and can finally cause pulmonary damage and the mortality of the patients (Jendrossek, Grassme et al. 2001, Lau, Hassett et al. 2004, Ryall, Davies et al. 2008, Manago, Becker et al. 2015).

The production of most virulence factors in *P. aeruginosa* is mediated by GacS/GacA two-components signal transduction system (de Souza, Mazzola et al. 2003, Brencic, McFarland et al. 2009). Membrane-bound sensor kinase

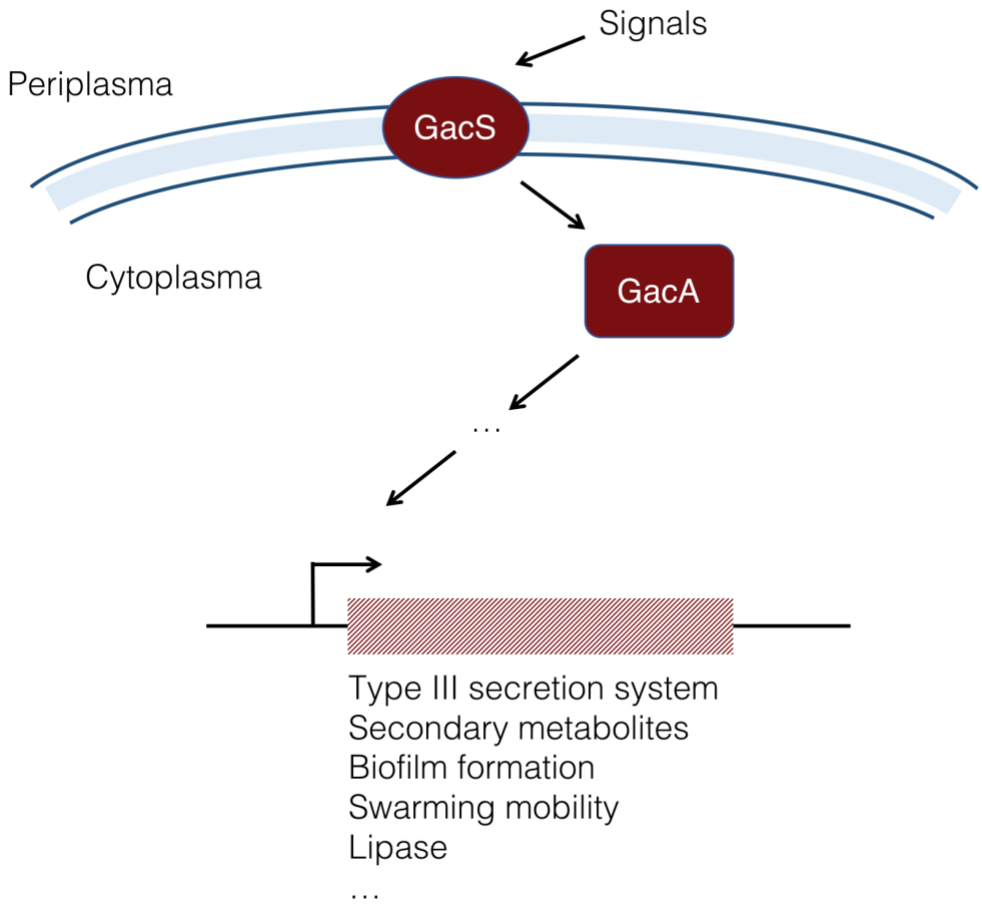

Figure 3.1 GacS/GacA two-component virulence system in *P. aeruginosa*

Environmental stimuli activate the signaling cascade led by GacS/GacA two component system, and result in the production of secondary metabolites and virulence factors.

GacS recognizes inconclusive environmental stimuli, and then activates cytoplasmic response regulator GacA. GacA in turn triggers the production of secondary metabolites and virulence factors via regulatory cascade (Figure 3.1) (de Souza, Mazzola et al. 2003). *Pseudomonas-ΔgacA* strain, the *P. aeruginosa* mutant without functional GacA, exhibits less virulence and toxicity in worms and mice (Heeb and Haas 2001, Liberati, Urbach et al. 2006).

Virulence of *P. aeruginosa* is multifactorial. *P. aeruginosa* produces secondary metabolites, which are partially GasS/GacA-dependent (Reimmann, Beyeler et al. 1997), to promote its infection to hosts. Several secondary metabolites are mitochondrial toxins, including: cyanide, an inhibitor of cytochrome c oxidase, an enzyme in complex IV of the respiratory chain and causes the rapid death of nematodes (Gallagher and Manoil 2001); pyoverdine, which removes ferric iron from hosts and thus compromises electron transfer and ATP production (Kang, Kirienko et al. 2018); and redox-active compounds phenazines, which increase reactive oxygen species generation and perturb the oxidative phosphorylation (Pierson and Pierson 2010, Ray, Rentas et al. 2015).

3.2 Protective role of the UPR^{mt} during *P. aeruginosa* infection

Consistent with the conclusion that *P. aeruginosa* produces of mitochondrial toxins and virulence factors during infection, *C. elegans* exposed to UCBPP-PA14, a clinical isolate of *P. aeruginosa* (Mahajan-Miklos, Tan et al. 1999),

showed decreased mitochondrial membrane potential and reduced oxygen consumption rate, while GacA is required for the toxicity (Figure 3.2).

Mitochondrial dysfunction caused by *P. aeruginosa* leads to the activation of the UPR^{mt}. (Liu, Samuel et al. 2014, Pellegrino, Nargund et al. 2014). The UPR^{mt} in turn alleviates the mitochondrial stress induced by pathogen infection and invokes innate immune response to detect and eliminate pathogens. Studies showed that, pre-activation of the UPR^{mt} via *spg-7* knock-down prolonged the survival and promoted the resistance of worms exposed to *P. aeruginosa* (Pellegrino, Nargund et al. 2014), indicating a protective role of the UPR^{mt} during pathogen infection. The enhanced resistance is also observed in *atfs-1* gain-of-function mutant with constitutively activation of the UPR^{mt} independent of mitochondrial stress (Rauthan, Ranji et al. 2013). Moreover, worms treated with *atfs-1*(RNAi) were more vulnerable to *P. aeruginosa* infection (Pellegrino, Nargund et al. 2014). These results demonstrated that the UPR^{mt} is the specific mitochondrial stress response pathway that promotes the defending to *P. aeruginosa* infection in worms.

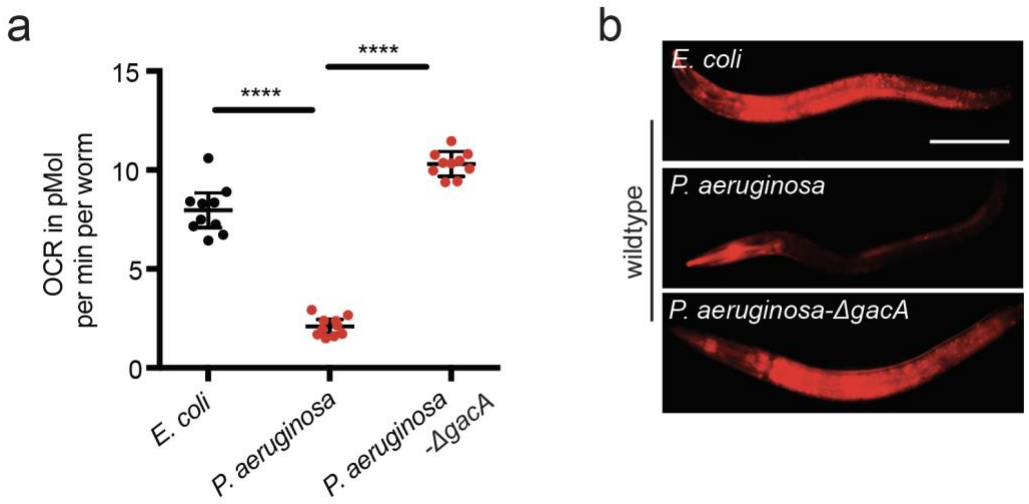

Figure 3.2 *P. aeruginosa* depolarizes mitochondria and perturbs mitochondrial function

a, Oxygen consumption rates (OCR) of wildtype worms on *E. coli*, *P. aeruginosa*, or *P. aeruginosa*-Δ***gacA***. n = 10; error bars, mean ±s.d.; **P* < 0.03 (Student's *t*-test). **b**, Images of TMRE-stained wildtype worms on *E. coli*, *P. aeruginosa*, or *P. aeruginosa*-Δ***gacA***. Scale bar, 0.1 mm.

3.3 UPR^{mt} repression during *P. aeruginosa* infection

Despite previous studies showing that the activation of the UPR^{mt} is protective for worms exposed to *P. aeruginosa*, interestingly, we observed that the UPR^{mt} was no longer activated in worms after treated with *P. aeruginosa* for 18 hours (Figure 3.3a).

As UPR^{mt} is a dynamic response, it is possible that the UPR^{mt} is turned off after exposed to *P. aeruginosa* for 18 hours. However, it is also possible that the UPR^{mt} is repressed despite the presence of mitochondrial stress. To distinguish the hypotheses, we exposed worms to both *P. aeruginosa* and mitochondrial toxin ethidium bromide. Ethidium bromide activates the UPR^{mt} via depleting the mtDNA and disrupting OXPHOS machinery assembly. While the UPR^{mt} is strongly induced in ethidium bromide-treated worms raised on *E. coli,* as indicated by *hsp-6$_{pr}$::gfp* reporter, ethidium bromide-treated worms raised on *P. aeruginosa* barely showed UPR^{mt} activity. In addition, UPR^{mt} activity is also repressed in *clk-1(qm30)* and *isp-1(qm150)* mutant worms (Figure 3.3b, c). These results demonstrated that *P. aeruginosa* infection impairs the UPR^{mt} activity. Interestingly, UPR^{mt} repression required the *P. aeruginosa* two-component regulator GacA (Figure 3.3a), which suggests that the virulence factors mediated by GacS/GacA system are responsible for the UPR^{mt} repression during *P. aeruginosa* infection.

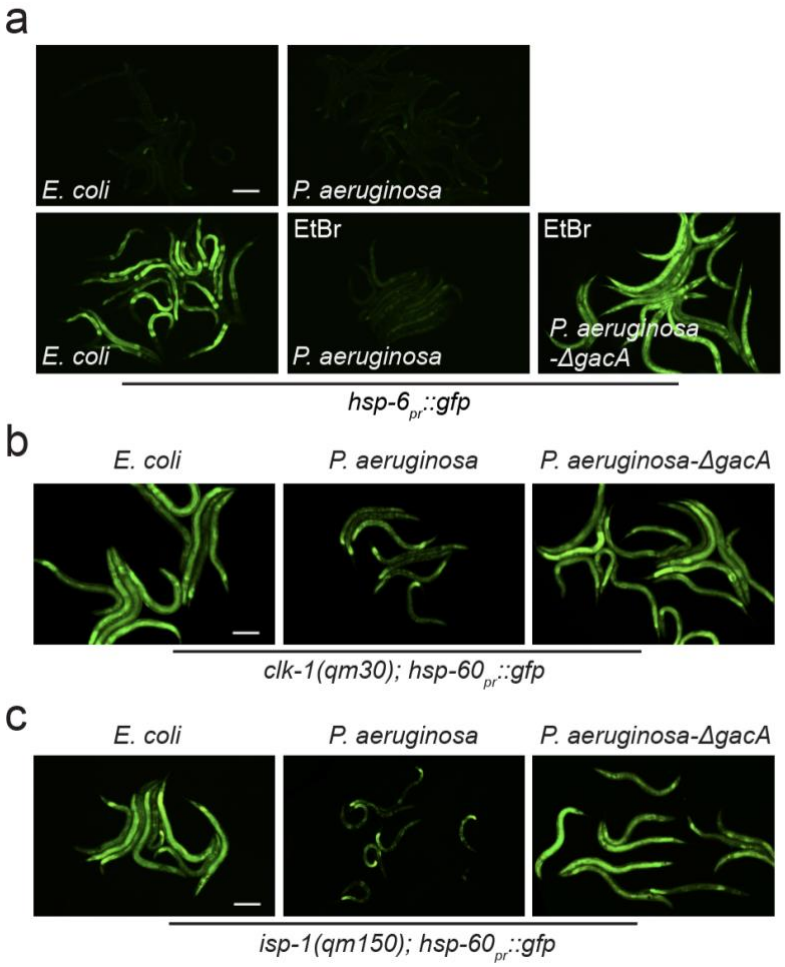

Figure 3.3 Prolonged exposure to *P. aeruginosa* represses the UPR^{mt}

a, *hsp-6$_{pr}$::gfp* worms on *E. coli*, *P. aeruginosa*, or *P. aeruginosa*-Δ*gacA* exposed to a control or 30 µg/ml ethidium bromide. Scale bar, 0.1 mm. **b**, *clk-1(qm30);hsp-60$_{pr}$::gfp* worms *on E. coli*, *P. aeruginosa*, or *P. aeruginosa*-Δ*gacA*. Scale bar, 0.1 mm. **c**, *isp-1(qm150);hsp-60$_{pr}$::gfp* worms on *E. coli*, *P. aeruginosa*, or *P. aeruginosa*-Δ*gacA*. Scale bar, 0.1 mm.

Together, these data suggest that *P. aeruginosa* evolved a mechanism to impair the UPR^{mt}.

3.4 Loss of ZIP-3 enhances *P. aeruginosa* resistance via inducing the mitochondrial UPR in *C. elegans*

To investigate whether ZIP-3 negatively regulates the UPR^{mt} during *P. aeruginosa* infection, we exposed *zip-3(gk3164);hsp-6$_{pr}$::gfp* and *hsp-6$_{pr}$::gfp* worms to *P. aeruginosa* strains with different pathogenicity (Lee, Urbach et al. 2006). While the UPR^{mt} activity in wildtype worms was repressed after 18 hours, the UPR^{mt} activity in *zip-3(gk3164)* worms remained robust when raised on different pathogenic *P. aeruginosa* strains (Figure 3.4a). Moreover, while UPR^{mt} activation in *clk-1(qm30)* worms was repressed during *P. aeruginosa* infection, *clk-1(qm30);zip-3(gk3164)* worms displayed robust activation of the UPR^{mt} during prolonged *P. aeruginosa* exposure (Figure 3.4b). Combined, these data demonstrate that ZIP-3 is required for UPR^{mt} inhibition during *P. aeruginosa* infection.

To determine if the *zip-3*-mediated UPR^{mt} induction leads to enhanced pathogen resistance in worms, we examined the phenotypes of *zip-3(gk3164)* worms. Impressively, *zip-3(gk3164)* worms survived longer during *P. aeruginosa* exposure, compared to wildtype worms (Figure 3.5a), in a manner

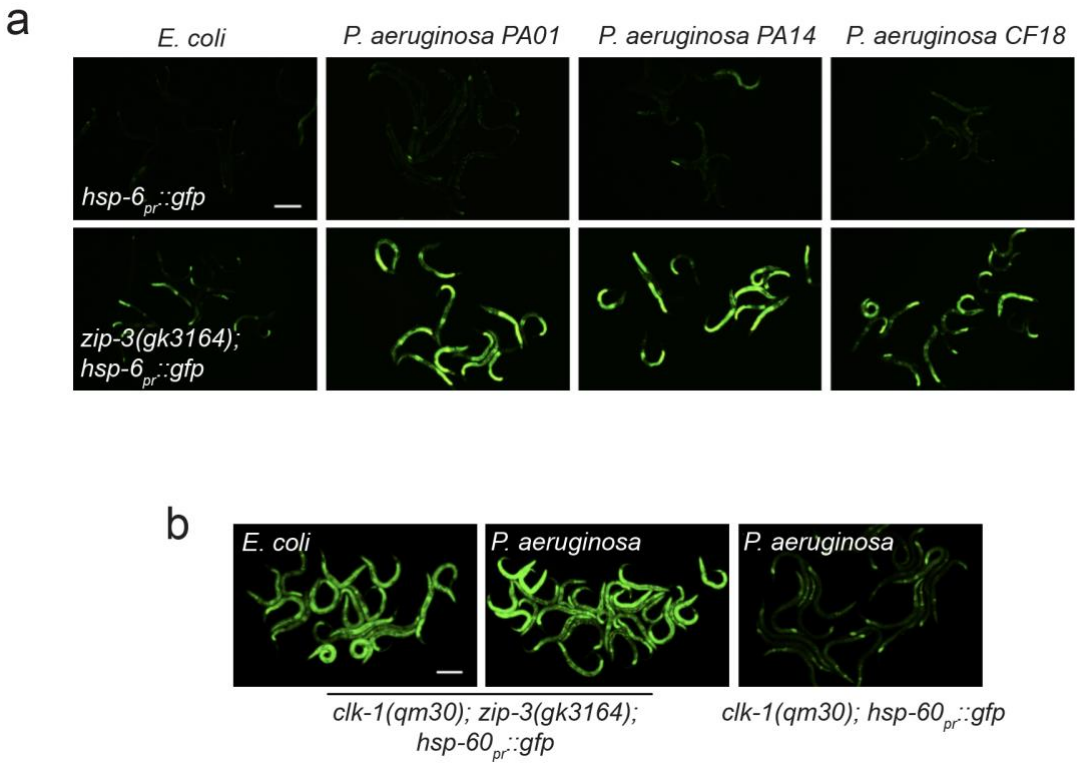

Figure 3.4 Loss of ZIP-3 induced the UPR^{mt} during *P. aeruginosa* infection

a, *hsp-6$_{pr}$::gfp* or *zip-3(gk3164);hsp-6$_{pr}$::gfp* worms on *E. coli* or pathogenic *P. aeruginosa* strains PA01, PA14 or CF18(Lee, Urbach et al. 2006). Scale bar, 0.1 mm. **b**, *clk-1(qm30);zip-3(gk3164);hsp-60$_{pr}$::gfp* and *clk-1(qm30);hsp-60$_{pr}$::gfp* worms on *E. coli* or *P. aeruginosa*. Scale bar, 0.1 mm.

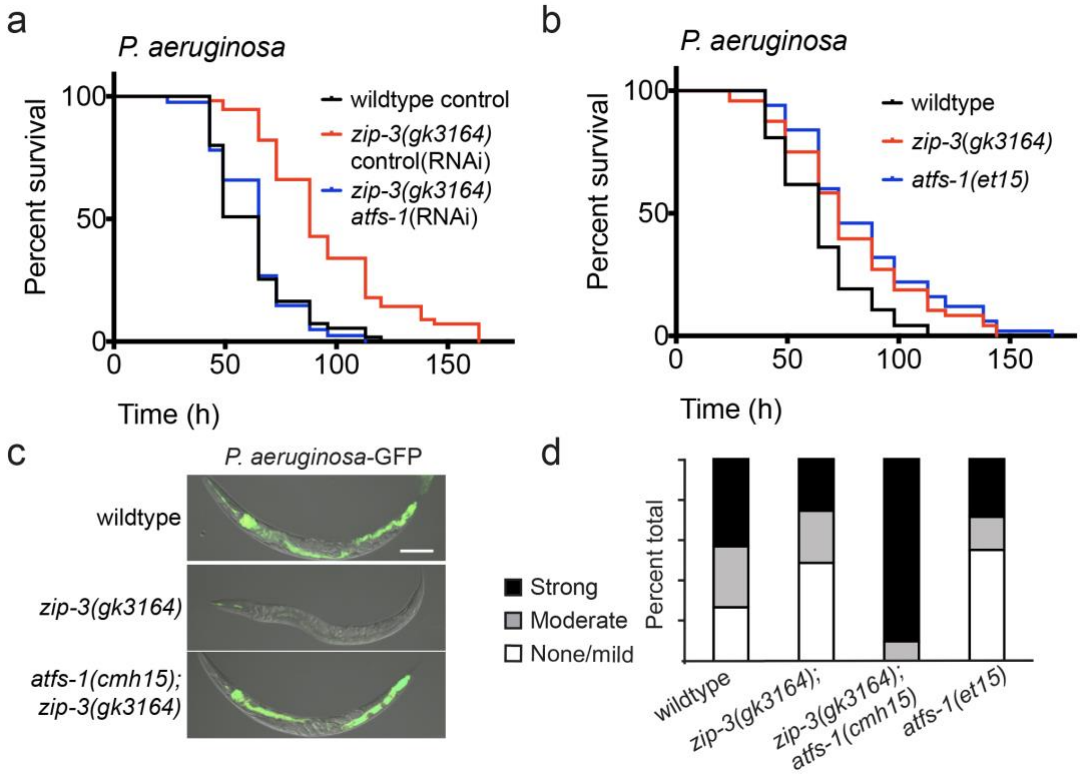

Figure 3.5 Loss of ZIP-3 promoted the resistance of *C. elegans* to *P. aeruginosa*

a, Survival of wildtype and *zip-3(gk3164)* worms on control or *atfs-1*(RNAi) exposed to *P. aeruginosa*. Statistics are in Table A.4. **b**, Survival of wildtype, *zip-3(gk3164)* and *atfs-1(et15)* worms exposed to *P. aeruginosa*. Statistics are in Table A.4. **c**, Representative photomicrographs of wildtype, *zip-3(gk3164)* and *zip-3(gk3164);atfs-1(cmh15)* worms raised on *E. coli* and exposed to *P. aeruginosa*–GFP. Images are overlays of DIC and GFP. Scale bar, 0.1 mm. **d**, Quantification of intestinal colonization in Figure 3.5c. White, grey and black bars denote no/mild infection, moderate infection and strong infection, respectively. Thirty worms were analyzed per treatment.

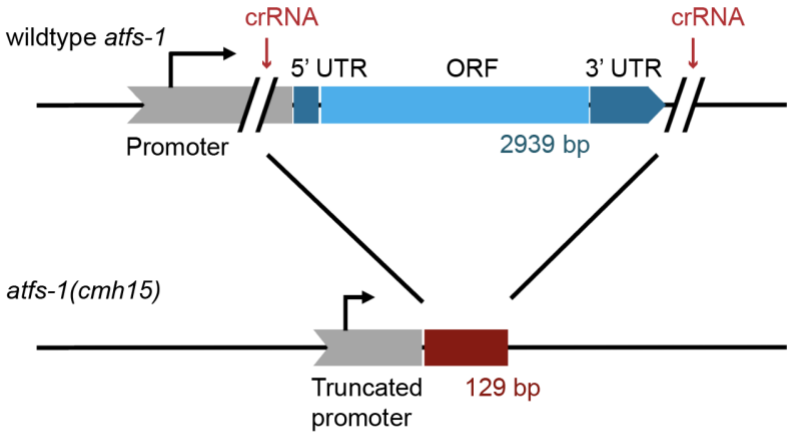

Figure 3.6 Schematic of the CRISPR-Cas9 generated *atfs-1(cmh15)* mutant

atfs-1(cmh15) allele harbors a deletion that removes the entire *atfs-1* 5'-untranslated region, 3'-untranslated region and the open reading frame. CRISPR-Cas9 engineering resulted in a 129 base pairs insertion at the *atfs-1* locus that contained no detectable open reading frames.

dependent on *atfs-1* (Figure 3.5a). Furthermore, the prolonged survival of *zip-3(gk3164)* worms on *P. aeruginosa* was comparable to the prolonged survival conferred by the constitutively active allele *atfs-1(et15)* (Figure 3.5b), which shows robust UPR^{mt} activity during *P. aeruginosa* infection (Pellegrino, Nargund et al. 2014). As with the *atfs-1(et15)* strain (Pellegrino, Nargund et al. 2014), the intestinal colonization of *P. aeruginosa* was reduced in *zip-3(gk3164)* relative to wildtype worms (Figure 3.5c). *atfs-1(cmh15)* is an *atfs-1* loss-of-function strain generated by CRISPR-Cas9 (Figure 3.6), with the entire *atfs-1* 5'-untranslated region, 3'-untranslated region and the open reading frame removed. *zip-3(gk3164);atfs-1(cmh15)* lost the resistance to pathogen intestinal colonization, demonstrating that the active UPRmt is required for the resistance in *zip-3* deletion worms (Figure 3.5c,). Combined, these data indicate that *zip-3*-deletion worms are resistant to *P. aeruginosa* in a manner dependent on UPR^{mt} activation, and further suggest that ZIP-3 negatively regulates ATFS-1.

Because the resistance of *zip-3*-deletion worms to *P. aeruginosa* required *atfs-1*, we sought to identify the *atfs-1*-dependent transcripts that are increased in *zip-3(gk3164)* relative to wildtype worms exposed to *P. aeruginosa*, as they potentially comprise genes and pathways that confer pathogen resistance. 1082 mRNAs were induced in *zip-3(gk3164)* worms relative to wildtype worms following 18 hours of *P. aeruginosa* exposure (Figure 3.7a). Of those, the induction of 143 mRNAs required *atfs-1* during mitochondrial dysfunction

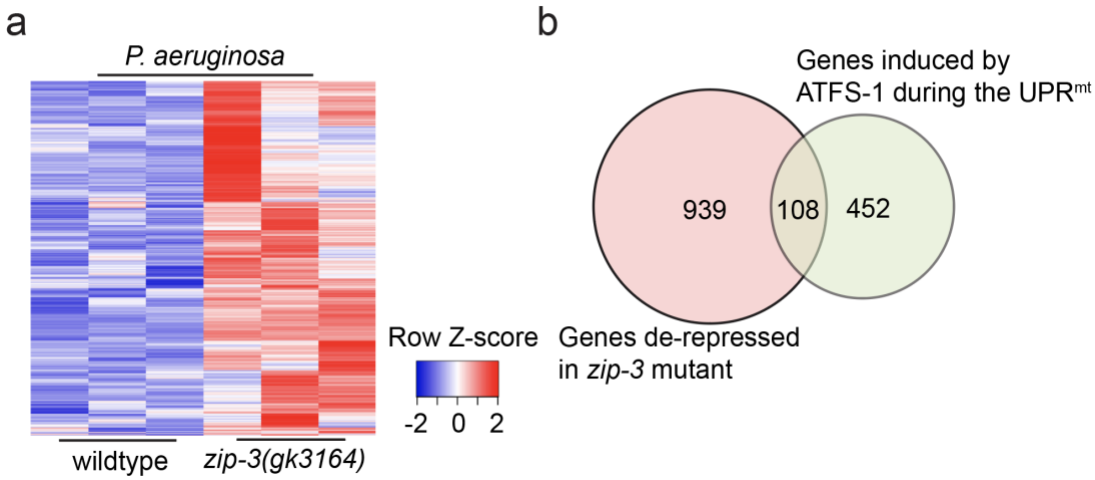

Figure 3.7 ZIP-3 represses 1082 genes during exposure to *P. aeruginosa*, a subset of which requires ATFS-1

a, Heat map of the 1082 genes induced in *zip-3(gk3164)* worms compared to wildtype worms raised on *P. aeruginosa* as determined by RNA-seq. **b**, Diagram of *atfs-1*-dependent UPR^{mt} genes induced when raised on *spg-7*(RNAi) and the mRNAs induced in *zip-3(gk3164)* worms raised on *P. aeruginosa*.

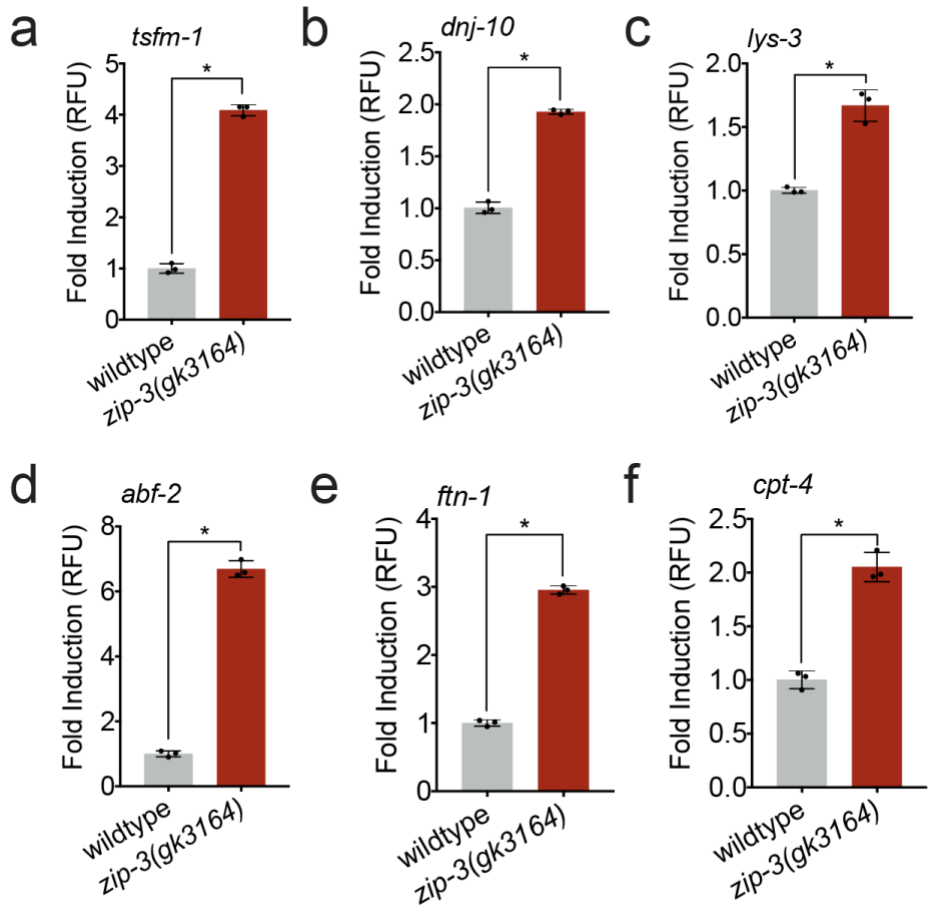

Figure 3.8 Representative transcripts induced in *zip-3(gk3164)* worms during *P. aeruginosa* infection

a-f, *tsfm-1*, *dnj-10*, *lys-3*, *abf-2*, *ftn-1* and *cpt-4* transcripts as determined by qRT-PCR in wildtype or *zip-3(gk3164)* worms on *P. aeruginosa* (n = 3, ±s.d.); **P* < 0.05 (Student's *t*-test).

Table 2. UPR^{mt} genes induced in *zip-3* deletion worms exposed to *P. aeruginosa*

Gene name	Description
Mitochondrial proteostasis	
hsp-6	mitochondrial chaperone, Hsp70 superfamily
dnj-10	mitochondrial-localized protein chaperone
Oxidative phosphorylation	
cchl-1	cytochrome C heme-lyase
C35D10.5	ubiquinol-cytochrome c reductase chaperone
B0035.15	NDUFAF4 ortholog; OXPHOS complex I assembly factor
Mitochondrial translation	
tsfm-1	mitochondrial translation elongation factor Ts (EF-Ts)
gfm-1	mitochondrial translation elongation factor g
Coenzyme Q synthesis	
D2023.6	coenzyme Q biosynthesis (ubiquinone)
coq-5	coenzyme Q biosynthesis (ubiquinone)
Mitochondrial	
phb-2	prohibitin, required for mitochondrial organization
haf-3	mitochondrial localized ABC transporter
cps-6	mitochondrial endonuclease G
Innate immunity	
lys-3	secreted lysozyme
irg-2	infection response gene
clec-160	C-type lectin
clec-17	CLEC3B homolog: C-type lectin
clec-56	CDCP2 homolog: C-type lectin
abf-2	antimicrobial peptide
Xenobiotic detoxification	
ugt-19	UDP-glucosyltransferase family 3

(Table 2 Continued)

ugt-2	UDP-glucosyltransferase family 3
ugt-50	UDP-glucosyltransferase family 3
ugt-62	UDP-glucuronosyltransferase
cyp-13A8	cytochrome P450
cyp-14A1	cytochrome P450
cyp-33C4	cytochrome P450
cyp-33C8	cytochrome P450
C23H4.2	unknown
Antioxidant	
Y38F2AR.12	glutathione and cytochrome P450 metabolism
gst-12	glutathione S-transferase; mitochondrial
gpx-7	glutathione peroxidase
F56C11.3	thiol oxidase acitivity
cdr-2	cadmium responsive, heavy metal detox
alh-5	aldehyde dehydrogenase
C35B1.5	Nucleoredoxin ortholog; thioredoxin ortholog
Iron metabolism	
ftn-1	ferritin; intracellular iron storage
Amino acid metabolism	
glna-1	GLS2 homolog; glutaminase
Glycolysis and glucose metabolism	
hxk-1	hexokinase; glycolysis
Lipid and Cholesterol metabolism	
Y71G12B.10	HMGCL homolog; HMG-CoA lyase
perm-5	predicted to have lipid binding activity
oac-14	o-acyltransferase
faah-2	fatty acid amide hydrolase
ckb-2	choline kinase B; phosphotidly choline biosynthesis enzyme
dsc-4	Large subunit of the microsomal triglyceride transfer protein
C50D2.9	malonyl-CoA-acyl carrier protein transacylase

(Table 2 Continued)

abhd-5.2	ABHydrolase domain containiing protein, lipid storage
C37H5.13	acyl-CoA thioesterase; peroxisomal thioesterase
acs-19	fatty acid CoA synthetase
dhs-14	short chain dehydrogenase, mitochondrial
Protein and lipid trafficking	
R186.1	Tango2 homolog; transport and golgi organization
Membrane transporters	
Y32F6B.1	SLC05A1; solute carrier, anion transport
slc-17.3	solute carrier protein
F58G6.3	SLC31A2 homolog; predicted to be a copper transporter
F58G6.7	SLC31A2 homolog; predicted to be a copper transporter
F58G6.9	SLC31A2 homolog; predicted to be a copper transporter
catp-3	cation transporting ATPase
amt-1	ammonium transporter ortholog
Transcription factors	
nhr-178	nuclear hormone receptor, PPARD family
nhr-193	nuclear hormone receptor, PPARD family
nhr-265	nuclear hormone receptor, PPARD family
Signaling	
gcy-5	guanylyl cyclase; potentially in a G protein cascade
grd-7	hedge-hog like, intercellular signaling
Proteolysis	
T05F1.11	F-box protein
fbxa-166	F-box protein
asp-8	aspartyl protease

caused by *spg-7*(RNAi) (Figure 3.7b, c, Table 2, Table A.2), consistent with ZIP-3 inhibiting activated or nuclear ATFS-1. These mRNAs include components involved in mitochondrial recovery (Figure 3.8a, b), innate immunity (Figure 3.8c, d), iron acquisition (Figure 3.8e) and fat metabolism (Figure 3.8f).

3.5 Phenazines as the UPR^{mt} inducer during pathogen infection

Next, we took advantage of the robust UPR^{mt} activation that occurred in *zip-3(gk3164)* worms exposed to *P. aeruginosa*, to identify the pathogen-produced molecule(s) that perturb mitochondrial function and activate the UPR^{mt}. Interestingly, *P. aeruginosa* unable to produce phenazines (*P. aeruginosa*-Δ***phz***) (Dietrich, Price-Whelan et al. 2006, Liberati, Urbach et al. 2006) did not activate the UPR^{mt} in worms lacking *zip-3* (Figure 3.9a). Moreover, exposure of phenazines to worms raised on non-pathogenic *E. coli* was sufficient to perturb mitochondrial function (Figure 3.9b) and activate the UPR^{mt} (Figure 3.9c). These data are consistent with phenazines being redox-active compounds that perturb OXPHOS and increase reactive oxygen species generation (Pierson and Pierson 2010, Ray, Rentas et al. 2015). Of note, *P. aeruginosa* strains unable to produce cyanide or multiple siderophores still caused UPR^{mt} activation suggesting that in this assay, the most potent mitochondrial toxins are phenazines (Figure 3.9d).

Last, we sought to gain insight into the relationship between virulence-mediated

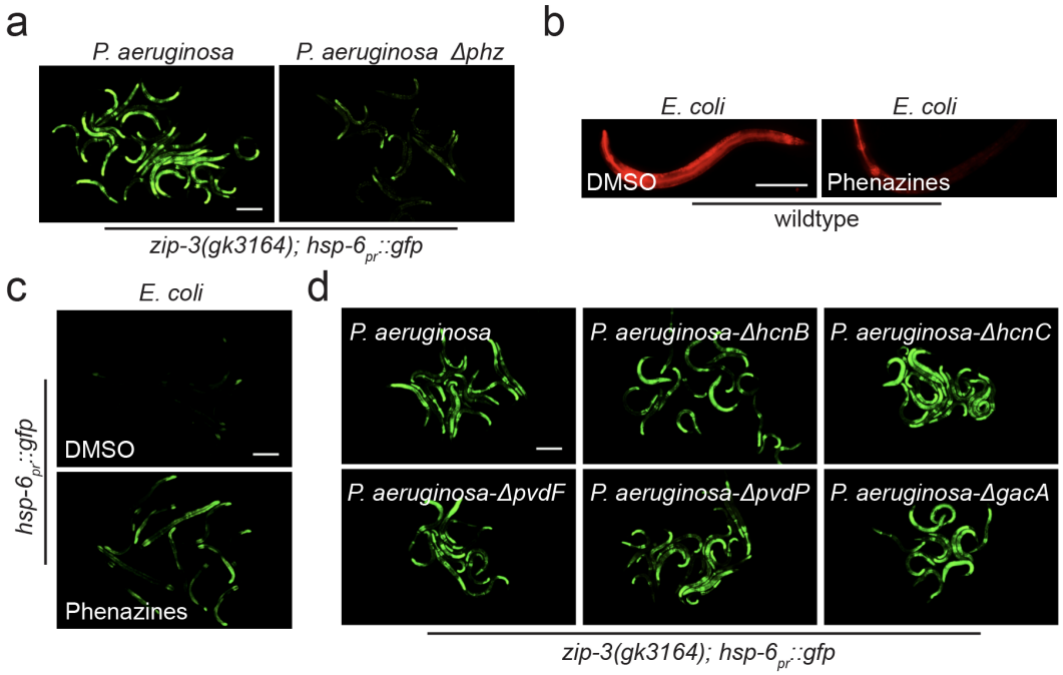

Figure 3.9 *P. aeruginosa*-secreted phenazines disturbs mitochondrial functions and is required for the activation of UPR^{mt}

a, *zip-3(gk3164);hsp-6$_{pr}$::gfp* worms on wildtype *P. aeruginosa* or *P. aeruginosa-*Δ*phz*. Scale bar, 0.1 mm. **b,** Representative images of TMRE-stained wildtype worms on *E. coli* treated with DMSO or phenazines. Scale bar, 0.1 mm. **c,** *hsp-6$_{pr}$::gfp* worms raised on *E. coli* treated with DMSO or phenazines. Scale bar, 0.1 mm.

UPR^{mt} repression (Figure 3.3) and the *P. aeruginosa*-produced phenazines that perturb mitochondrial function and activate the UPR^{mt} via the *zip-3* loss-of-function model. One possibility is that UPR^{mt} repression increases the potency of the mitochondrial-toxic phenazines via synthetic toxicity, similar to both *P. aeruginosa* and *atfs-1*(RNAi) impairing the development of worms with mitochondrial dysfunction (Baker, Nargund et al. 2012, Pellegrino, Nargund et al. 2014). However, the host survival upon exposure to *P. aeruginosa*-Δ***phz*** was similar to wildtype *P. aeruginosa*, suggesting that the associated mitochondrial dysfunction (Figure 3.2b and Figure 3.9b) did not impact survival (Figure 3.10). Alternatively, UPR^{mt} repression may prevent the activation of an anti-microbial response initiated in response phenazine-dependent mitochondrial perturbation (Figure 3.9c).

To examine these models, wildtype and *zip-3*-deletion worms were exposed to wildtype or *P. aeruginosa*-Δ***phz***. Surprisingly, *zip-3(gk3164)* worms were not resistant to *P. aeruginosa*-Δ***phz*** relative to wildtype *P. aeruginosa*. In fact, the pathogenic strain unable to produce phenazines was considerably more toxic to worms lacking *zip-3* (Figure 3.10), consistent with phenazines activating a host-protective anti-microbial response. These findings suggest that phenazine-specific mitochondrial perturbation allows the host to initiate an anti-microbial response to prolong its survival. Consistent with this model, UPR^{mt} repression is dependent on the pathogenicity of *P. aeruginosa* (Figure 3.3) and occurs

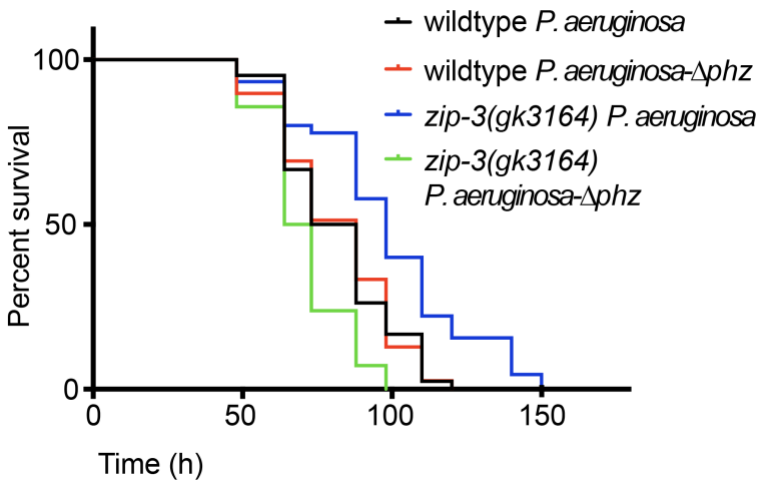

Figure 3.10 Survival of wildtype and *zip-3(gk3164)* worms exposed to wildtype *P. aeruginosa* and *P. aeruginosa*-Δ*phz*

Lack of phenazines in *P. aeruginosa*-Δ*phz* didn't affect the survival of wildtype worms. However, *zip3* deletion strain survives shorter on *P. aeruginosa*-Δ*phz* compared to wildtype *P. aeruginosa*.

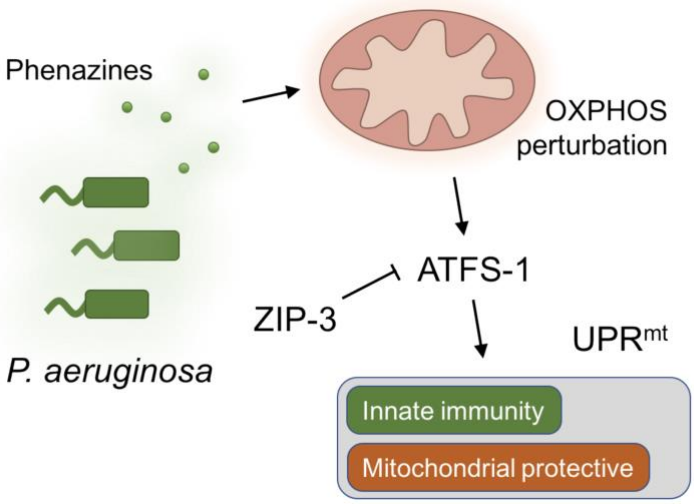

Figure 3.11 Schematics of the interaction between *P. aeruginosa*, mitochondrial perturbation and UPR^{mt} repression via ZIP-3

Phenazines produced by P. aeruginosa during the infection of the pathogen impairs the mitochondrial function of *C. elegans*. Mitochondrial stress leads to the activation of ATFS-1-depedent UPR^{mt}, which then induces the host defense response. However, the bZIP transcription factor ZIP-3 represses the host UPR^{mt} response during infection, which promotes the infection of *P. aeruginosa.*

following prolonged pathogen exposure, while the phenazines that perturb mitochondrial function and activate the UPR^{mt} are secreted independent of the virulence response, albeit at reduced levels (Figure 3.11) (Dietrich, Price-Whelan et al. 2006, Pierson and Pierson 2010, Recinos, Sekedat et al. 2012, Ray, Rentas et al. 2015).

In summary, *C. elegans* detect *P. aeruginosa* through phenazine-mediated disruption of OXPHOS and responds by initiating the UPR^{mt} via the transcription factor ATFS-1. However, once the virulence response is initiated, *P. aeruginosa* engages a host negative regulatory mechanism requiring ZIP-3 that impairs active ATFS-1 and the associated mitochondrial-protective and anti-bacterial response, limiting a pathway that impairs intestinal colonization by the pathogen and prolongs host survival.

Chapter 4 Discussion

4.1 Dynamic regulation of the UPR^{mt} via ATFS-1, ZIP-3 and WWP-1

As we have discussed in Chapter 1.3.3, mis-regulated UPR^{mt} activity impairs the normal development, differentiation and activities of cells. We also showed that *atfs-1* gain-of-function worms caused severe growth defects in worms with mitochondrial dysfunction (Figure 2.7). Thus, UPR^{mt} activity requires tight regulation.

In Chapter 2, we showed that ZIP-3, a bZIP protein transcriptionally regulated by ATFS-1, serves as a UPR^{mt} repressor via composing the negative feedback loop with ATFS-1. To match the UPR^{mt} activity to the level of mitochondrial stress in cells, we expected dynamic regulation of the UPR^{mt} repressor as well. We have identified two pieces of evidence suggesting that ZIP-3 is dynamically regulated. First, in worms exposed to various mitochondrial stressors, including paraquat, *spg-7*(RNAi), and *clk-1* mutation, ATFS-1 is required for the accumulation of nuclear ZIP-3 (Figure 2.8), suggesting that ATFS-1 is crucial for ZIP-3 regulation during mitochondrial stress. Also, the E3 ubiquitin ligase WWP-1 which acts as the negative regulator of ZIP-3, is transcriptionally induced during *spg-7*(RNAi) (Figure 2.9), indicating that the turnover rate of ZIP-3 protein is increased during mitochondrial stress. Thus, we speculate that during mitochondrial stress, the UPR^{mt} repressor ZIP-3 is induced by ATFS-1

and rapidly degraded to ensure appropriate level of UPR^{mt} activity. With the stress decreasing, continued UPR^{mt} activity will activate the UPR^{mt} repressor, and finally attenuates the UPR^{mt} (Figure 4.1). Therefore, the tight regulation of ZIP-3 by ATFS-1 and WWP-1 enables the UPR^{mt} activity level to reach a balance during mitochondrial stress and to elicit an adequate amount of response.

4.2 The mechanism of ZIP-3 mediated UPR^{mt} repression using the *P. aeruginosa* model of mitochondrial stress

Although we have identified several lines of evidence indicating that ZIP-3 functions as the negative regulator of ATFS-1 and the UPR^{mt}, mechanistically how ZIP-3 represses the UPR^{mt} remains unclear. The difficulty in understanding the mechanism arises partially due to the poor stability of ZIP-3 and ATFS-1 proteins, as it is not trivial to assess whether ATFS-1 and ZIP-3 form heterodimers *in vivo* or have any other interactions at protein level.

With *P. aeruginosa* infection experiments described in Chapter 3, we observed the co-presence of mitochondrial stress and the strong ZIP-3-mediated repression of the UPR^{mt}, which suggests that *P. aeruginosa* serves as a perfect tool to study the regulation of UPR^{mt} by ZIP-3.

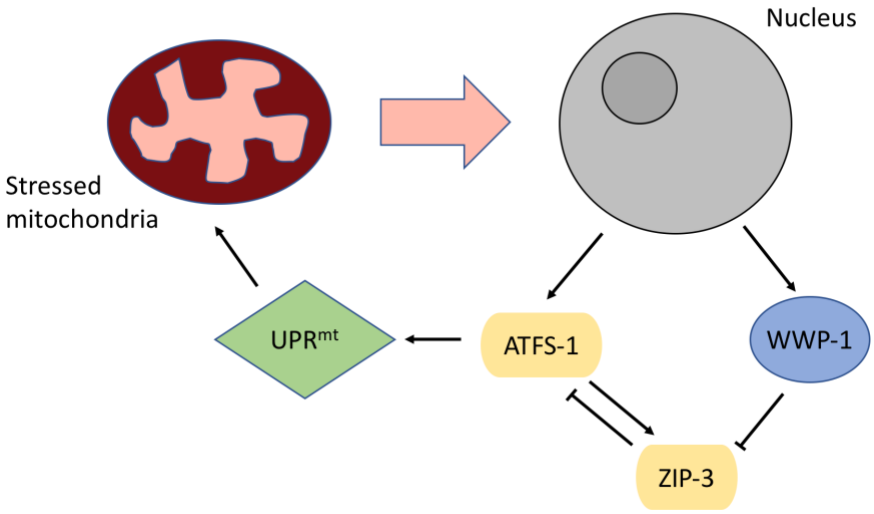

Figure 4.1 Schematics of the feedback loops between ATFS-1, UPR^{mt}, ZIP-3 and the ZIP-3 negative regulator WWP-1

Mitochondrial stress activates the UPR^{mt} mediated by ATFS-1, which promotes the recovery of mitochondria, as well as the transcription of E3 ubiquitin ligase WWP-1. ATFS-1 induces the expression of *zip-3*, which has been demonstrated to be the negative regulator of ATFS-1, and thus forms a negative feedback loop between ATFS-1 and ZIP-3. In addition, WWP-1 degrades ZIP-3 protein. Therefore, ATFS-1, ZIP-3 and WWP-1 forms the feedback regulation that fulfills the dynamic regulation of UPR^{mt} activity, to match the activity of UPR^{mt} to mitochondrial stress level in cells.

We first hypothesized that *P. aeruginosa* stabilizes ZIP-3 via repressing WWP-1 and thus, leads to the UPR^{mt} repression. However, no nuclear ZIP-3::GFP accumulation was observed during the first 18 hours of *P. aeruginosa* exposure, suggesting ZIP-3 was not stabilized during infection. It is also reasonable to infer that ZIP-3 negatively regulates ATFS-1 via turning over ZIP-3/ATFS-1 heterodimer, as the study showing that ZIP-3 and ATFS-1 proteins form heterodimer *in vitro* (Reinke, Baek et al. 2013). Knock-down of *wwp-1* stabilizes ZIP-3::GFP in worms exposed to *P. aeruginosa*, but didn't rescue the UPR^{mt} repression on *P. aeruginosa.* Thus, it is unlikely that *P. aeruginosa* represses the UPR^{mt} by ZIP-3 via WWP-1. However, as we have no evidence suggesting that WWP-1 degrades nuclear ZIP-3, or WWP-1 is the only negative regulator of ZIP-3, we cannot rule out the possibility that *P. aeruginosa* regulates ZIP-3 and the UPR^{mt} via altering the stability of ZIP-3 protein.

In previous experiments, we showed that the phosphorylation-dead mutation tyrosine (Tyr) - phenylalanine (Phe) in -PPxY- motif of ZIP-3 protein blocked the WWP-1 binding. The result implies that the phosphorylation at Tyr167 is important for the WWP-1-dependent degradation of ZIP-3. Therefore, the phosphorylation at Tyr167, or other amino acids, may also contribute to ZIP-3 mediated inhibition of ATFS-1. Thus, we next asked whether *P. aeruginosa* alters the activity of ZIP-3 via phosphorylation. With *hsp-6$_{pr}$::gfp* strain as a tool, we used genetic approaches to identify the mutants that rescued the UPR^{mt} repression and hence, could possibly be the upstream regulators of ZIP-3.

Innate immunity in worms can be achieved by several MAP Kinase cascades. MAP kinases PMK-1 and KGB-1 are activated during pathogen infection (Kim, Liberati et al. 2004, Sakaguchi, Matsumoto et al. 2004). Moreover, over-activating the kinases via knocking-down MAPK phosphatase VHP-1 (Mizuno, Hisamoto et al. 2004) represses the UPR^{mt} upon mitochondrial stress (data not published). Thus, we then investigated whether the MAP kinases could possibly regulate ZIP-3 via phosphorylation. However, we failed to activate the UPR^{mt} in worms exposed to *P. aeruginosa* with *kgb-1*, *pmk-1*, *pmk-3*, *sek-1* and *vhp-1* mutant strains, which are either MAP kinase loss-of-function or gain-of-function strains, suggesting the MAP kinases are not involved in *P. aeruginosa*-mediated UPR^{mt} repression.

Several studies have shown that *P. aeruginosa* suppresses host immune response via activating the DAF-2 insulin/IGF-I like signaling pathway in worms (Garsin, Villanueva et al. 2003, Evans, Kawli et al. 2008, Portal-Celhay, Bradley et al. 2012). Loss of *daf-2* induces the transcription of several innate immune genes, including antimicrobial peptide *abf-2* (Evans, Kawli et al. 2008). Also, *daf-2* mutants survived longer and had less intestinal colonization compared to wildtype worms when exposed to *P. aeruginosa*, which is similar to *zip-3* deletion strain (Garsin, Villanueva et al. 2003, Portal-Celhay, Bradley et al. 2012). In addition, DAF-2 is a membrane-associated receptor tyrosine kinase. As both WWP-1 (Sanarico, Ronchini et al. 2018) and ZIP-3 (Nakai and Horton

1999) are predicted to be plasma membrane-localized, we reasoned that DAF-2 phosphorylates ZIP-3 during pathogen infection. However, we were not able to activate the UPR^{mt} in *daf-2(e1370)*, *daf-2* loss-of-function worms exposed to *P. aeruginosa*, suggesting that DAF-2 is unlikely to be the positively regulator of ZIP-3. However, as the activation of DAF-2 insulin-like signaling pathway has been shown to be required for UPR^{mt} activation (Schieber and Chandel 2014), we were not able to rule out the possibility that ZIP-3 is regulated by DAF-2 pathway.

4.3 Role of ZIP-3 beyond UPR^{mt} repressor

We showed that ZIP-3 is important for balancing the UPR^{mt} activity in cells. However, ZIP-3 may also have functions beyond being a UPR^{mt} repressor. From the RNA-seq experiments, we identified many mRNAs whose expressions are altered in *zip-3(gk3164)* worms exposed to *spg*-7(RNAi) or *P. aeruginosa*, yet not affected by ATFS-1 during mitochondrial stress (Figure 2.4, 3.7), suggesting ZIP-3 also functions independent of ATFS-1. Supporting the idea, we also observed that *zip-3(gk3164);atfs-1(cmh15)* worms developed slower than either the *zip-3(gk3164)* or *atfs-1(cmh15)* mutant alone (Figure 4.2), indicating that ZIP-3 and ATFS-1 function in different pathways.

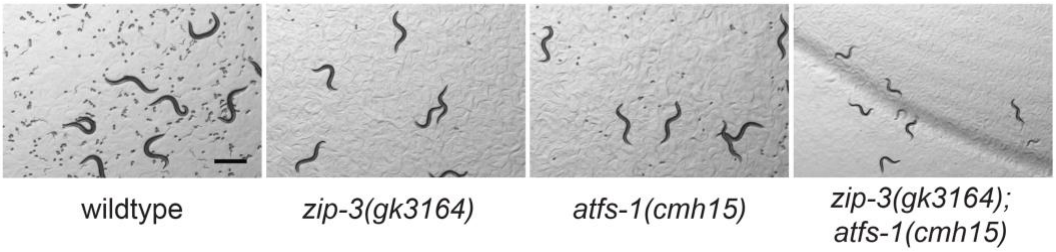

Figure 4.2 Growth of wildtype, *zip-3(gk3164)*, *atfs-1(cmh15)* and *zip-3(gk3164);atfs-1(cmh15)* strain raised on *E. coli*

zip-3 and *atfs-1(cmh15)* double deletion strain grows slower compared to *zip-3* deletion or *atfs-1* deletion worms, indicating the ATFS-1 independent role of ZIP-3 protein.

Though ATFS-1 is the only protein we know of that regulates the expression level of *zip-3* gene, the basal transcription of *zip-3* gene is ATFS-1 independent (Figure 2.1). Thus, it would be intriguing to examine the ATFS-1-independent function of ZIP-3 protein during mitochondrial stress, via expressing *zip-3* gene under an ATFS-1 independent promoter or *zip-3* promoter with ATFS-1-binding motif mutated.

In conclusion, we identified a negative feedback loop that regulates the UPR^{mt} activity in cells via the UPR^{mt} repressor ZIP-3. ZIP-3 is a bZIP transcription factor, whose transcription is partially regulated by UPR^{mt} mediator ATFS-1 and is degraded by E3 ubiquitin ligase WWP-1. Also, we showed that the negative regulator is exploited by pathogen *P. aeruginosa* during infection, to repress the UPR^{mt}-mediated defense response in worms. For the next step, we will investigate the mechanism by which ZIP-3 represses ATFS-1 and the UPR^{mt}, which will shed light on how the UPR^{mt} is regulated intrinsically, and how pathogens interact with hosts during infection.

Chapter 5 Methodology

Worm strains and plasmids. The reporter strains *hsp-6$_{pr}$::gfp* and *hsp-60$_{pr}$::gfp* for visualizing UPR^{mt} activation were previously described (Yoneda, Benedetti et al. 2004). The *hsp-6$_{pr}$::gfp* was constructed by ligating a 1.7 kb *Hind*III-*Bam*HI PCR fragment derived by amplification of *C. elegans* genomic DNA with the primers: C37H5.5.2AS (TCGAGTCCATACAAGCACTC) and C37H5.8.2AS (GGGGGGATCCGAAGACAAGAATGATCGTGC) into the GFP reporter plasmid pPD95.75 (a gift of Andy Fire, Baltimore MD, USA). *hsp-6 $_{pr}$::gfp* contains the 5′ flanking region and encodes the predicted first 10 amino acids of HSP-6 fused to GFP. The *hsp-60$_{pr}$::gfp* reporter was constructed by ligating a 2.3 kb *Sal*I-*Bam*HI PCR fragment derived by amplification of *C. elegans* genomic DNA with the primers: CeHSP10.6AS (AAGAGTCGACTCGCGGAAGATTGAGTATTCC) and CeHSP60.2AS (CTGAGGATCCTTTCTGGCGAGGGGAAGCATC) into pPD95.75. *hsp-60$_{pr}$::gfp* contains the 5′ flanking region and encodes the predicted first 7 amino acids of HSP-60 fused to GFP.

N2 (wildtype), *isp-1(qm150)*, *clk-1(qm30*), and *zip-3(gk3164)* were obtained from the *Caenorhabditis* Genetics Center. The *atfs-1(et15)* strain was a gift from Mark Pilon.

The *zip-3$_{pr}$::gfp* plasmid was constructed by PCR amplifying 2.4 kb of the *zip-3* promoter and ligating it into the plasmid pPD95.75. The *zip-3$_{pr}$::zip-3::gfp* plasmid was constructed by PCR amplifying and ligating 6.3 kb of genomic DNA including 2.4 kb of the *zip-3* promoter and the z*ip-3* open reading frame (without the stop codon) into the plasmid pPD95.75. The plasmid expressing *zip-3$_{pr}$::zip-3^{PPxA}* was constructed by mutating the corresponding tyrosine codon (-TAC-) to the alanine codon (-GCC-) via PCR. Transgenic lines were generated by injecting 12 ng/µl of the *zip-3$_{pr}$::zip-3::gfp* plasmid, the *zip-3$_{pr}$::gfp* plasmid or the *zip-3$_{pr}$::zip-3^{PPxA}* plasmid into wildtype worms along with 8 ng/µl of the co-injection marker plasmid pCFJ90 *(myo-2$_{pr}$::mCherry)*. The extrachromosomal arrays of *zip-3$_{pr}$::zip-3::gfp* and *zip-3$_{pr}$::zip-3^{PPxA}* were then integrated into the genome via gamma irradiation (Appendices 1) (Mello and Fire 1995).

The *atfs-1(cmh15)* deletion strain was generated via CRISPR-Cas9 in wildtype worms. The crRNAs (Dharmacon) were co-injected with purified Cas9 protein, tracrRNA (Dharmacon), and the *dpy-10* co-injection markers as described(Paix, Folkmann et al. 2015). Deletion of the entire *atfs-1* open reading frame by CRISPR-Cas9 resulted in the insertion of a 129 base pair sequence with little apparent homology (Fig. S5A). The crRNAs used to delete the complete open reading frame of ATFS-1 are listed in Table A.3.

The z*ip-3$_{pr}$::gfp::zip-3^{PPxA}* and *zip-3$_{pr}$::gfp::zip-3^{PPxF}* worm strains were generated by multiple rounds of CRISPR-Cas9 genome engineering as

described (Paix, Folkmann et al. 2015). First, a sequence encoding GFP was PCR amplified from the plasmid pPD95.75, purified using the QIAquick® Gel Extraction Kit, and inserted into the genome after the start codon of the *zip-3* open reading frame in frame with the remainder of the gene. Second, synthesized single-stranded oligo donors (ssODN) (IDT) were used to make point mutations to substitute PPxY motif to PPxA (Y167A) or PPxF(Y167F) in the ZIP-3 protein. In both steps, the crRNA and repair templates were co-injected with purified Cas9 protein (IDT), tracrRNA (IDT), and the *rol-6* co-injection marker as described(Paix, Folkmann et al. 2015). The tracrRNA is 74nt long (Jinek, Chylinski et al. 2012): AACAGCAUAGCAAGUUAAAAUAAGGCUAGUCCGUUAUCAACUUGAAAAA GUGGCACCGAGUCGGUGCUUUUUUU. Sequences of crRNA and repair templates are listed in Table A.3. The injection mix used for CRISPR is:

Cas9 prep (10µg/µl): 5µl

tracrRNA (4µg/µl): 5µl

rol-6 crRNA (8µg/µl): 0.4µl

rol-6 ssODN (500ng/µl): 0.55µl

Targeted gene crRNA (8µg/µl): 1µl

(Optional: PCR template: 500ng/µl final in the mix)

(Optional: ssODN (1µg/µl): 2.2µl)

KCl (1M): 0.5µl

Hepes pH7.4 (200mM): 0.75µl

H2O: add if necessary to reach a final volume of 20µl

All worms were confirmed by sequencing and outcrossed at least three times prior to experimentation or crossing them into the *hsp-6$_{pr}$::gfp* or *hsp-60$_{pr}$::gfp* backgrounds.

Bacterial strains. Worms were raised on the OP50 strain of *E. coli*, and on the HT115 strain for RNAi treatment (Rual, Ceron et al. 2004). For RNAi treatment, overnight HT115 bacterial culture was spread on NGM plates supplemented with 100µg/ml Ampicillin and 0.3mM IPTG. For *P. aeruginosa* experiments, worms were exposed to the UCBPP-PA14 strain of *P. aeruginosa* unless otherwise indicated. PA01, PA14, CF18 are pathogenic *P. aeruginosa* strains (Lee, Urbach et al. 2006). *P. aeruginosa* mutants: *P. aeruginosa*-Δ*gacA*, *P. aeruginosa*-Δ*phz*, *P. aeruginosa*-Δ*hcnB, P. aeruginosa*-Δ*hcnC, P. aeruginosa*-Δ*pvdF* and *P. aeruginosa*-Δ*pvdP* are from UCBPP-PA14 Transposon Insertion Mutant Library (Liberati, Urbach et al. 2006).

***P. aeruginosa* slow killing and intestinal accumulation assays**. UPR^{mt} activity assay were performed as previously described (Pellegrino, Nargund et al. 2014) with minor modifications. *P. aeruginosa* strains were streaked to LB plates and incubated at 37°C for 18 hours, followed by room temperature for 6 hours, and transferred to liquid LB for 24-hours (LB) at 16°C. 300 µl of the bacterial culture was added to agar plates and incubated at 25°C for 24 hours. Eggs were first allowed to hatch on unseeded NGM plates for 2 days at 20°C.

Starved L1s were then transferred to *P. aeruginosa* plates and incubated at 20°C. Images were taken after 18 hours. For the ethidium bromide experiments, 30 μg/ml ethidium bromide was spread to slow-killing plates (Tan, Mahajan-Miklos et al. 1999) before seeding *P. aeruginosa* or *E. coli*.

Slow killing assays were performed as described (Tan, Mahajan-Miklos et al. 1999, Pellegrino, Nargund et al. 2014), with minor modifications. For the RNAi experiments, worms were first raised on control, *atfs-1*(RNAi) or *zip-3*(RNAi) for two generations prior to transferring them to *P. aeruginosa* slow-killing plates. Each experiment was performed in triplicate and *P* values were evaluated with log rank (Mantel-Cox) statistical test. Statistics are in Table A.4.

The *P. aeruginosa* intestinal accumulation assays were performed as described (Pellegrino, Nargund et al. 2014). Overnight cultures of *P. aeruginosa* expressing GFP (*P. aeruginosa*–GFP) were seeded onto slow-killing NGM plates, allowed to dry overnight at room temperature and then incubated at 37°C for 24 h. To exclude pathogen avoidance as a means of decreased intestinal colonization, where indicated *P. aeruginosa*–GFP was also spread across the entire surface of the slow-killing plate. Synchronized L4 worms were transferred to plates coated with *P. aeruginosa*–GFP and were imaged following 48 hours of exposure to *P. aeruginosa*-GFP at 25°C.

Phenazine treatment. Phenazine exposure was performed as described (Cezairliyan, Vinayavekhin et al. 2013, Pukkila-Worley, Feinbaum et al. 2014). In short, 1-hydroxyphenazine (TCI America), pyocyanin (Cayman Chemicals) and phenazine-1-carboxylic acid (Apollo Scientific) were dissolved in DMSO at 5 mg/ml. The molecules were then added to sterilized modified NGM (0.25% peptone, 0.3% NaCl, 1.6% agar, 50 mM sodium citrate, the pH was adjusted to 5 with HCl), to final concentrations of 1 ng/µl 1-hydroxyphenazine, 5 ng/µl pyocyanin and 5 ng/µl phenazine-1-carboxylic acid prior to pouring the media into 3.5 cm petri dishes. Plates were then seeded with *E. coli* and incubated at 25°C for 20 hours. Worms were first synchronized by bleaching and starved for 2 days at 20°C, and then transferred to phenazine or control plates. Worms were examined 48 hours following exposure to phenazines.

TMRE staining. *P. aeruginosa* was streaked to a LB plate and incubated at 37°C for 24 hours, and then for 24 hours in LB liquid at 37°C. TMRE-coated plates (1 mM) were seeded with 70 µl of bacterial culture and incubated at 25°C for 24 hours. Worms were synchronized and raised on *E. coli* OP50 plates until the L3 stage, then transferred to *P. aeruginosa* or *E. coli* plates containing TMRE for 15 hours. The worms were transferred to plates lacking TMRE for 3 hours prior to imaging. Worms were incubated at 20°C throughout the experiment.

Oxygen consumption. Oxygen consumption rates (OCR) were measured using a Seahorse Extracellular Flux Analyzer XFe96 as described (Koopman, Michels et al. 2016, Lin, Schulz et al. 2016). Worms at L4 stage were transferred to unseeded NGM plates and allowed to completely digest the remaining bacteria in their intestine for 1 hour, after which 10 worms were transferred to each well of a 96-well microplate containing 200 µl M9 buffer. Basal respiration was measured for a total of 60 min, in 6-min intervals that included a 2 minute mix, a 2 minute time delay and a 2 minute measurement. To measure respiratory capacity, 15 µM FCCP was injected. Subsequently, non-mitochondrial respiration was measured by injection 40 mM sodium azide. For *P. aeruginosa* experiments, *P. aeruginosa* was streaked to a LB plate and incubated at 37°C for 24 hours, transferred to LB liquid for 24 hours at 37°C, and lastly to NGM plates for 24 hours at 37°C. Worms were exposed to *P. aeruginosa* for 12 hours prior to being transferred to the unseeded plates followed by OCR analysis.

RNA isolation and qRT-PCR. Total RNA was extracted from frozen worm pellets with RNA STAT (Tel-Test) and used for cDNA synthesis with qScript™ cDNA SuperMix (QuantaBio). qRT-PCR was performed using iQ™ SYBR® Green Supermix (Bio-Rad Laboratories).

For RNA extracted from worms treated with *P. aeruginosa*, the worms were first raised in on the HT115 strain of *E. coli* for two generations (control, *atfs-1*, or

zip-3(RNAi)). They were then bleached to unseeded NGM plates for 1 hour, and transferred to *P. aeruginosa* or *E. coli* control plates for 18 hours at 20°C before being harvested. For the experiments not involving *P. aeruginosa*, worms were synchronized and harvested at the L4 state. qRT-PCR primers are listed in Table A.3.

RNA-sequencing and differential gene expression analysis. cDNA libraries were constructed with standard Illumina P5 and P7 adapter sequences. For the RNA-sequencing experiments in which worms were exposed to *P. aeruginosa*, cDNA libraries were run on an Illumina HiSEq2000 instrument with single-read 50-bp (SR50). For RNA-sequencing experiment involving *spg-7*(RNAi), cDNA libraries were run on an Illumina HiSEq3000 instrument with pair-end 50-bp (PE50). RNA reads were then aligned to WBcel235/ce11 reference genome and differential gene expression analysis was performed with edgeR.

Statistics. All experiments were performed at least three times yielding similar results and comprised of biological replicates. The sample size and statistical tests were chosen based on previous studies with similar methodologies and the data met the assumptions for each statistical test performed. No statistical method was used in deciding sample sizes. No blinded experiments were performed and randomization was not used. For all figures, the mean ± standard deviation (s.d.) is represented unless otherwise noted.

Microscopy. *C. elegans* were imaged using either a Zeiss AxioCam 506 mono camera mounted on a Zeiss Axio Imager Z2 microscope or a Zeiss AxioCam MRc camera mounted on a Zeiss SteREO Discovery.V12 stereoscope. Images with high magnification (63×) were obtained using the Zeiss ApoTome.2. Exposure times were the same in each experiment.

Data Availability. The RNA-sequencing data have been deposited in a MIAME-compliant format to the Gene Expression Omnibus database under accession numbers GSE111325 and GSE113136.

APPENDICES

Table A. 1. UPR^{mt} genes induced in *zip-3(gk3164)* strain during *spg-7*(RNAi) treatment

Sequence Name	Gene Symbol	Description	*zip-3(gk3164)* /wildtype *spg-7*(RNAi)	*p*-value	*atfs-1(tm4919)* / wildtype *spg-7*(RNAi)	*p*-value
AMPK pathway						
T01B6.3	aakg-4	AMPK gamma subunit	1.63254	0.04332	0.25018	0.00011
Glycolysis and glucose metabolism						
T26H5.8		galactoside 2-alpha-L-fucosyltransferase	3.02230	0.00017	0.32618	0.00946
Oxidative phosphorlation						
C15H9.1	nnt-1	nicotinamide nucleotide transhydrogenase	2.78598	0.00000	0.33186	0.00018
Innate Immunity						
C50F2.10	abf-2	antimicrobial peptide	1.84104	0.04087	0.19798	0.00033
T08A9.12	spp-2	antimicrobial peptide	1.89243	0.00039	0.43257	0.00128
F55G11.5	dod-22	Involved in innate immune response	1.53431	0.03482	0.34243	0.00030
Xenobiotic detoxification						
T10B9.7	cyp-13A2	cytochrome P450	2.67818	0.00000	0.54347	0.03362
T10B9.5	cyp-13A3	cytochrome P450	2.11502	0.01569	0.35741	0.02655
C45H4.2	cyp-33C1	cytochrome P450	2.66054	0.00093	0.02590	0.00000
C45H4.17	cyp-33C2	cytochrome P450	1.88211	0.03332	0.04223	0.00000
B0213.10	cyp-34A5	cytochrome P450	1.94524	0.04076	0.22983	0.00388
B0213.12	cyp-34A7	cytochrome P450	2.88332	0.00285	0.10336	0.00044
B0213.15	cyp-34A9	cytochrome P450	1.60365	0.00890	0.19358	0.00000
F37B1.2	gst-12	glutathione S-transferase	2.15710	0.00506	0.40754	0.02415
C02A12.1	gst-33	glutathione S-transferase	1.90186	0.00812	0.16915	0.00000
T08B1.3	alh-5	aldehyde dehydrogenase	2.14029	0.00003	0.24606	0.00000
T23F4.3	dlhd-1	dienelactone hydrolase	2.32246	0.00031	0.43351	0.01334
C52A10.2		carboxylic ester hydrolase	2.29708	0.00427	0.15910	0.00003
Antioxidant						
C08A9.1	sod-3	superoxide dismutase, mitochondrial	2.37167	0.00185	0.39772	0.02199
Lipid and cholesterol metabolism						
Y56A3A.5	faah-5	fatty acid amide hydrolase	1.90071	0.04816	0.26934	0.00947
W06D12.3	fat-5	delta(9)-fatty-acid desaturase	3.69483	0.00000	0.35403	0.00006
F09B9.1	oac-14	o-acyltransferase	2.11766	0.00003	0.40700	0.00050
C06E4.3		hydroxysteroid dehydrogenase	2.83160	0.00002	0.15761	0.00000
C06E4.6		hydroxysteroid dehydrogenase	2.95923	0.00032	0.22454	0.00094
F12E12.12		hydroxysteroid dehydrogenase	2.78656	0.00134	0.31085	0.01630
F11A5.12	stdh-2	putative steroid dehydrogenase	2.67667	0.00226	0.18638	0.00097
F14E5.5	lips-10	lipase related	1.46120	0.03832	0.55848	0.02792
Transporters						
C54G7.4	ifta-1	intraflagellar transport associated	2.54701	0.00133	0.25772	0.00164
ZC196.2		VAPA and VAPB ortholog	3.03140	0.00121	0.15194	0.00122
B0281.6		potassium channel tetramerization domain	2.38413	0.01658	0.25171	0.02316
Iron metabolism						
C54F6.14	ftn-1	ferritin; intracellular iron storage	1.68103	0.00495	0.28548	0.00000
Proteolysis						
Y51A2A.9	fbxa-117	F-box protein	2.74219	0.00232	0.17191	0.00119
M162.8	fbxa-118	F-box protein	3.52109	0.00055	0.02030	0.00000
C08E3.8	fbxa-165	F-box protein	2.57769	0.00299	0.36994	0.03851
Transcription factors						
C25E10.1	nhr-30	nuclear hormone receptor	3.27629	0.00058	0.31395	0.03644
F44E7.8	nhr-142	nuclear hormone receptor	1.80884	0.01281	0.25595	0.00010

(Table A. 1. Continued)

F41D3.3	nhr-265	nuclear hormone receptor	2.89823	0.00114	0.02071	0.00000
R03E9.1	mdl-1	bHLH transcription factor	1.44504	0.03564	0.49422	0.00546
Signaling						
Y73B3A.12	cal-6	calmodulin related genes	3.75795	0.00049	0.09865	0.00200
K02E2.4	ins-35	insulin-related peptides	8.00809	0.00000	0.33736	0.00534
C54D10.7	dct-3	DAF-16/FOXO controlled	5.27821	0.00000	0.39169	0.03249
Cell structure						
R09D1.5	chil-18	chitinase-like	8.25710	0.00000	0.01964	0.00000
Y53H1B.1	cutl-10	cuticlin-like	2.30481	0.00393	0.26974	0.00227
Orphans						
B0205.2	srz-85	serpentine receptor	1.83374	0.03693	0.29330	0.00417
C25E10.7		TIL-domain protease inhibitor	5.39257	0.00000	0.02737	0.00000
F40B1.1	bath-13	BTB and MATH domain containing	3.11731	0.00028	0.05459	0.00000
B0047.1	bath-20	BTB and MATH domain containing	2.05161	0.02654	0.23553	0.00436
Y73B3A.13		RCOR1 homolog	2.97090	0.00196	0.11613	0.00066
C41D11.8	cps-6	endonuclease G, mitochondrial	1.58838	0.00863	0.56715	0.02571
C50F7.2	clx-1	collagan related	6.15015	0.00000	0.16385	0.00004
Unknowns						
F21C10.10		unknown; mitochondrial localized	2.48377	0.00000	0.59795	0.04730
AC8.1	pme-6	unknown; induced by oxidants and mitochondrial dysfunction	2.19777	0.01630	0.11333	0.00008
C40A11.8		unknown; induced by oxidants and mitochondrial dysfunction	3.15443	0.00034	0.12575	0.00008
T28A11.16		unknown; induced by oxidants and mitochondrial dysfunction	2.75949	0.00040	0.20314	0.00018
Y46H3C.6		unknown; induced by oxidants and mitochondrial dysfunction	2.42023	0.00452	0.18805	0.00058
B0547.3	srd-14	unknown; induced by oxidants and mitochondrial dysfunction	2.29977	0.00834	0.19563	0.00097
Y37D8A.4		unknown; induced by oxidants and mitochondrial dysfunction	1.70940	0.01358	0.36111	0.00132
K01A11.3		unknown; induced by oxidants and mitochondrial dysfunction	2.26370	0.01974	0.15192	0.00165
ZC395.5		unknown; induced by oxidants and mitochondrial dysfunction	2.55483	0.00007	0.37484	0.00409
T28A11.2		unknown; induced by oxidants and mitochondrial dysfunction	2.00135	0.00023	0.52663	0.01814
C03G6.5		unknown; induced by oxidants and mitochondrial dysfunction	2.29924	0.00014	0.49628	0.02630
F21C10.11		unknown; induced by oxidants and mitochondrial dysfunction	1.70927	0.00284	0.56871	0.02932
C37A5.2	fipr-22	unknown	2.09730	0.02656	0.35547	0.04533
C07G1.7		unknown	3.39688	0.00001	0.00958	0.00000
ZK262.9		unknown	3.98695	0.00009	0.00109	0.00000
F09E10.1		unknown	2.18546	0.00893	0.05881	0.00000
Y68A4A.13		unknown	9.47243	0.00000	0.20873	0.00000
R09D1.4		unknown	7.93866	0.00000	0.03554	0.00000
F40D4.13		unknown	4.92957	0.00000	0.05151	0.00000
F42C5.6		unknown	2.83689	0.00114	0.04790	0.00000
T28A11.19		unknown	3.86164	0.00001	0.08187	0.00000
T11F9.10		unknown	2.72429	0.00239	0.06250	0.00000
T20D4.10		unknown	4.06899	0.00000	0.17165	0.00000
C54E10.1		unknown	2.11284	0.01808	0.09523	0.00001
F35F10.5		unknown	2.77552	0.00031	0.15943	0.00001
T20D4.11		unknown	2.06091	0.00208	0.22556	0.00002
Y45F10C.6		unknown	3.02046	0.00061	0.09842	0.00002
ZC15.3		unknown	4.39493	0.00003	0.05243	0.00004
T13G4.5		unknown	2.72021	0.00420	0.07223	0.00005
C50F7.5		unknown	5.33592	0.00000	0.22606	0.00009
F55B11.6		unknown	4.91922	0.00001	0.08403	0.00015
C38D9.2		unknown	3.47466	0.00007	0.15306	0.00016
Y54G2A.21		unknown	1.88809	0.02059	0.21560	0.00017
ZC15.4		unknown	6.01624	0.00000	0.09182	0.00042
Y46H3C.6		unknown	2.42023	0.00452	0.18805	0.00058
H25P06.5		unknown	2.56661	0.01217	0.08066	0.00062
Y116F11B.10		unknown	2.14109	0.02267	0.15018	0.00063
B0563.9		unknown	82.75700	0.00000	0.10731	0.00076
T20D4.12		unknown	6.27838	0.00000	0.20851	0.00083
F59H6.14		unknown	2.57493	0.00916	0.11032	0.00094

(Table A. 1. Continued)

C17B7.2	unknown	3.21663	0.00035	0.17622	0.00096
R05D8.11	unknown	3.96818	0.00011	0.11806	0.00104
K09H11.11	unknown	3.08978	0.00073	0.16596	0.00115
F55H12.2	unknown	1.63803	0.03982	0.32416	0.00137
F01G10.4	unknown	12.61376	0.00000	0.03919	0.00247
Y73B3B.1	unknown	2.99653	0.00168	0.20388	0.00694
F57G4.11	unknown	12.71408	0.00000	0.20375	0.00957
F48G7.12	unknown	3.59464	0.00030	0.21108	0.00965
F55B12.10	unknown	2.93408	0.00152	0.24381	0.01003
C54F6.6	unknown	1.99632	0.02305	0.31208	0.01027
B0207.5	unknown	2.04125	0.02808	0.27657	0.01090
K02A2.5	unknown	1.81669	0.04801	0.32037	0.01132
T23B12.14	unknown	3.17819	0.00081	0.23948	0.01251
B0507.10	unknown	24.65986	0.00000	0.45595	0.03652
C54F6.15	unknown	3.03578	0.00066	0.28738	0.01363
T26H5.4	unknown	2.19029	0.00801	0.40041	0.03445
C18B10.6	unknown	2.51454	0.00422	0.35480	0.03545
F14F9.2	unknown	12.73638	0.00000	0.23354	0.01907
F48G7.2	unknown	4.92355	0.00000	0.27342	0.02048
Y102A5C.35	unknown	2.26162	0.03342	0.23198	0.02802
Y53F4B.6	unknown	4.17041	0.00005	0.27740	0.02841
C39E9.8	unknown	1.90214	0.00028	0.56564	0.02497

Table A. 2. Subset of UPR^{mt} genes induced in *zip-3(gk3164)* strain during *P. aeruginosa* treatment

Sequence Name	Gene Symbol	Description	*zip-3(gk3164)* /wildtype *P. aeruginosa*	*p*-value	*atfs-1(tm4919)* / wildtype *spg-7*(RNAi)	*p*-value
Mitochondrial proteostasis						
C37H5.8	*hsp-6*	mitochondrial chaperone, Hsp70 superfamily	1.50329	0.00475	0.62726	0.01538
F22B7.5	*dnj-10*	mitochondrial-localized protein chaperone	1.52025	0.00737	0.47577	0.00003
Oxidative phosphorylation						
MTCE.34	*nduo-3*	NADH-ubiquinone oxidoreductase subunit, mtDNA encoded	2.16487	0.00003	0.61979	0.01559
T06D8.6	*cchl-1*	cytochrome C heme-lyase; attaches heme to cytochrome c	1.44185	0.04715	0.65944	0.01868
C35D10.5		ubiquinol-cytochrome c reductase chaperone	2.33002	0.01658	0.49457	0.00015
B0035.15		NDUFAF4 ortholog; OXPHOS complex I assembly factor	1.70322	0.03190	0.59460	0.00526
Mitochondrial translation						
F55C5.5	*tsfm-1*	mitochondrial translation elongation factor Ts (EF-Ts)	2.22348	0.00016	0.43382	0.00000
C43E11.4	*tufm-2*	mitochondrial translation elongation factor Tu (EF-Tu)	1.67453	0.00431	0.47400	0.00003
T01E8.6	*mrps-14*	mitochondrial ribosomal subunit, small	1.52363	0.03528	0.54724	0.00066
F29C12.4	*gfm-1*	mitochondrial translation elongation factor g	1.47148	0.01225	0.44080	0.00001
E02H1.2		ERAL1 homolog; 12S mitochondrial rRNA chaperone 1	1.55921	0.02621	0.54355	0.00355
Coenzyme Q synthesis						
D2023.6		Coenzyme Q biosynthesis (ubiquinone); COQ-8	1.55302	0.04110	0.46327	0.00002
Mitochondrial						
T24H7.1	*phb-2*	prohibitin, required for mitochondrial organization	1.39333	0.02345	0.56808	0.00274
F57A10.3	*haf-3*	mitochondrial localized ABC transporter	1.67037	0.00120	0.52359	0.00024
Innate immunity						
Y22F5A.6	*lys-3*	secreted lysozyme	2.00269	0.00795	0.40560	0.00274
C49G7.5	*irg-2*	infection response gene	1.74916	0.01035	0.44202	0.00037
F09G8.8	*clec-160*	C-type lectin	1.96921	0.01308	0.57643	0.00219
E03H4.10	*clec-17*	CLEC3B homolog: C-type lectin	2.93324	0.00438	0.06231	0.00000
C50F2.10	*abf-2*	antimicrobial peptide	18.47726	0.00580	0.32543	0.00033
Xenobiotic detoxification						
AC3.8	*ugt-2*	UDP-glucosyltransferase family 3	1.55362	0.01928	0.40416	0.00000
T07C5.1	*ugt-50*	UDP-glucosyltransferase family 3	1.46890	0.01831	0.54492	0.00107
M88.1	*ugt-62*	UDP-glucuronosyltransferase	1.88961	0.00023	0.35037	0.00000
K08B4.3	*ugt-19*	UDP-glucosyltransferase family 3	2.37197	0.00003	0.25346	0.00000
T10B9.4	*cyp-13A8*	cytochrome P450	2.99672	0.04677	0.03808	0.00000
K09A11.2	*cyp-14A1*	cytochrome P450	6.28458	0.00058	0.10589	0.00000
F44C8.1	*cyp-33C4*	cytochrome P450	2.67153	0.00395	0.48288	0.00096
R08F11.3	*cyp-33C8*	cytochrome P450	2.45231	0.00000	0.36683	0.00000
C23H4.2		unknown	2.28969	0.00270	0.37529	0.00000
T08B1.3	*alh-5*	aldehyde dehydrogenase, [NAD(P)+] activity	1.94939	0.02500	0.37835	0.00000
Antioxidant						
Y38F2AR.12		glutathione and cytochrome P450 metabolism	1.61519	0.00327	0.60236	0.00428
F43E2.5	*msra-1*	methionine sulfoxide reductase	1.59719	0.00788	0.40892	0.00000
F56C11.3		thiol oxidase acitivity	2.07887	0.02174	0.57096	0.01506
C54D10.1	*cdr-2*	cadmium responsive, heavy metal detox	2.19767	0.00016	0.33415	0.00000
C35B1.5		Nucleoredoxin ortholog; thioredoxin ortholog	1.61873	0.01048	0.69107	0.04598
Iron metabolism						
C54F6.14	*ftn-1*	ferritin; intracellular iron storage	2.31207	0.00004	0.41941	0.00000
Amino acid metabolism						
C09F9.3	*glna-1*	glutaminase; catalyzes glutamine to glutamate and ammonia	2.16525	0.00014	0.53566	0.00221
Glycolysis and glucose metabolism						
F14B4.2	*hxk-1*	hexokinase; glycolysis	1.48374	0.02150	0.55973	0.00109

(Table A. 2. Continued)

Lipid and Cholesterol metabolism						
Y71G12B.10		HMG-CoA lyase; synthesizes acetoacetate in mitochondria	1.66101	0.00421	0.67974	0.02977
Y62E10A.6		ferredoxin reductase	1.51564	0.03456	0.60331	0.00891
T28D9.3		PLPP3 homolog; phospholipid phosphatase	1.75665	0.04043	0.68523	0.04107
C55C3.5	*perm-5*	predicted to have lipid binding activity	1.61767	0.00894	0.43077	0.00000
F09B9.1	*oac-14*	o-acyltransferase	1.58479	0.00184	0.53628	0.00050
B0218.2	*faah-2*	FAAH homolog; fatty acid amide hydrolase	1.41682	0.04074	0.54973	0.00069
F35C8.5		cholesterol 25-hydroxylase; cholesterol and lipid metabolism	1.78074	0.03142	0.56543	0.00145
F16B4.4		delta-12 fatty acyl desaturase	2.32258	0.00001	0.68745	0.03364
K11D12.4	*cpt-4*	Carnitine palmitoyl transferase; essential for beta oxidation	1.56477	0.00498	0.62633	0.01573
C50D2.9		malonyl-CoA-acyl carrier protein transacylase	2.26911	0.00002	0.36781	0.00000
C37H5.13		acyl-CoA thioesterase; peroxisomal thioesterase	1.55326	0.01683	0.62490	0.00857
C17C3.3		acyl-CoA thioesterase; peroxisomal thioesterase	3.28578	0.02569	0.30796	0.00233
C37H5.3	*abhd-5.2*	ABHydrolase domain containiing protein, lipid storage	1.97029	0.00080	0.64342	0.01479
F55E10.6	*drd-5*	shrot chain dehydrogenase/reductase; mitochondrial	1.70999	0.00789	0.59931	0.00384
R05D8.8	*dhs-14*	short chain dehydrogenase, mitochondrial	5.74850	0.00002	0.44055	0.00001
Nucleotide metabolism						
K11C4.4	*odc-1*	ornithine decarboxylase, polyamine biosynthesis,	1.39354	0.03729	0.50902	0.00022
Protein and lipid trafficking						
T03F7.7		SEC14 related, Golgi trafficking	1.51932	0.02216	0.59702	0.01941
R186.1		Tango2 homolog; transport and golgi organization	2.04731	0.00424	0.46974	0.00100
Membrane transporters						
Y32F6B.1		SLC05A1; solute carrier, anion transport	2.25956	0.00000	0.45756	0.00002
C33D12.3	*twk-26*	Potassium channel	2.13305	0.00020	0.52037	0.00273
C02C2.4	*slc-17.3*	solute carrier protein	2.81749	0.00146	0.23543	0.00000
F58G6.3		SLC31A2 homolog; predicted to be a copper transporter	2.44794	0.02055	0.68698	0.03866
F58G6.7		SLC31A2 homolog; predicted to be a copper transporter	3.14959	0.00088	0.65487	0.01740
F58G6.9		SLC31A2 homolog; predicted to be a copper transporter	3.62925	0.00001	0.29066	0.00000
C09H5.2	*catp-3*	cation transporting ATPase	1.60681	0.00098	0.62171	0.01096
C29F4.2	*best-7*	BESTrophin homolog: chloride channel	2.98624	0.00000	0.57808	0.00583
C05E11.4	*amt-1*	ammonium transporter ortholog	17.44587	0.00654	0.25643	0.00001
T28F3.3	*hke-4.1*	KE4 homolog; predicted to be a zinc transporter	5.26843	0.00000	0.58327	0.00900
Transcription factors						
F16B4.9	*nhr-178*	nuclear hormone receptor, involved in lipid storage	1.69149	0.02671	0.17658	0.00000
F57G8.6	*nhr-193*	nuclear hormone receptor	2.91015	0.02401	0.52172	0.00252
F41D3.3	*nhr-265*	nuclear hormone receptor	4.35208	0.03400	0.06805	0.00000
Signaling						
ZK970.6	*gcy-5*	guanylyl cyclase; potentially in a G protein cascade	5.54436	0.00003	0.28692	0.00079
Cell Adhesion						
ZC376.3		neruoligin ortholog	3.16028	0.00000	0.66698	0.04734
Proteolysis						
T05F1.11		F-box protein	2.25928	0.00000	0.49259	0.00024
T16G12.1		ERAP1 homolog; endoplasmic reticulum aminopeptidase	1.61594	0.00091	0.44273	0.00001
C08E3.9	*fbxa-166*	F-box protein	11.62209	0.00004	0.27921	0.00001
F59D6.3	*asp-8*	aspartyl protease	1.60280	0.01980	0.25840	0.00000
Orphan						
ZK1073.1		ortholog of NDRG1 (N-myc downstream regulated 1).	1.48650	0.02963	0.44028	0.00000
Y32H12A.8		GATOR complex amino acid sensing branch of mTORC1	1.36676	0.03028	0.64535	0.01268
C13D9.1	*srr-6*	serpentine receptor	1.91109	0.00440	0.44458	0.00866
B0205.2	*srz-85*	serpentine receptor	8.14517	0.00610	0.42734	0.00417
F56A3.4	*spd-5*	coiled-coil domain, interacts with CED-9, limits apoptosis	1.37928	0.03169	0.51026	0.00022
R119.7	*rnp-8*	RRM RNA binding protein	1.37928	0.03169	0.51026	0.00022
D2030.6	*prg-1*	Piwi family protein	4.43849	0.00024	0.62067	0.00893

(Table A. 2. Continued)

Y71H2AM.16	*pho-9*	intestinal acid phosphatase, lysosomal	2.34641	0.00011	0.51569	0.00230
R12A1.4	*ges-1*	B carboxylesterase	1.83058	0.00082	0.52368	0.00033
Y76A2A.2		copper-transporting E1-E2 ATPase	1.45788	0.01228	0.65579	0.01890
R09D1.5	*chil-18*	OVGP1 homolog; chitinase-like	11.41291	0.00076	0.06559	0.00000
Unknown						
Y68A4A.13		unknown; induced by oxidants and mitochondrial dysfunction	3.89313	0.00000	0.33758	0.00000
Y54G2A.45		unknown; induced by oxidants and mitochondrial dysfunction	1.66584	0.00425	0.40946	0.00000
Y48E1C.4		unknown; induced by oxidants and mitochondrial dysfunction	1.91261	0.00217	0.62512	0.01241
T28A11.2		unknown; induced by oxidants and mitochondrial dysfunction	3.13228	0.00000	0.64115	0.01814
T22B7.3		unknown; induced by oxidants and mitochondrial dysfunction	1.81376	0.00146	0.55293	0.00935
T20D4.10		unknown; induced by oxidants and mitochondrial dysfunction	10.39029	0.00000	0.29478	0.00000
T05B11.4		unknown; induced by oxidants and mitochondrial dysfunction	1.84282	0.03323	0.54774	0.03853
R08F11.4		unknown; induced by oxidants and mitochondrial dysfunction	1.87951	0.00742	0.13054	0.00000
K06G5.3		unknown; induced by oxidants and mitochondrial dysfunction	4.81175	0.00462	0.21069	0.00000
F58B4.5		unknown; induced by oxidants and mitochondrial dysfunction	1.73814	0.01130	0.65319	0.02115
F35F10.5		unknown; induced by oxidants and mitochondrial dysfunction	37.18101	0.00012	0.28007	0.00001
F22G12.7		unknown; induced by oxidants and mitochondrial dysfunction	4.94425	0.00332	0.53180	0.03982
F18E3.11		unknown; induced by oxidants and mitochondrial dysfunction	2.37826	0.00994	0.62924	0.03255
F18E3.13		unknown; induced by oxidants and mitochondrial dysfunction	1.45472	0.03966	0.64707	0.03987
F13H6.3		unknown; induced by oxidants and mitochondrial dysfunction	1.62673	0.00196	0.51808	0.00021
F14F9.2		unknown; induced by oxidants and mitochondrial dysfunction	17.18376	0.00000	0.36490	0.01907
C18A11.3		unknown; induced by oxidants and mitochondrial dysfunction	1.71180	0.01257	0.65892	0.01991
C17B7.2		unknown; induced by oxidants and mitochondrial dysfunction	6.44123	0.00027	0.30020	0.00096
C05D2.8		unknown; induced by oxidants and mitochondrial dysfunction	1.46481	0.02254	0.51793	0.00024
B0507.6		unknown; induced by oxidants and mitochondrial dysfunction	2.74603	0.00005	0.29152	0.00000
B0507.10		unknown; induced by oxidants and mitochondrial dysfunction	5.84595	0.00000	0.58020	0.03652
T28A11.16		unknown	4.74686	0.00000	0.33128	0.00018
T20D4.11		unknown	3.90055	0.00000	0.35622	0.00002
T20D4.12		unknown	17.15909	0.00000	0.33733	0.00083
T20D3.3		unknown	1.35728	0.04304	0.64961	0.01507
T16G1.4		unknown	1.72175	0.02925	0.24166	0.00000
R119.1		unknown	3.82438	0.00317	0.49156	0.00447
R08E5.3		unknown	1.60648	0.01002	0.56733	0.00227
F15D4.5		unknown	4.07636	0.00191	0.34741	0.00007
F13D12.3		unknown	4.27412	0.00000	0.51951	0.00079
F07E5.9		unknown	14.86654	0.00010	0.45129	0.02485
C38D9.2		unknown	1.92717	0.03957	0.27226	0.00016
C46A5.5		unknown; required for development	3.64155	0.00332	0.28265	0.00000
C04E6.11		unknown	1.49396	0.01980	0.65676	0.02147
B0205.13		unknown	12.30373	0.00000	0.63047	0.01516
B0205.14		unknown	25.74182	0.00000	0.42702	0.00000
B0391.10		unknown	5.71294	0.00263	0.44620	0.00265
Y54G2A.21		unknown	4.90389	0.00014	0.34524	0.00017
T12B5.9		unknown	2.80977	0.02296	0.53474	0.04529

Table A. 3. qRT-PCR primers, crRNAs and repair templates for CRISPR

qRT-PCR primers	
abf-2	CGTGGCTGCCGACATCGACTT
	ATGCACAACCCCTGAGCCGC
cpt-4	GAACACATAAAAGAAGATGCTCAAAAACTCCT
	GGAAAAGTAAAAGTATTTTAGAATGTGGCGGAGAA
cyp-14A1	CATTTCCGGCAATTGTGTTGA
	GTGAACTGGCAGAAGGGTTT
dnj-10	GCGGGCTCATTCATCGATCTGTAC
	CAGATTTTTTGTCGACACCCAAAG
ftn-1	GCGGCCGTCAATAAACAGATTAA
	CAATGTTCCGAAGTGCGAT
lys-3	CAAGATATGATTAGAAGTGCGAAGAATCT
	TCAGAACATGCCAGTACCACAA
tsfm-1	AGACTGGTTATAGTTATGTGAATTGTCGT
	CGATGTTACACGAGTTCCAAGTTTT
zip-3	CGCACCCGATTCCAGTTGATAC
	CATTCCAGATGATGAGGATTGTGG
crRNAs	
atfs-1(cmh15)	AGTGGTATGAGGTCAGAATG
	GTAATATCATCGCCATGAGA
zip-3 $_{pr}$ ::gfp::zip-3	AAGTCGTCCGCATCGTATGA
zip-3 $_{pr}$ ::gfp::zip-3 ^{Y167A}	TGTGGAGCAAAGGAAGAGTA
zip-3 $_{pr}$ ::gfp::zip-3 ^{Y167F}	TGTGGAGCAAAGGAAGAGTA
Primers for amplifying repair template (GFP)	
zip-3 $_{pr}$ ::gfp::zip-3	CCAGTGAAAAAACCTTCCCTGTCTCCAAAAATGagtaaaggagaagaacttttcactgg
	TCCACGCCGCATGAAGTCGTCCGCATCGTAACTAGGCTGtttgtatagttcatccatgccatg
Repair templates	
zip-3 $_{pr}$ ::gfp::zip-3 ^{Y167A}	AAAGAAAAAATTTCCAGAATGTCCAATGGCTCCACCACCAgcaagTTCCTTTGCTCCACAAT
	CCTCATCATCTGGcATGCTTCAGCAACAACCACAGGATCTAGTGATTCCCCAG
zip-3 $_{pr}$ ::gfp::zip-3 ^{Y167F}	AAAGAAAAAATTTCCAGAATGTCCAATGGCTCCACCACCATtCTCTTCCTTTGCTCCACA
	ATCCTCATCATCTGGcATGCTTCAGCAACAACCACAGGATCTAGTGATTCCCCAG

Table A. 4. Statistics for survival analysis

Strain comparison	*p* values	Number of worms	Figure
Lifespan			
wildtype control vs *zip-3(gk3164)* control	0.1945	wildtype control: 82/100, *zip-3(gk3164)* control: 83/100	2.2b
wildtype control vs wildtype *zip-3* (RNAi)	0.4048	wildtype control: 49/60, wildtype *zip-3* (RNAi): 49/60	2.2b
clk-1(qm30) vs *clk-1(qm30);zip-3(gk3164)*	0.0154	*clk-1(qm30)* : 58/90, *clk-1(qm30);zip-3(gk3164)* : 62/90	2.3d
isp-1(qm150) vs *isp-1(qm150);zip-3(gk3164)*	0.0156	*isp-1(qm150)* : 75/90, *isp-1(qm150);zip-3(gk3164)* : 70/90	2.3e
survival on *P. aeruginosa*			
wildtype control vs *zip-3(gk3164)* control	<0.0001	wildtype control: 55/60, *zip-3(gk3164)* control: 56/60	3.5a
zip-3(gk3164) control vs *zip-3(gk3164) atfs-1* (RNAi)	<0.0001	*zip-3(gk3164)* control: 56/60, *zip-3(gk3164) atfs-1* (RNAi): 41/60	3.5a
wildtype vs *atfs-1(et15)*	0.0003	wildtype: 47/60, *atfs-1(et15)* : 50/60	3.5b
wildtype vs *zip-3(gk3164) atfs-1(et15)* vs *zip-3(gk3164)*	0.006 0.3804	wildtype: 47/60, *zip-3(gk3164)* : 48/60 *atfs-1(et15)* : 50/60, *zip-3(gk3164)* : 48/60	3.5b 3.5b
zip-3(gk3164) P. aeruginosa vs *zip-3(gk3164) P. aeruginosa*-∆*phz*	<0.0001	*zip-3(gk3164) P. aeruginosa: 45/60, zip-3(gk3164) P. aeruginosa*-∆*phz: 42/60*	3.10
wildtype P. aeruginosa vs *wildtype P. aeruginosa*-∆*phz*	0.9876	wildtype *P. aeruginosa* : 42/60, wildtype *P. aeruginosa*-∆*phz* : 39/60	3.10
zip-3(gk3164) P. aeruginosa-∆*phz* vs *wildtype P. aeruginosa*-∆*phz*	0.0017	*zip-3(gk3164) P. aeruginosa*-∆*phz: 42/60, wildtype P. aeruginosa*-∆*phz: 39/60*	3.10

Statistical analysis was performed using the log rank (Mantel–Cox) statistical test. Number of worms represents the number of dead worms scored relative to the number of worms alive at the start of the experiment. The difference in numbers indicates those worms that were excluded (see Methods).

Appendices 5. Gamma Irradiation of *C. elegans* to integrate extrachromosomal transgenes

Procedure:

It is advisable to integrate at least 2-3 independent extachromasomal lines per construct since some arrays integrate more readily than others. The transmission freque ncy for these strains should be 25-35%.

1. Synchronize transgenic worms by either egg lay or bleaching.
    a. Egg Lay: Pick 10 gravid adult transgenic worms onto each of four 6cm seeded plates (40 worms total). Let the worms lay eggs for 6 hours and then remove the adult worms.
    b. Bleaching: Use a 20% alkaline hypochlorite solution to bleach gravid worms for several minutes or until worms begin to dissolve. Wash eggs at least three times with M9 to remove residual bleach/ NaOH. Let eggs hatch overnight in M9 with gen tle rocking and then distribute the liquid onto 6cm seeded plates.
2. Incubate worms at 20°C for approximately 48 hours until they reach the late L4 stage.

    Note: When your transgenic line is developmentally delayed it will take longer than 48 hours to reach t he late L4 stage. As a result, the transgenic worms may be overgrown by the non-transgenic worms causing the plates to starve before they are ready.
3. Irradiate the worm with 4000rads of gamma rays for 10 minutes.
4. Pick 5 irradiated L4 transgenic worms onto each of 20 10cm *enriched* NGM plates (100 worms total).
5. Incubate worms for 12-14 days at 20°C or until the worms are starved.

    Note: After 10 days you can wrap the plates in Parafilm to avoid loss of moisture.
6. Chunk the worms onto 6cm plates and incubate at 20°C for 24-36 hours.
7. Single 20 worms from each plate onto 3cm plates (400 worms total) .
8. Incubate at 20°C for 24-36 hours.
9. Identify plates where 100% of worms are transgenic.

    Note: A small bacterial lawn can make it easier to screen for transgenic progeny. Try to avoid contamination as it makes it harder to screen.
10. Since gamma irradiation can cause background mutations, it is wise to outcross the recovered integrated strains by mating with wild type males several times.
11. Sequence for the integrated gene using appropriate primers.

REFERENCES

Alberts, B., A. Johnson, J. Lewis, M. Raff, K. Roberts and P. Walter (2002). "Electron-transport chains and their proton pumps." Molecular biology of the cell **4**.

Alexandre, A. and A. L. Lehninger (1984). "Bypasses of the antimycin a block of mitochondrial electron transport in relation to ubisemiquinone function." Biochim Biophys Acta **767**(1): 120-129.

Angelastro, J. M., T. N. Ignatova, V. G. Kukekov, D. A. Steindler, G. B. Stengren, C. Mendelsohn and L. A. Greene (2003). "Regulated expression of ATF5 is required for the progression of neural progenitor cells to neurons." J Neurosci **23**(11): 4590-4600.

Angelastro, J. M., J. L. Mason, T. N. Ignatova, V. G. Kukekov, G. B. Stengren, J. E. Goldman and L. A. Greene (2005). "Downregulation of activating transcription factor 5 is required for differentiation of neural progenitor cells into astrocytes." J Neurosci **25**(15): 3889-3899.

Apel, K. and H. Hirt (2004). "Reactive oxygen species: metabolism, oxidative stress, and signal transduction." Annu Rev Plant Biol **55**: 373-399.

Arosio, P., R. Ingrassia and P. Cavadini (2009). "Ferritins: a family of molecules for iron storage, antioxidation and more." Biochim Biophys Acta **1790**(7): 589-599.

Baker, B. M. and C. M. Haynes (2011). "Mitochondrial protein quality control during biogenesis and aging." Trends Biochem Sci **36**(5): 254-261.

Baker, B. M., A. M. Nargund, T. Sun and C. M. Haynes (2012). "Protective coupling of mitochondrial function and protein synthesis via the eIF2alpha kinase GCN-2." PLoS Genet **8**(6): e1002760.

Baker, M. J., T. Tatsuta and T. Langer (2011). "Quality control of mitochondrial proteostasis." Cold Spring Harb Perspect Biol **3**(7).

Balaban, R. S., S. Nemoto and T. Finkel (2005). "Mitochondria, oxidants, and aging." Cell **120**(4): 483-495.

Bennett, C. F., J. J. Kwon, C. Chen, J. Russell, K. Acosta, N. Burnaevskiy, M. M. Crane, A. Bitto, H. Vander Wende, M. Simko, V. Pineda, R. Rossner, B. M. Wasko, H. Choi, S. Chen, S. Park, G. Jafari, B. Sands, C. Perez Olsen, A. R. Mendenhall, P. G. Morgan and M. Kaeberlein (2017). "Transaldolase inhibition impairs mitochondrial respiration and induces a starvation-like longevity response in Caenorhabditis elegans." PLoS Genet **13**(3): e1006695.

Berendzen, K. M., J. Durieux, L. W. Shao, Y. Tian, H. E. Kim, S. Wolff, Y. Liu and A. Dillin (2016). "Neuroendocrine Coordination of Mitochondrial Stress Signaling and Proteostasis." Cell **166**(6): 1553-1563 e1510.

Bonora, E., A. M. Porcelli, G. Gasparre, A. Biondi, A. Ghelli, V. Carelli, A. Baracca, G. Tallini, A. Martinuzzi, G. Lenaz, M. Rugolo and G. Romeo (2006). "Defective oxidative phosphorylation in thyroid oncocytic carcinoma is associated with pathogenic mitochondrial DNA mutations affecting complexes I and III." Cancer Res **66**(12): 6087-6096.

Boroughs, L. K. and R. J. DeBerardinis (2015). "Metabolic pathways promoting cancer cell survival and growth." Nat Cell Biol **17**(4): 351-359.

Brencic, A., K. A. McFarland, H. R. McManus, S. Castang, I. Mogno, S. L. Dove and S. Lory (2009). "The GacS/GacA signal transduction system of Pseudomonas aeruginosa acts exclusively through its control over the transcription of the RsmY and RsmZ regulatory small RNAs." Mol Microbiol **73**(3): 434-445.

Brown, G. C. (1992). "Control of respiration and ATP synthesis in mammalian mitochondria and cells." Biochem J **284 (Pt 1)**: 1-13.

Bruce, M. C., V. Kanelis, F. Fouladkou, A. Debonneville, O. Staub and D. Rotin (2008). "Regulation of Nedd4-2 self-ubiquitination and stability by a PY motif located within its HECT-domain." Biochem J **415**(1): 155-163.

Bulua, A. C., A. Simon, R. Maddipati, M. Pelletier, H. Park, K. Y. Kim, M. N. Sack, D. L. Kastner and R. M. Siegel (2011). "Mitochondrial reactive oxygen species promote production of proinflammatory cytokines and are elevated in TNFR1-associated periodic syndrome (TRAPS)." J Exp Med **208**(3): 519-533.

Cano, M., L. Wang, J. Wan, B. P. Barnett, K. Ebrahimi, J. Qian and J. T. Handa (2014). "Oxidative stress induces mitochondrial dysfunction and a protective unfolded protein response in RPE cells." Free Radic Biol Med **69**: 1-14.

Carrano, A. C., A. Dillin and T. Hunter (2014). "A Kruppel-like factor downstream of the E3 ligase WWP-1 mediates dietary-restriction-induced longevity in Caenorhabditis elegans." Nat Commun **5**: 3772.

Cerami, E., J. Gao, U. Dogrusoz, B. E. Gross, S. O. Sumer, B. A. Aksoy, A. Jacobsen, C. J. Byrne, M. L. Heuer, E. Larsson, Y. Antipin, B. Reva, A. P. Goldberg, C. Sander and N. Schultz (2012). "The cBio cancer genomics portal: an open platform for exploring multidimensional cancer genomics data." Cancer Discov **2**(5): 401-404.

Cezairliyan, B., N. Vinayavekhin, D. Grenfell-Lee, G. J. Yuen, A. Saghatelian and F. M. Ausubel (2013). "Identification of Pseudomonas aeruginosa phenazines that kill Caenorhabditis elegans." PLoS Pathog **9**(1): e1003101.

Cizkova, A., V. Stranecky, R. Ivanek, H. Hartmannova, L. Noskova, L. Piherova, M. Tesarova, H. Hansikova, T. Honzik, J. Zeman, P. Divina, A. Potocka, J. Paul, W. Sperl, J. A. Mayr, S. Seneca, J. Houstek and S. Kmoch (2008). "Development of a human mitochondrial oligonucleotide microarray (h-MitoArray) and gene expression analysis of fibroblast cell lines from 13 patients with isolated F1Fo ATP synthase deficiency." BMC Genomics **9**: 38.

Cocheme, H. M. and M. P. Murphy (2008). "Complex I is the major site of mitochondrial superoxide production by paraquat." J Biol Chem **283**(4): 1786-1798.

Cole, A., Z. Wang, E. Coyaud, V. Voisin, M. Gronda, Y. Jitkova, R. Mattson, R. Hurren, S. Babovic, N. Maclean, I. Restall, X. Wang, D. V. Jeyaraju, M. A. Sukhai, S. Prabha, S. Bashir, A. Ramakrishnan, E. Leung, Y. H. Qia, N. Zhang, K. R. Combes, T. Ketela, F. Lin, W. A. Houry, A. Aman, R. Al-Awar, W. Zheng, E. Wienholds, C. J. Xu, J. Dick, J. C. Wang, J. Moffat, M. D. Minden, C. J. Eaves, G. D. Bader, Z. Hao, S. M. Kornblau, B. Raught and A. D. Schimmer (2015). "Inhibition of the Mitochondrial Protease ClpP as a Therapeutic Strategy for Human Acute Myeloid Leukemia." Cancer Cell **27**(6): 864-876.

Czarnecka, A. M., C. Campanella, G. Zummo and F. Cappello (2006). "Mitochondrial chaperones in cancer: from molecular biology to clinical diagnostics." Cancer Biol Ther **5**(7): 714-720.

Dang, L., D. W. White, S. Gross, B. D. Bennett, M. A. Bittinger, E. M. Driggers, V. R. Fantin, H. G. Jang, S. Jin, M. C. Keenan, K. M. Marks, R. M. Prins, P. S. Ward, K. E. Yen, L. M. Liau, J. D. Rabinowitz, L. C. Cantley, C. B. Thompson, M. G. Vander Heiden and S. M. Su (2010). "Cancer-associated IDH1 mutations produce 2-hydroxyglutarate." Nature **465**(7300): 966.

Dasgupta, S., M. O. Hoque, S. Upadhyay and D. Sidransky (2009). "Forced cytochrome B gene mutation expression induces mitochondrial proliferation and prevents apoptosis in human uroepithelial SV-HUC-1 cells." Int J Cancer **125**(12): 2829-2835.

de Souza, J. T., M. Mazzola and J. M. Raaijmakers (2003). "Conservation of the response regulator gene gacA in Pseudomonas species." Environ Microbiol **5**(12): 1328-1340.

Deichmann, M., B. Kahle, A. Benner, M. Thome, B. Helmke and H. Naher (2004). "Somatic mitochondrial mutations in melanoma resection specimens." Int J Oncol **24**(1): 137-141.

Dickinson, A., K. Y. Yeung, J. Donoghue, M. J. Baker, R. D. Kelly, M. McKenzie, T. G. Johns and J. C. St John (2013). "The regulation of mitochondrial DNA copy number in glioblastoma cells." Cell Death Differ **20**(12): 1644-1653.

Dietrich, L. E., A. Price-Whelan, A. Petersen, M. Whiteley and D. K. Newman (2006). "The phenazine pyocyanin is a terminal signalling factor in the quorum sensing network of Pseudomonas aeruginosa." Mol Microbiol **61**(5): 1308-1321.

Dillin, A., A. L. Hsu, N. Arantes-Oliveira, J. Lehrer-Graiwer, H. Hsin, A. G. Fraser, R. S. Kamath, J. Ahringer and C. Kenyon (2002). "Rates of behavior and aging specified by mitochondrial function during development." Science **298**(5602): 2398-2401.

Dogan, S. A., C. Pujol, P. Maiti, A. Kukat, S. Wang, S. Hermans, K. Senft, R. Wibom, E. I. Rugarli and A. Trifunovic (2014). "Tissue-specific loss of DARS2 activates stress responses independently of respiratory chain deficiency in the heart." Cell Metab **19**(3): 458-469.

Durieux, J., S. Wolff and A. Dillin (2011). "The cell-non-autonomous nature of electron transport chain-mediated longevity." Cell **144**(1): 79-91.

Emerson, J., M. Rosenfeld, S. McNamara, B. Ramsey and R. L. Gibson (2002). "Pseudomonas aeruginosa and other predictors of mortality and morbidity in young children with cystic fibrosis." Pediatr Pulmonol **34**(2): 91-100.

Endo, J., M. Sano, T. Katayama, T. Hishiki, K. Shinmura, S. Morizane, T. Matsuhashi, Y. Katsumata, Y. Zhang, H. Ito, Y. Nagahata, S. Marchitti, K. Nishimaki, A. M. Wolf, H. Nakanishi, F. Hattori, V. Vasiliou, T. Adachi, I. Ohsawa, R. Taguchi, Y. Hirabayashi, S. Ohta, M. Suematsu, S. Ogawa and K. Fukuda (2009). "Metabolic remodeling induced by mitochondrial aldehyde stress stimulates tolerance to oxidative stress in the heart." Circ Res **105**(11): 1118-1127.

Evans, E. A., T. Kawli and M. W. Tan (2008). "Pseudomonas aeruginosa suppresses host immunity by activating the DAF-2 insulin-like signaling pathway in Caenorhabditis elegans." PLoS Pathog **4**(10): e1000175.

Evans, S. A., S. M. Turner, B. J. Bosch, C. C. Hardy and M. A. Woodhead (1996). "Lung function in bronchiectasis: the influence of Pseudomonas aeruginosa." Eur Respir J **9**(8): 1601-1604.

Ewbank, J. J., T. M. Barnes, B. Lakowski, M. Lussier, H. Bussey and S. Hekimi (1997). "Structural and functional conservation of the Caenorhabditis elegans timing gene clk-1." Science **275**(5302): 980-983.

Feng, J., F. Bussiere and S. Hekimi (2001). "Mitochondrial electron transport is a key determinant of life span in Caenorhabditis elegans." Dev Cell **1**(5): 633-644.

Fiorese, C. J., A. M. Schulz, Y. F. Lin, N. Rosin, M. W. Pellegrino and C. M. Haynes (2016). "The Transcription Factor ATF5 Mediates a Mammalian Mitochondrial UPR." Curr Biol **26**(15): 2037-2043.

Gallagher, L. A. and C. Manoil (2001). "Pseudomonas aeruginosa PAO1 kills Caenorhabditis elegans by cyanide poisoning." J Bacteriol **183**(21): 6207-6214.

Gao, J., B. A. Aksoy, U. Dogrusoz, G. Dresdner, B. Gross, S. O. Sumer, Y. Sun, A. Jacobsen, R. Sinha, E. Larsson, E. Cerami, C. Sander and N. Schultz (2013). "Integrative analysis of complex cancer genomics and clinical profiles using the cBioPortal." Sci Signal **6**(269): pl1.

Gariani, K., K. J. Menzies, D. Ryu, C. J. Wegner, X. Wang, E. R. Ropelle, N. Moullan, H. Zhang, A. Perino, V. Lemos, B. Kim, Y. K. Park, A. Piersigilli, T. X. Pham, Y. Yang, C. S. Ku, S. I. Koo, A. Fomitchova, C. Canto, K. Schoonjans, A. A. Sauve, J. Y. Lee and J. Auwerx (2016). "Eliciting the mitochondrial unfolded protein response by nicotinamide adenine dinucleotide repletion reverses fatty liver disease in mice." Hepatology **63**(4): 1190-1204.

Garsin, D. A., J. M. Villanueva, J. Begun, D. H. Kim, C. D. Sifri, S. B. Calderwood, G. Ruvkun and F. M. Ausubel (2003). "Long-lived C. elegans daf-2 mutants are resistant to bacterial pathogens." Science **300**(5627): 1921.

Gasparre, G., E. Hervouet, E. de Laplanche, J. Demont, L. F. Pennisi, M. Colombel, F. Mege-Lechevallier, J. Y. Scoazec, E. Bonora, R. Smeets, J. Smeitink, V. Lazar, J. Lespinasse, S. Giraud, C. Godinot, G. Romeo and H. Simonnet (2008). "Clonal expansion

of mutated mitochondrial DNA is associated with tumor formation and complex I deficiency in the benign renal oncocytoma." Hum Mol Genet **17**(7): 986-995.

Gaude, E. and C. Frezza (2014). "Defects in mitochondrial metabolism and cancer." Cancer Metab **2**: 10.

Gems, D. and L. Partridge (2013). "Genetics of longevity in model organisms: debates and paradigm shifts." Annu Rev Physiol **75**: 621-644.

Goard, C. A. and A. D. Schimmer (2014). "Mitochondrial matrix proteases as novel therapeutic targets in malignancy." Oncogene **33**(21): 2690-2699.

Hansen, M. B., C. Mitchelmore, K. M. Kjaerulff, T. E. Rasmussen, K. M. Pedersen and N. A. Jensen (2002). "Mouse Atf5: molecular cloning of two novel mRNAs, genomic organization, and odorant sensory neuron localization." Genomics **80**(3): 344-350.

Harman, D. (1956). "Aging: a theory based on free radical and radiation chemistry." J Gerontol **11**(3): 298-300.

Hartl, F. U. (1996). "Molecular chaperones in cellular protein folding." Nature **381**(6583): 571-579.

Hartl, F. U., N. Pfanner, D. W. Nicholson and W. Neupert (1989). "Mitochondrial protein import." Biochim Biophys Acta **988**(1): 1-45.

Harvey, K. F. and S. Kumar (1999). "Nedd4-like proteins: an emerging family of ubiquitin-protein ligases implicated in diverse cellular functions." Trends Cell Biol **9**(5): 166-169.

Haynes, C. M., Y. Yang, S. P. Blais, T. A. Neubert and D. Ron (2010). "The matrix peptide exporter HAF-1 signals a mitochondrial UPR by activating the transcription factor ZC376.7 in C. elegans." Mol Cell **37**(4): 529-540.

Heeb, S. and D. Haas (2001). "Regulatory roles of the GacS/GacA two-component system in plant-associated and other gram-negative bacteria." Mol Plant Microbe Interact **14**(12): 1351-1363.

Hernandez, I. H., J. Torres-Peraza, M. Santos-Galindo, E. Ramos-Moron, M. R. Fernandez-Fernandez, M. J. Perez-Alvarez, A. Miranda-Vizuete and J. J. Lucas (2017).

"The neuroprotective transcription factor ATF5 is decreased and sequestered into polyglutamine inclusions in Huntington's disease." Acta Neuropathol **134**(6): 839-850.

Hoogenraad, N. J., L. A. Ward and M. T. Ryan (2002). "Import and assembly of proteins into mitochondria of mammalian cells." Biochim Biophys Acta **1592**(1): 97-105.

Houtkooper, R. H., L. Mouchiroud, D. Ryu, N. Moullan, E. Katsyuba, G. Knott, R. W. Williams and J. Auwerx (2013). "Mitonuclear protein imbalance as a conserved longevity mechanism." Nature **497**(7450): 451-457.

Infantino, V., P. Convertini, L. Cucci, M. A. Panaro, M. A. Di Noia, R. Calvello, F. Palmieri and V. Iacobazzi (2011). "The mitochondrial citrate carrier: a new player in inflammation." Biochem J **438**(3): 433-436.

Isaacs, J. S., Y. J. Jung, D. R. Mole, S. Lee, C. Torres-Cabala, Y. L. Chung, M. Merino, J. Trepel, B. Zbar, J. Toro, P. J. Ratcliffe, W. M. Linehan and L. Neckers (2005). "HIF overexpression correlates with biallelic loss of fumarate hydratase in renal cancer: novel role of fumarate in regulation of HIF stability." Cancer Cell **8**(2): 143-153.

Ishikawa, K., K. Takenaga, M. Akimoto, N. Koshikawa, A. Yamaguchi, H. Imanishi, K. Nakada, Y. Honma and J. Hayashi (2008). "ROS-generating mitochondrial DNA mutations can regulate tumor cell metastasis." Science **320**(5876): 661-664.

Ito, K. and T. Suda (2014). "Metabolic requirements for the maintenance of self-renewing stem cells." Nat Rev Mol Cell Biol **15**(4): 243-256.

Janssen-Heininger, Y. M., B. T. Mossman, N. H. Heintz, H. J. Forman, B. Kalyanaraman, T. Finkel, J. S. Stamler, S. G. Rhee and A. van der Vliet (2008). "Redox-based regulation of signal transduction: principles, pitfalls, and promises." Free Radic Biol Med **45**(1): 1-17.

Jay, J. W., P.D. (1987). "Krebs' Citric Acid Cycle-Half a Century and Still Turning." Biochemical Society Symposia.

Jendrossek, V., H. Grassme, I. Mueller, F. Lang and E. Gulbins (2001). "Pseudomonas aeruginosa-induced apoptosis involves mitochondria and stress-activated protein kinases." Infect Immun **69**(4): 2675-2683.

Jinek, M., K. Chylinski, I. Fonfara, M. Hauer, J. A. Doudna and E. Charpentier (2012). "A programmable dual-RNA-guided DNA endonuclease in adaptive bacterial immunity." Science **337**(6096): 816-821.

Jovaisaite, V. and J. Auwerx (2015). "The mitochondrial unfolded protein response-synchronizing genomes." Curr Opin Cell Biol **33**: 74-81.

Kang, D., D. R. Kirienko, P. Webster, A. L. Fisher and N. V. Kirienko (2018). "Pyoverdine, a siderophore from Pseudomonas aeruginosa, translocates into C. elegans, removes iron, and activates a distinct host response." Virulence **9**(1): 804-817.

Karpel-Massler, G., B. A. Horst, C. Shu, L. Chau, T. Tsujiuchi, J. N. Bruce, P. Canoll, L. A. Greene, J. M. Angelastro and M. D. Siegelin (2016). "A Synthetic Cell-Penetrating Dominant-Negative ATF5 Peptide Exerts Anticancer Activity against a Broad Spectrum of Treatment-Resistant Cancers." Clin Cancer Res **22**(18): 4698-4711.

Kasahara, A. and L. Scorrano (2014). "Mitochondria: from cell death executioners to regulators of cell differentiation." Trends Cell Biol **24**(12): 761-770.

Kato, Y., T. Aizawa, H. Hoshino, K. Kawano, K. Nitta and H. Zhang (2002). "abf-1 and abf-2, ASABF-type antimicrobial peptide genes in Caenorhabditis elegans." Biochem J **361**(Pt 2): 221-230.

Kim, D. H., N. T. Liberati, T. Mizuno, H. Inoue, N. Hisamoto, K. Matsumoto and F. M. Ausubel (2004). "Integration of Caenorhabditis elegans MAPK pathways mediating immunity and stress resistance by MEK-1 MAPK kinase and VHP-1 MAPK phosphatase." Proc Natl Acad Sci U S A **101**(30): 10990-10994.

Kim, K. H., Y. T. Jeong, H. Oh, S. H. Kim, J. M. Cho, Y. N. Kim, S. S. Kim, D. H. Kim, K. Y. Hur, H. K. Kim, T. Ko, J. Han, H. L. Kim, J. Kim, S. H. Back, M. Komatsu, H. Chen, D. C. Chan, M. Konishi, N. Itoh, C. S. Choi and M. S. Lee (2013). "Autophagy deficiency leads to protection from obesity and insulin resistance by inducing Fgf21 as a mitokine." Nat Med **19**(1): 83-92.

Kim, K. H. and M. S. Lee (2014). "FGF21 as a Stress Hormone: The Roles of FGF21 in Stress Adaptation and the Treatment of Metabolic Diseases." Diabetes Metab J **38**(4): 245-251.

Kirkwood, T. B. (2005). "Understanding the odd science of aging." Cell **120**(4): 437-447.

Koopman, M., H. Michels, B. M. Dancy, R. Kamble, L. Mouchiroud, J. Auwerx, E. A. Nollen and R. H. Houtkooper (2016). "A screening-based platform for the assessment of cellular respiration in Caenorhabditis elegans." Nat Protoc **11**(10): 1798-1816.

Koshiba, T., K. Yasukawa, Y. Yanagi and S. Kawabata (2011). "Mitochondrial membrane potential is required for MAVS-mediated antiviral signaling." Sci Signal **4**(158): ra7.

Kujoth, G. C., A. Hiona, T. D. Pugh, S. Someya, K. Panzer, S. E. Wohlgemuth, T. Hofer, A. Y. Seo, R. Sullivan, W. A. Jobling, J. D. Morrow, H. Van Remmen, J. M. Sedivy, T. Yamasoba, M. Tanokura, R. Weindruch, C. Leeuwenburgh and T. A. Prolla (2005). "Mitochondrial DNA mutations, oxidative stress, and apoptosis in mammalian aging." Science **309**(5733): 481-484.

Kumar, H., T. Kawai and S. Akira (2011). "Pathogen recognition by the innate immune system." International reviews of immunology **30**(1): 16-34.

Larman, T. C., S. R. DePalma, A. G. Hadjipanayis, N. Cancer Genome Atlas Research, A. Protopopov, J. Zhang, S. B. Gabriel, L. Chin, C. E. Seidman, R. Kucherlapati and J. G. Seidman (2012). "Spectrum of somatic mitochondrial mutations in five cancers." Proc Natl Acad Sci U S A **109**(35): 14087-14091.

Lau, G. W., D. J. Hassett, H. Ran and F. Kong (2004). "The role of pyocyanin in Pseudomonas aeruginosa infection." Trends Mol Med **10**(12): 599-606.

Laukka, T., C. J. Mariani, T. Ihantola, J. Z. Cao, J. Hokkanen, W. G. Kaelin, Jr., L. A. Godley and P. Koivunen (2016). "Fumarate and Succinate Regulate Expression of Hypoxia-inducible Genes via TET Enzymes." J Biol Chem **291**(8): 4256-4265.

LeBleu, V. S., J. T. O'Connell, K. N. Gonzalez Herrera, H. Wikman, K. Pantel, M. C. Haigis, F. M. de Carvalho, A. Damascena, L. T. Domingos Chinen, R. M. Rocha, J. M. Asara and R. Kalluri (2014). "PGC-1alpha mediates mitochondrial biogenesis and oxidative phosphorylation in cancer cells to promote metastasis." Nat Cell Biol **16**(10): 992-1003, 1001-1015.

Lee, D. G., J. M. Urbach, G. Wu, N. T. Liberati, R. L. Feinbaum, S. Miyata, L. T. Diggins, J. He, M. Saucier, E. Deziel, L. Friedman, L. Li, G. Grills, K. Montgomery, R. Kucherlapati, L. G. Rahme and F. M. Ausubel (2006). "Genomic analysis reveals that Pseudomonas aeruginosa virulence is combinatorial." Genome Biol **7**(10): R90.

Lee, S. J., A. B. Hwang and C. Kenyon (2010). "Inhibition of respiration extends C. elegans life span via reactive oxygen species that increase HIF-1 activity." Curr Biol **20**(23): 2131-2136.

Lee, S. S., R. Y. Lee, A. G. Fraser, R. S. Kamath, J. Ahringer and G. Ruvkun (2003). "A systematic RNAi screen identifies a critical role for mitochondria in C. elegans longevity." Nat Genet **33**(1): 40-48.

Lemasters, J. J. (2005). "Selective mitochondrial autophagy, or mitophagy, as a targeted defense against oxidative stress, mitochondrial dysfunction, and aging." Rejuvenation Res **8**(1): 3-5.

Liberati, N. T., J. M. Urbach, S. Miyata, D. G. Lee, E. Drenkard, G. Wu, J. Villanueva, T. Wei and F. M. Ausubel (2006). "An ordered, nonredundant library of Pseudomonas aeruginosa strain PA14 transposon insertion mutants." Proc Natl Acad Sci U S A **103**(8): 2833-2838.

Lill, R. and U. Muhlenhoff (2008). "Maturation of iron-sulfur proteins in eukaryotes: mechanisms, connected processes, and diseases." Annu Rev Biochem **77**: 669-700.

Lin, M. T. and M. F. Beal (2006). "Mitochondrial dysfunction and oxidative stress in neurodegenerative diseases." Nature **443**(7113): 787-795.

Lin, Y. F., A. M. Schulz, M. W. Pellegrino, Y. Lu, S. Shaham and C. M. Haynes (2016). "Maintenance and propagation of a deleterious mitochondrial genome by the mitochondrial unfolded protein response." Nature **533**(7603): 416-419.

Liu, L., D. R. Wise, J. A. Diehl and M. C. Simon (2008). "Hypoxic reactive oxygen species regulate the integrated stress response and cell survival." J Biol Chem **283**(45): 31153-31162.

Liu, X., N. Jiang, B. Hughes, E. Bigras, E. Shoubridge and S. Hekimi (2005). "Evolutionary conservation of the clk-1-dependent mechanism of longevity: loss of mclk1 increases cellular fitness and lifespan in mice." Genes Dev **19**(20): 2424-2434.

Liu, X., C. N. Kim, J. Yang, R. Jemmerson and X. Wang (1996). "Induction of apoptotic program in cell-free extracts: requirement for dATP and cytochrome c." Cell **86**(1): 147-157.

Liu, X., C. Pei, S. Yan, G. Liu, G. Liu, W. Chen, Y. Cui and Y. Liu (2015). "NADPH oxidase 1-dependent ROS is crucial for TLR4 signaling to promote tumor metastasis of non-small cell lung cancer." Tumour Biol **36**(3): 1493-1502.

Liu, Y., B. S. Samuel, P. C. Breen and G. Ruvkun (2014). "Caenorhabditis elegans pathways that surveil and defend mitochondria." Nature **508**(7496): 406-410.

Liu, Z. and R. A. Butow (2006). "Mitochondrial retrograde signaling." Annu Rev Genet **40**: 159-185.

Lopez-Otin, C., M. A. Blasco, L. Partridge, M. Serrano and G. Kroemer (2013). "The hallmarks of aging." Cell **153**(6): 1194-1217.

Losman, J. A., R. E. Looper, P. Koivunen, S. Lee, R. K. Schneider, C. McMahon, G. S. Cowley, D. E. Root, B. L. Ebert and W. G. Kaelin, Jr. (2013). "(R)-2-hydroxyglutarate is sufficient to promote leukemogenesis and its effects are reversible." Science **339**(6127): 1621-1625.

Lowell, B. B. and G. I. Shulman (2005). "Mitochondrial dysfunction and type 2 diabetes." Science **307**(5708): 384-387.

Ma, C., M. E. Wickham, J. A. Guttman, W. Deng, J. Walker, K. L. Madsen, K. Jacobson, W. A. Vogl, B. B. Finlay and B. A. Vallance (2006). "Citrobacter rodentium infection causes both mitochondrial dysfunction and intestinal epithelial barrier disruption in vivo: role of mitochondrial associated protein (Map)." Cell Microbiol **8**(10): 1669-1686.

Mahajan-Miklos, S., M. W. Tan, L. G. Rahme and F. M. Ausubel (1999). "Molecular mechanisms of bacterial virulence elucidated using a Pseudomonas aeruginosa-Caenorhabditis elegans pathogenesis model." Cell **96**(1): 47-56.

Mahla, R. S., M. C. Reddy, D. V. Prasad and H. Kumar (2013). "Sweeten PAMPs: Role of Sugar Complexed PAMPs in Innate Immunity and Vaccine Biology." Front Immunol **4**: 248.

Manago, A., K. A. Becker, A. Carpinteiro, B. Wilker, M. Soddemann, A. P. Seitz, M. J. Edwards, H. Grassme, I. Szabo and E. Gulbins (2015). "Pseudomonas aeruginosa pyocyanin induces neutrophil death via mitochondrial reactive oxygen species and mitochondrial acid sphingomyelinase." Antioxid Redox Signal **22**(13): 1097-1110.

Martin, J. (1997). "Molecular chaperones and mitochondrial protein folding." J Bioenerg Biomembr **29**(1): 35-43.

Martinez, B. A., D. A. Petersen, A. L. Gaeta, S. P. Stanley, G. A. Caldwell and K. A. Caldwell (2017). "Dysregulation of the Mitochondrial Unfolded Protein Response Induces Non-Apoptotic Dopaminergic Neurodegeneration in C. elegans Models of Parkinson's Disease." J Neurosci **37**(46): 11085-11100.

Martinus, R. D., G. P. Garth, T. L. Webster, P. Cartwright, D. J. Naylor, P. B. Hoj and N. J. Hoogenraad (1996). "Selective induction of mitochondrial chaperones in response to loss of the mitochondrial genome." Eur J Biochem **240**(1): 98-103.

Mello, C. and A. Fire (1995). "DNA transformation." Methods Cell Biol **48**: 451-482.

Miller, F. J., F. L. Rosenfeldt, C. Zhang, A. W. Linnane and P. Nagley (2003). "Precise determination of mitochondrial DNA copy number in human skeletal and cardiac muscle by a PCR-based assay: lack of change of copy number with age." Nucleic Acids Res **31**(11): e61.

Mizuno, T., N. Hisamoto, T. Terada, T. Kondo, M. Adachi, E. Nishida, D. H. Kim, F. M. Ausubel and K. Matsumoto (2004). "The Caenorhabditis elegans MAPK phosphatase VHP-1 mediates a novel JNK-like signaling pathway in stress response." EMBO J **23**(11): 2226-2234.

Mohrin, M., J. Shin, Y. Liu, K. Brown, H. Luo, Y. Xi, C. M. Haynes and D. Chen (2015). "Stem cell aging. A mitochondrial UPR-mediated metabolic checkpoint regulates hematopoietic stem cell aging." Science **347**(6228): 1374-1377.

Moreira, P. I., C. Carvalho, X. Zhu, M. A. Smith and G. Perry (2010). "Mitochondrial dysfunction is a trigger of Alzheimer's disease pathophysiology." Biochim Biophys Acta **1802**(1): 2-10.

Morrison, A. J., Jr. and R. P. Wenzel (1984). "Epidemiology of infections due to Pseudomonas aeruginosa." Rev Infect Dis **6 Suppl 3**: S627-642.

Munch, C. and J. W. Harper (2016). "Mitochondrial unfolded protein response controls matrix pre-RNA processing and translation." Nature **534**(7609): 710-713.

Munkacsy, E. and S. L. Rea (2014). "The paradox of mitochondrial dysfunction and extended longevity." Exp Gerontol **56**: 221-233.

Nakai, K. and P. Horton (1999). "PSORT: a program for detecting sorting signals in proteins and predicting their subcellular localization." Trends Biochem Sci **24**(1): 34-36.

Nargund, A. M., C. J. Fiorese, M. W. Pellegrino, P. Deng and C. M. Haynes (2015). "Mitochondrial and nuclear accumulation of the transcription factor ATFS-1 promotes OXPHOS recovery during the UPR(mt)." Mol Cell **58**(1): 123-133.

Nargund, A. M., M. W. Pellegrino, C. J. Fiorese, B. M. Baker and C. M. Haynes (2012). "Mitochondrial import efficiency of ATFS-1 regulates mitochondrial UPR activation." Science **337**(6094): 587-590.

Naviaux, R. K., W. L. Nyhan, B. A. Barshop, J. Poulton, D. Markusic, N. C. Karpinski and R. H. Haas (1999). "Mitochondrial DNA polymerase gamma deficiency and mtDNA depletion in a child with Alpers' syndrome." Ann Neurol **45**(1): 54-58.

Neft, N. and T. M. Farley (1972). "Conditions influencing antimycin production by a Streptomyces species grown in chemically defined medium." Antimicrob Agents Chemother **1**(3): 274-276.

Obregon, D., H. Hou, J. Deng, B. Giunta, J. Tian, D. Darlington, M. Shahaduzzaman, Y. Zhu, T. Mori, M. P. Mattson and J. Tan (2012). "Soluble amyloid precursor protein-alpha modulates beta-secretase activity and amyloid-beta generation." Nat Commun **3**: 777.

Osman, C., D. R. Voelker and T. Langer (2011). "Making heads or tails of phospholipids in mitochondria." J Cell Biol **192**(1): 7-16.

Ostermann, J., A. L. Horwich, W. Neupert and F. U. Hartl (1989). "Protein folding in mitochondria requires complex formation with hsp60 and ATP hydrolysis." Nature **341**(6238): 125-130.

Owusu-Ansah, E., W. Song and N. Perrimon (2013). "Muscle mitohormesis promotes longevity via systemic repression of insulin signaling." Cell **155**(3): 699-712.

Paix, A., A. Folkmann, D. Rasoloson and G. Seydoux (2015). "High Efficiency, Homology-Directed Genome Editing in Caenorhabditis elegans Using CRISPR-Cas9 Ribonucleoprotein Complexes." Genetics **201**(1): 47-54.

Parrish, J., L. Li, K. Klotz, D. Ledwich, X. Wang and D. Xue (2001). "Mitochondrial endonuclease G is important for apoptosis in C. elegans." Nature **412**(6842): 90-94.

Pellegrino, M. W., A. M. Nargund, N. V. Kirienko, R. Gillis, C. J. Fiorese and C. M. Haynes (2014). "Mitochondrial UPR-regulated innate immunity provides resistance to pathogen infection." Nature **516**(7531): 414-417.

Petros, J. A., A. K. Baumann, E. Ruiz-Pesini, M. B. Amin, C. Q. Sun, J. Hall, S. Lim, M. M. Issa, W. D. Flanders, S. H. Hosseini, F. F. Marshall and D. C. Wallace (2005). "mtDNA mutations increase tumorigenicity in prostate cancer." Proc Natl Acad Sci U S A **102**(3): 719-724.

Pickart, C. M. (2001). "Mechanisms underlying ubiquitination." Annu Rev Biochem **70**: 503-533.

Pierson, L. S., 3rd and E. A. Pierson (2010). "Metabolism and function of phenazines in bacteria: impacts on the behavior of bacteria in the environment and biotechnological processes." Appl Microbiol Biotechnol **86**(6): 1659-1670.

Portal-Celhay, C., E. R. Bradley and M. J. Blaser (2012). "Control of intestinal bacterial proliferation in regulation of lifespan in Caenorhabditis elegans." BMC Microbiol **12**: 49.

Pukkila-Worley, R., R. L. Feinbaum, D. L. McEwan, A. L. Conery and F. M. Ausubel (2014). "The evolutionarily conserved mediator subunit MDT-15/MED15 links protective innate immune responses and xenobiotic detoxification." PLoS Pathog **10**(5): e1004143.

Rainbolt, T. K., N. Atanassova, J. C. Genereux and R. L. Wiseman (2013). "Stress-regulated translational attenuation adapts mitochondrial protein import through Tim17A degradation." Cell Metab **18**(6): 908-919.

Rauthan, M., P. Ranji, R. Abukar and M. Pilon (2015). "A Mutation in Caenorhabditis elegans NDUF-7 Activates the Mitochondrial Stress Response and Prolongs Lifespan via ROS and CED-4." G3 (Bethesda) **5**(8): 1639-1648.

Rauthan, M., P. Ranji, N. Aguilera Pradenas, C. Pitot and M. Pilon (2013). "The mitochondrial unfolded protein response activator ATFS-1 protects cells from inhibition of the mevalonate pathway." Proc Natl Acad Sci U S A **110**(15): 5981-5986.

Ray, A., C. Rentas, G. A. Caldwell and K. A. Caldwell (2015). "Phenazine derivatives cause proteotoxicity and stress in C. elegans." Neurosci Lett **584**: 23-27.

Ray, P. D., B. W. Huang and Y. Tsuji (2012). "Reactive oxygen species (ROS) homeostasis and redox regulation in cellular signaling." Cell Signal **24**(5): 981-990.

Rea, S. L., N. Ventura and T. E. Johnson (2007). "Relationship between mitochondrial electron transport chain dysfunction, development, and life extension in Caenorhabditis elegans." PLoS Biol **5**(10): e259.

Recinos, D. A., M. D. Sekedat, A. Hernandez, T. S. Cohen, H. Sakhtah, A. S. Prince, A. Price-Whelan and L. E. Dietrich (2012). "Redundant phenazine operons in Pseudomonas aeruginosa exhibit environment-dependent expression and differential roles in pathogenicity." Proc Natl Acad Sci U S A **109**(47): 19420-19425.

Reimmann, C., M. Beyeler, A. Latifi, H. Winteler, M. Foglino, A. Lazdunski and D. Haas (1997). "The global activator GacA of Pseudomonas aeruginosa PAO positively controls the production of the autoinducer N-butyryl-homoserine lactone and the formation of the virulence factors pyocyanin, cyanide, and lipase." Mol Microbiol **24**(2): 309-319.

Reinke, A. W., J. Baek, O. Ashenberg and A. E. Keating (2013). "Networks of bZIP protein-protein interactions diversified over a billion years of evolution." Science **340**(6133): 730-734.

Rodriguez-Torres, M. and A. L. Allan (2016). "Aldehyde dehydrogenase as a marker and functional mediator of metastasis in solid tumors." Clin Exp Metastasis **33**(1): 97-113.

Rotin, D. and S. Kumar (2009). "Physiological functions of the HECT family of ubiquitin ligases." Nat Rev Mol Cell Biol **10**(6): 398-409.

Rual, J. F., J. Ceron, J. Koreth, T. Hao, A. S. Nicot, T. Hirozane-Kishikawa, J. Vandenhaute, S. H. Orkin, D. E. Hill, S. van den Heuvel and M. Vidal (2004). "Toward improving Caenorhabditis elegans phenome mapping with an ORFeome-based RNAi library." Genome Res **14**(10B): 2162-2168.

Russell, A. P., V. C. Foletta, R. J. Snow and G. D. Wadley (2014). "Skeletal muscle mitochondria: a major player in exercise, health and disease." Biochim Biophys Acta **1840**(4): 1276-1284.

Ryall, B., J. C. Davies, R. Wilson, A. Shoemark and H. D. Williams (2008). "Pseudomonas aeruginosa, cyanide accumulation and lung function in CF and non-CF bronchiectasis patients." Eur Respir J **32**(3): 740-747.

Sabharwal, S. S. and P. T. Schumacker (2014). "Mitochondrial ROS in cancer: initiators, amplifiers or an Achilles' heel?" Nat Rev Cancer **14**(11): 709-721.

Sakaguchi, A., K. Matsumoto and N. Hisamoto (2004). "Roles of MAP kinase cascades in Caenorhabditis elegans." J Biochem **136**(1): 7-11.

Sanarico, A. G., C. Ronchini, A. Croce, E. M. Memmi, U. A. Cammarata, A. De Antoni, S. Lavorgna, M. Divona, L. Giaco, G. E. M. Melloni, A. Brendolan, G. Simonetti, G. Martinelli, P. Mancuso, F. Bertolini, F. L. Coco, G. Melino, P. G. Pelicci and F. Bernassola (2018). "The E3 ubiquitin ligase WWP1 sustains the growth of acute myeloid leukaemia." Leukemia **32**(4): 911-919.

Scandalios, J. G. (1993). "Oxygen Stress and Superoxide Dismutases." Plant Physiol **101**(1): 7-12.

Schatz, G. and B. Dobberstein (1996). "Common principles of protein translocation across membranes." Science **271**(5255): 1519-1526.

Schieber, M. and N. S. Chandel (2014). "TOR signaling couples oxygen sensing to lifespan in C. elegans." Cell Rep **9**(1): 9-15.

Schreiner, B., H. Westerburg, I. Forne, A. Imhof, W. Neupert and D. Mokranjac (2012). "Role of the AAA protease Yme1 in folding of proteins in the intermembrane space of mitochondria." Mol Biol Cell **23**(22): 4335-4346.

Schwarz, K., N. Siddiqi, S. Singh, C. J. Neil, D. K. Dawson and M. P. Frenneaux (2014). "The breathing heart - mitochondrial respiratory chain dysfunction in cardiac disease." Int J Cardiol **171**(2): 134-143.

Sciacovelli, M., G. Guzzo, V. Morello, C. Frezza, L. Zheng, N. Nannini, F. Calabrese, G. Laudiero, F. Esposito, M. Landriscina, P. Defilippi, P. Bernardi and A. Rasola (2013). "The mitochondrial chaperone TRAP1 promotes neoplastic growth by inhibiting succinate dehydrogenase." Cell Metab **17**(6): 988-999.

Selak, M. A., S. M. Armour, E. D. MacKenzie, H. Boulahbel, D. G. Watson, K. D. Mansfield, Y. Pan, M. C. Simon, C. B. Thompson and E. Gottlieb (2005). "Succinate links TCA cycle dysfunction to oncogenesis by inhibiting HIF-alpha prolyl hydroxylase." Cancer Cell **7**(1): 77-85.

Semenza, G. L. (2010). "HIF-1: upstream and downstream of cancer metabolism." Curr Opin Genet Dev **20**(1): 51-56.

Sena, L. A., S. Li, A. Jairaman, M. Prakriya, T. Ezponda, D. A. Hildeman, C. R. Wang, P. T. Schumacker, J. D. Licht, H. Perlman, P. J. Bryce and N. S. Chandel (2013). "Mitochondria are required for antigen-specific T cell activation through reactive oxygen species signaling." Immunity **38**(2): 225-236.

Seth, R. B., L. Sun, C. K. Ea and Z. J. Chen (2005). "Identification and characterization of MAVS, a mitochondrial antiviral signaling protein that activates NF-kappaB and IRF 3." Cell **122**(5): 669-682.

Shao, L. W., R. Niu and Y. Liu (2016). "Neuropeptide signals cell non-autonomous mitochondrial unfolded protein response." Cell Res **26**(11): 1182-1196.

Sharma, L. K., H. Fang, J. Liu, R. Vartak, J. Deng and Y. Bai (2011). "Mitochondrial respiratory complex I dysfunction promotes tumorigenesis through ROS alteration and AKT activation." Hum Mol Genet **20**(23): 4605-4616.

Shigenaga, M. K., T. M. Hagen and B. N. Ames (1994). "Oxidative damage and mitochondrial decay in aging." Proc Natl Acad Sci U S A **91**(23): 10771-10778.

Shimizu, Y. I., M. Morita, A. Ohmi, S. Aoyagi, H. Ebihara, D. Tonaki, Y. Horino, M. Iijima, H. Hirose, S. Takahashi and Y. Takahashi (2009). "Fasting induced up-regulation of activating transcription factor 5 in mouse liver." Life Sci **84**(25-26): 894-902.

Shin, D. Y., H. J. Shin, G. Y. Kim, J. Cheong, I. W. Choi, S. K. Kim, S. K. Moon, H. S. Kang and Y. H. Choi (2008). "Streptochlorin isolated from Streptomyces sp. Induces apoptosis in human hepatocarcinoma cells through a reactive oxygen species-mediated mitochondrial pathway." J Microbiol Biotechnol **18**(11): 1862-1868.

Simon, S. M., C. S. Peskin and G. F. Oster (1992). "What drives the translocation of proteins?" Proc Natl Acad Sci U S A **89**(9): 3770-3774.

Singh, K. K., V. Ayyasamy, K. M. Owens, M. S. Koul and M. Vujcic (2009). "Mutations in mitochondrial DNA polymerase-gamma promote breast tumorigenesis." J Hum Genet **54**(9): 516-524.

Stavru, F., F. Bouillaud, A. Sartori, D. Ricquier and P. Cossart (2011). "Listeria monocytogenes transiently alters mitochondrial dynamics during infection." Proc Natl Acad Sci U S A **108**(9): 3612-3617.

Subramaniam, S. R. and M. F. Chesselet (2013). "Mitochondrial dysfunction and oxidative stress in Parkinson's disease." Prog Neurobiol **106-107**: 17-32.

Swerdlow, R. H. and S. M. Khan (2004). "A "mitochondrial cascade hypothesis" for sporadic Alzheimer's disease." Med Hypotheses **63**(1): 8-20.

Taanman, J. W. (1999). "The mitochondrial genome: structure, transcription, translation and replication." Biochim Biophys Acta **1410**(2): 103-123.

Tan, A. S., J. W. Baty, L. F. Dong, A. Bezawork-Geleta, B. Endaya, J. Goodwin, M. Bajzikova, J. Kovarova, M. Peterka, B. Yan, E. A. Pesdar, M. Sobol, A. Filimonenko, S. Stuart, M. Vondrusova, K. Kluckova, K. Sachaphibulkij, J. Rohlena, P. Hozak, J. Truksa, D. Eccles, L. M. Haupt, L. R. Griffiths, J. Neuzil and M. V. Berridge (2015). "Mitochondrial genome acquisition restores respiratory function and tumorigenic potential of cancer cells without mitochondrial DNA." Cell Metab **21**(1): 81-94.

Tan, M. W., S. Mahajan-Miklos and F. M. Ausubel (1999). "Killing of Caenorhabditis elegans by Pseudomonas aeruginosa used to model mammalian bacterial pathogenesis." Proc Natl Acad Sci U S A **96**(2): 715-720.

Tatsuta, T. and T. Langer (2008). "Quality control of mitochondria: protection against neurodegeneration and ageing." EMBO J **27**(2): 306-314.

Thannickal, V. J. and B. L. Fanburg (2000). "Reactive oxygen species in cell signaling." Am J Physiol Lung Cell Mol Physiol **279**(6): L1005-1028.

Tian, Y., G. Garcia, Q. Bian, K. K. Steffen, L. Joe, S. Wolff, B. J. Meyer and A. Dillin (2016). "Mitochondrial Stress Induces Chromatin Reorganization to Promote Longevity and UPR(mt)." Cell **165**(5): 1197-1208.

Torres-Peraza, J. F., T. Engel, R. Martin-Ibanez, A. Sanz-Rodriguez, M. R. Fernandez-Fernandez, M. Esgleas, J. M. Canals, D. C. Henshall and J. J. Lucas (2013). "Protective neuronal induction of ATF5 in endoplasmic reticulum stress induced by status epilepticus." Brain **136**(Pt 4): 1161-1176.

Truscott, K. N., N. Wiedemann, P. Rehling, H. Muller, C. Meisinger, N. Pfanner and B. Guiard (2002). "Mitochondrial import of the ADP/ATP carrier: the essential TIM complex of the intermembrane space is required for precursor release from the TOM complex." Mol Cell Biol **22**(22): 7780-7789.

Tyynismaa, H., C. J. Carroll, N. Raimundo, S. Ahola-Erkkila, T. Wenz, H. Ruhanen, K. Guse, A. Hemminki, K. E. Peltola-Mjosund, V. Tulkki, M. Oresic, C. T. Moraes, K. Pietilainen, I. Hovatta and A. Suomalainen (2010). "Mitochondrial myopathy induces a starvation-like response." Hum Mol Genet **19**(20): 3948-3958.

Uekusa, H., M. Namimatsu, Y. Hiwatashi, T. Akimoto, T. Nishida, S. Takahashi and Y. Takahashi (2009). "Cadmium interferes with the degradation of ATF5 via a post-ubiquitination step of the proteasome degradation pathway." Biochem Biophys Res Commun **380**(3): 673-678.

Vijg, J. and J. Campisi (2008). "Puzzles, promises and a cure for ageing." Nature **454**(7208): 1065-1071.

Wachsmuth, M., A. Hubner, M. Li, B. Madea and M. Stoneking (2016). "Age-Related and Heteroplasmy-Related Variation in Human mtDNA Copy Number." PLoS Genet **12**(3): e1005939.

Wang, X., W. Wang, L. Li, G. Perry, H. G. Lee and X. Zhu (2014). "Oxidative stress and mitochondrial dysfunction in Alzheimer's disease." Biochim Biophys Acta **1842**(8): 1240-1247.

Warburg, O., F. Wind and E. Negelein (1927). "The Metabolism of Tumors in the Body." J Gen Physiol **8**(6): 519-530.

Watatani, Y., N. Kimura, Y. I. Shimizu, I. Akiyama, D. Tonaki, H. Hirose, S. Takahashi and Y. Takahashi (2007). "Amino acid limitation induces expression of ATF5 mRNA at the post-transcriptional level." Life Sci **80**(9): 879-885.

Watts, J. L. and J. Browse (2000). "A palmitoyl-CoA-specific delta9 fatty acid desaturase from Caenorhabditis elegans." Biochem Biophys Res Commun **272**(1): 263-269.

Weinberg, F., R. Hamanaka, W. W. Wheaton, S. Weinberg, J. Joseph, M. Lopez, B. Kalyanaraman, G. M. Mutlu, G. R. Budinger and N. S. Chandel (2010). "Mitochondrial metabolism and ROS generation are essential for Kras-mediated tumorigenicity." Proc Natl Acad Sci U S A **107**(19): 8788-8793.

Weinberg, S. E., L. A. Sena and N. S. Chandel (2015). "Mitochondria in the regulation of innate and adaptive immunity." Immunity **42**(3): 406-417.

West, A. P., G. S. Shadel and S. Ghosh (2011). "Mitochondria in innate immune responses." Nat Rev Immunol **11**(6): 389-402.

White, M. J., K. McArthur, D. Metcalf, R. M. Lane, J. C. Cambier, M. J. Herold, M. F. van Delft, S. Bedoui, G. Lessene, M. E. Ritchie, D. C. Huang and B. T. Kile (2014). "Apoptotic caspases suppress mtDNA-induced STING-mediated type I IFN production." Cell **159**(7): 1549-1562.

Willhite, D. C. and S. R. Blanke (2004). "Helicobacter pylori vacuolating cytotoxin enters cells, localizes to the mitochondria, and induces mitochondrial membrane permeability changes correlated to toxin channel activity." Cell Microbiol **6**(2): 143-154.

Wong, A., P. Boutis and S. Hekimi (1995). "Mutations in the clk-1 gene of Caenorhabditis elegans affect developmental and behavioral timing." Genetics **139**(3): 1247-1259.

Wood, R. E. (1976). "Pseudomonas: the compromised host." Hosp Pract **11**(8): 91-100.

Wright, G., K. Terada, M. Yano, I. Sergeev and M. Mori (2001). "Oxidative stress inhibits the mitochondrial import of preproteins and leads to their degradation." Exp Cell Res **263**(1): 107-117.

Xia, D., C. A. Yu, H. Kim, J. Z. Xia, A. M. Kachurin, L. Zhang, L. Yu and J. Deisenhofer (1997). "Crystal structure of the cytochrome bc1 complex from bovine heart mitochondria." Science **277**(5322): 60-66.

Yap, Y. W., R. M. Llanos, S. La Fontaine, M. A. Cater, P. M. Beart and N. S. Cheung (2016). "Comparative Microarray Analysis Identifies Commonalities in Neuronal Injury: Evidence for Oxidative Stress, Dysfunction of Calcium Signalling, and Inhibition of Autophagy-Lysosomal Pathway." Neurochem Res **41**(3): 554-567.

Yoneda, T., C. Benedetti, F. Urano, S. G. Clark, H. P. Harding and D. Ron (2004). "Compartment-specific perturbation of protein handling activates genes encoding mitochondrial chaperones." J Cell Sci **117**(Pt 18): 4055-4066.

Youle, R. J. and D. P. Narendra (2011). "Mechanisms of mitophagy." Nat Rev Mol Cell Biol **12**(1): 9-14.

Youle, R. J. and A. M. van der Bliek (2012). "Mitochondrial fission, fusion, and stress." Science **337**(6098): 1062-1065.

Zhang, H., D. Ryu, Y. Wu, K. Gariani, X. Wang, P. Luan, D. D'Amico, E. R. Ropelle, M. P. Lutolf, R. Aebersold, K. Schoonjans, K. J. Menzies and J. Auwerx (2016). "NAD(+) repletion improves mitochondrial and stem cell function and enhances life span in mice." Science **352**(6292): 1436-1443.

Zhang, Q., M. Raoof, Y. Chen, Y. Sumi, T. Sursal, W. Junger, K. Brohi, K. Itagaki and C. J. Hauser (2010). "Circulating mitochondrial DAMPs cause inflammatory responses to injury." Nature **464**(7285): 104-107.

Zhang, X., R. Zhuang, H. Wu, J. Chen, F. Wang, G. Li and C. Wu (2018). "A novel role of endocan in alleviating LPS-induced acute lung injury." Life Sci **202**: 89-97.

Zhao, Q., J. Wang, I. V. Levichkin, S. Stasinopoulos, M. T. Ryan and N. J. Hoogenraad (2002). "A mitochondrial specific stress response in mammalian cells." EMBO J **21**(17): 4411-4419.